Thomas Creek (EL06/2013) Annual Report on Exploration 2019

Sorell Peninsula, Tasmania

For the period 21st October 2018 to 1st October 2019

By: Robert Reid, Andy Rust, Luke Vanzino and Jeremy Burton
30/09/2019. Datum used: GDA94, Zone 55

Accelerate Resources Ltd.
Unit 1/ 16 Ord Street
PO Box 938, West Perth
Western Australia, 6005

Summary

Accelerate Resources Ltd. has undertaken extensive exploration efforts on EL6/2013 following ASX listing in January 2018. The project is located on the Sorell Peninsula in western Tasmania, approximately 40km south of the township of Strahan. Exploration is being undertaken for Volcanic hosted massive sulphide and hydrid mineralisation host within the Cambrian Mount Read Volcanic equivalent strata, including porphyry / intrusive-related copper-cobalt-gold mineralisation at the Thomas Creek Prospect, as well as Nickel-sulphide and platinum-group element mineralisation associated with middle Cambrian mafic and ultramafic rocks of the Hibbs Ultramafic Belt.

Exploration work during the year to 01/10/2019 continued to target the Thomas Creek Prospect, completing an ongoing field program, following on from last year's work which included IP and EM geophysical surveys, drilling (3 holes for 831.7m), soil sampling and field reconnaissance.

A final drill hole TCDD004 (EOH 657m) was undertaken targeting a magnetic anomaly and soil Cu high as well as chargeability and a resistivity contrast at depth. TCDD004 was partly co-funded by the Tasmanian Government through MRT's Exploration Drilling Grant Initiative (EDGI) program. The hole intersected a sequence of altered andesitic lavas and volcanic breccias, cross-cut by several K feldspar altered monzodiorites, with zones of magnetite – chalcopyrite - pyrite – K feldspar veining intersected in the upper 300m of the hole. A number of zones of anomalous copper and gold were identified, including 4m at 0.19% copper from 292m, 2m at 1.65g/t gold from 424m, 2m at 0.41% copper from 458m and 4.3m at 0.11% copper from 605.7m. Significant was identification of a potential Cambrian seafloor exhalative volcanic hosted massive sulphide horizon at 519m. This narrow 30cm interval featured chemical precipitate like textures within locally massive to semi-massive pyrite, beneath pervasively silicified and sericitised banding up hole.

A 430line km Mobile Magnetotelurics (MobileMT) airborne survey aiming to map resistivity contrasts to ~1,000m was completed. The survey focused on the Thomas Creek area, but extended north encompassing Timbertops and south to Mt Lowran at the southern end of the Hibbs Ultramafic belt. This system is the latest innovation in airborne electromagnetics and the most advanced generation of airborne Audio-Frequency Magnetic Electromagnetic (AFMAG) technologies. 3D inversion of the MobileMT survey data identified a conductive anomaly in an unexplored area northeast of the Thomas Creek Copper-Gold-Cobalt prospect, as well as a lower tenor conductive zone spatially correlating with the initial Thomas Creek IP Chargeability and geochemical target area. The survey also revealed the presence of an untested resistive plug extending to depth from the centre of the Thomas Creek Intrusive Complex.

Field work and GIS-based data interpretation generated significant insights into the geology and mineralisation at Thomas Creek. Structure elements identified utilising all orientated drill hole data included principal NW and SW dipping chalcopyrite bearing vein orientations, as well as a significant thrust fault. Analysis of geochemical correlation trends in both soil and drill hole data resulted in definition of two key element associations for intrusion related K Feldspar-Silicate alteration (K, Ba, Tl & Rb) and vein (Cu, Co, P, Ni, W, Re) related styles. Comparison to Mt Lyell and other VHMS was undertaken in part through developing vectoring indices. A number of highly prospective Cu-Co targets have been identified, including in the south of the Thomas Creek Grid, as well as open potential in the north and north east.

Contents

Table of Figures

Introduction

This second annual report for Accelerate Resources Ltd. details the completion of significant exploration efforts undertaken to 1st October 2019 on Thomas Creek EL6/2013 (224km^2), located on the Sorell Peninsula ~40km south of Strahan, western Tasmania (Figure 1). The licence is a recent amalgamation of EL's 6 & 7/2013, transferred from Sherlock Minerals to form the foundation for the company's successful January 2018 IPO and ASX listing. Exploration Licence EL6/2013 is held 100% by Accelerate Resources Limited.

The company explores EL6/2013 as part of its Mt Read Project, comprising four adjoining exploration licences; EL6/2013, EL7/2018, EL8/2018 and EL9/2018, located in western Tasmania, approximately 40km south of the township of Strahan. Exploration is being undertaken for Volcanic hosted massive sulphide and hydrid mineralisation host within the Cambrian Mount Read Volcanic equivalent strata, including porphyry / intrusive-related copper-cobalt-gold mineralisation at the Thomas Creek Cu-Co-Au Prospect, as well as Nickel-sulphide and platinum-group element mineralisation associated with middle Cambrian mafic and ultramafic rocks of the Hibbs Ultramafic Belt, including the Henrietta and Young Henry Prospects.

Acknowledgement to contributing geological team members goes to Exploration Manager Andy Rust, consultants Robert Reid and Luke Vanzino, as well as Accelerate company geologist Jeremy Burton. Russell Mortimer from Southern Geoscience undertook geophysical data processing and interpretation. Drilling was undertaken by Edrill Pty. Ltd. Field crew from Rogers Exploration Services provided logistics, grid cutting and sampling support, principally through Ian Rogers.

At Thomas Creek, drilling (TCDD004; EOH 657m), soils and reconnaissance exploration was ongoing at the time of last year's annual reporting. Data was presented at the time, but interpretation relating to drill holes completed prior, awaited this presented. All drilling, map and location data provided in the report use the GDA 94 (Zone 55) reference datum.

Accelerate are advancing through the application of a multidisciplinary approach to exploration in this poorly understood area. The Thomas Creek tenement is little explored with scant geological mapping (including by Amoco, Plutonic, MHM Limited and Mineral Resources Tasmania more regionally) having been undertaken. Stream sediment sampling is relatively scant, mostly extending along the east and north of Thomas Creek, but associated rock chip sampling and geology reporting is sparse. Past exploration has intensely focused upon the immediate "Thomas Creek" area, and largely ignored the surrounding mineral potential. There is obvious potential to upgrade data sets, likely resulting in large gains in understanding of the area. The region to the south and west of Thomas Creek in particular is largely unknown, due to difficult access and minimal exploration to-date.

Location and Access

Access to the project area can be achieved via Macquarie Harbour coastal landing by boat or by helicopter from Strahan (Figure 1). Access within the project areas is achieved on foot via historical exploration tracks (all of which are currently unsuitable for vehicular egress) and cut lines.

The area has a high annual rainfall of approximately 1750 millimetres. The natural vegetation is dominated by rainforest and related scrub, most dominantly Nothofagus rainforest. Additionally

there are areas of wet eucalypt forest and woodland flora types, heathland and coastal vegetation complexes. Bauera scrub areas are very thick and generally impenetrable without prior line cutting work. Where tree canopy is high, undergrowth is significantly less and access over the ground can be achieved with some effort.

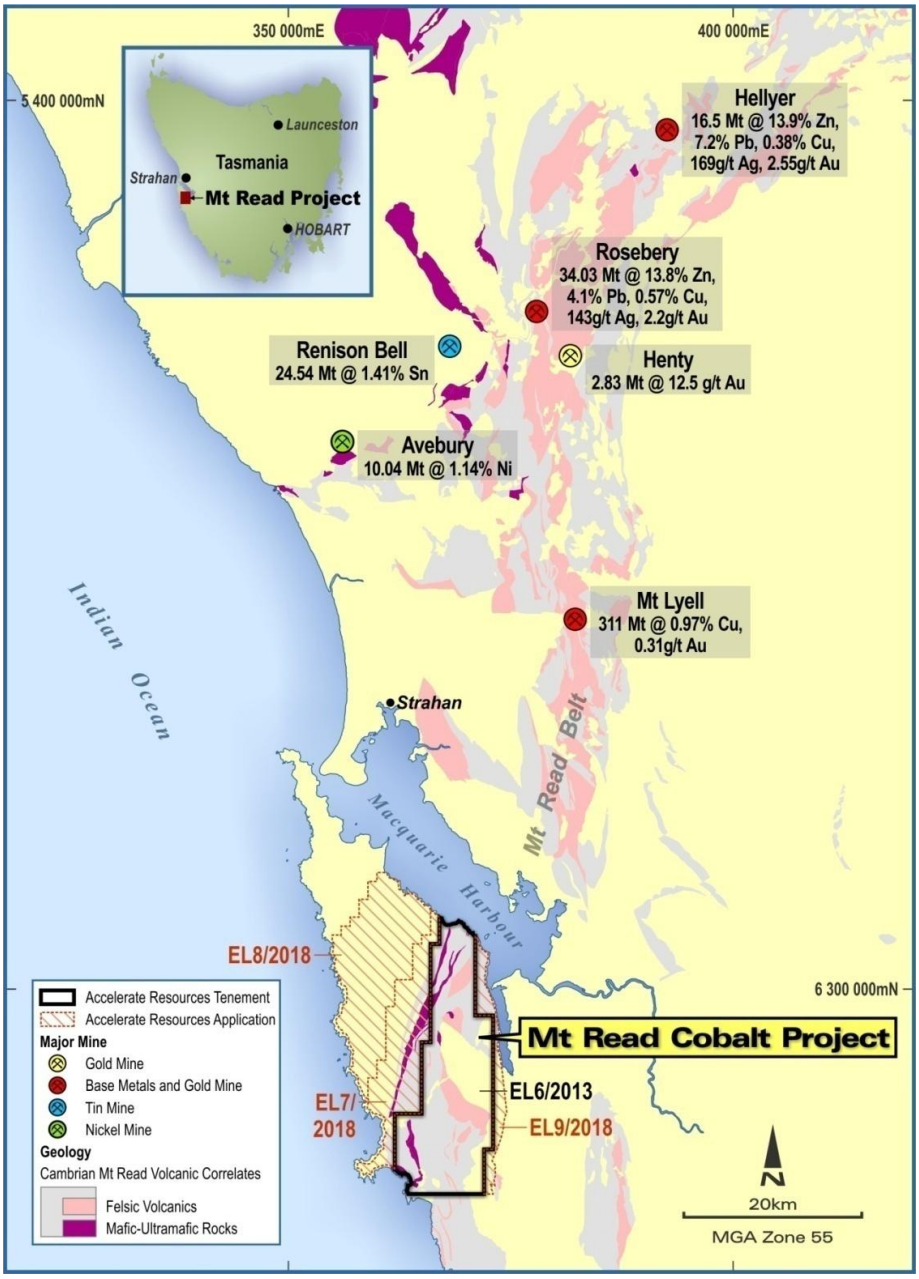

Figure 1: Location of EL06/2013.

Land Tenure

The tenement lies within the Southwest Conservation Area and is part of the Cape Sorell, Strategic Prospectivity Zone, which is protected by the Mining (strategic Prospectivity Zones) Act 1993 – An Act to ensure continuing access for mining purposes to areas of the State having high potential for mineral exploration. The tenements are abutted to the east by the Franklin Gordon Wild Rivers National Park, and to the northeast by the Macquarie Harbour Historical Site.

Geology

The geology of the Sorell Peninsula area (Figure 2) has been described in unpublished company reports of BHP and Amoco/Cyprus, and in White's (1975) PhD thesis. Mapping in the late 1960's by BHP was largely based on coastal exposures and a few inland traverses, with a large component relying upon aerial photo interpretation. Subsequent explorers have relied heavily upon BHP's initial mapping, with a re-interpretation provided by Close and Reid (1995). Limited description of the regional geology is given in Corbett and Solomon (1989).

South of the Sorell Peninsula is little known. Regional mapping by the Mines Department at 1:50,000 covers the area to the north of Varna Bay ("Macquarie Harbour" map sheet; McCleneghan and Findlay, 1989) and to the south of High Rocky Point ("Montgomery" map sheet; Brown, 1988). In between the Hibbs 1:50,000 sheet, encompassing the Thomas Creek area, has been partially mapped but remains incomplete due to lack of funding. A report by Brown et al. (1991) supplements this mapping and provides the most extensive discussion and interpretation of the Sorrell Peninsula geology thus far. Brown et al. (1991) recognised two Precambrian rock successions and six Eocambrian-Cambrian volcano-sedimentary associations in the region (Figure 4). Four of the volcanic associations are relevant to the tenement area.

These associations are: -

- Andesite-rhyolite association (Noddy Creek Volcanics);
- Boninitic association (Timbertops Volcanics);
- Picritic basalt- basalt association (Birch's Inlet-Mainwaring River Volcanics);
- Serpentinised ultramafic rock-gabbro association incorporating sheared blocks of 1. and 2. (Point Hibbs Melange Belt).

These multiple-deformed associations are bounded by a series of NE to NNE-trending faults and the distribution of these associations is interpreted by Brown et al (1991) to result from thrust sheet stacking. Their structural model of "thin skinned tectonics" probably incorporates a pre-Ordovician thrusting event, reworked by late (Devonian?) thrusting. Thrusts are interpreted as eastward dipping with west/north-west thrust direction. Younger transcurrent faulting further disrupted the Point Hibbs Melange Belt.

The Cambrian andesites and rhyolites of the Noddy Creek Volcanics (NCV) crop out in the southern portion of the Sorell Peninsula and are inferred to extend further south past Point Hibbs (Brown et al., 1991; Close and Reid, 1995). The NCV hosts a series of diorite intrusions, and an extensive intrusive complex of diorites occurs within the southern portion of the NCV, south west of the Ordovician – aged Timbertops Syncline. The Thomas Creek Cu Prospect is believed to be hosted by a roof pendant within this intrusive complex.

The relationship of the NCV to the Mt Read Volcanics (MRV) is somewhat enigmatic. The MRV crops out in a N-S trending belt to the east, and extends from Mount Darwin, disappearing beneath a Tertiary Graben to re-emerge further south in the D'Aguillar Range area. Corbett and Solomon (1989) have correlated the NCV with the MRV based on similar calc-alkaline composition, and suggest the NCV could be a smaller, separate arc or sub-arc west of the main Mt Read Belt. More recent work by Brown et al (1991) has suggested a more direct correlation based on geochemical similarities of the southernmost NCV to volcanics of the Que River-Hellyer area.

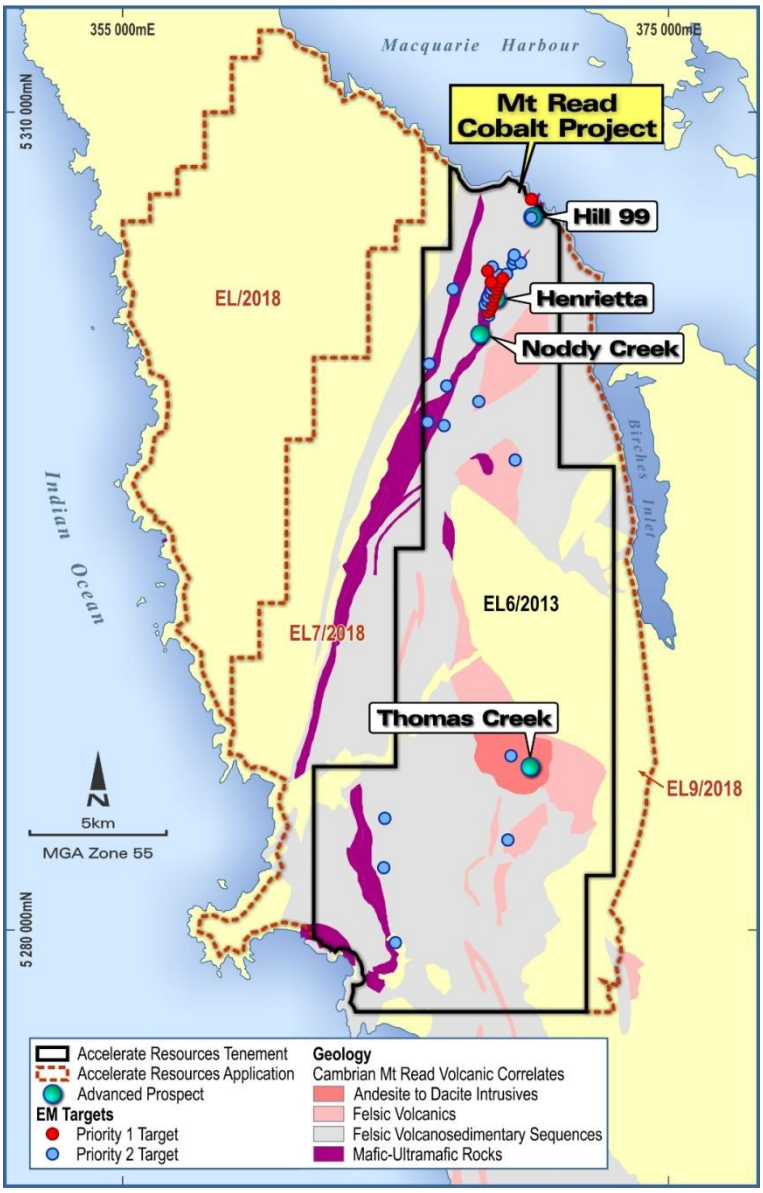

Figure 2: EL06/2013 Cambrian Geology.

Cambrian volcanics are mapped as overlain by Ordovician-aged upper Owen Sandstone forming the Timbertops Syncline, north east of Thomas Creek. Here, Calver (et al., 2014) report siliceous conglomerate and quartz arenite overlain by grey siltstone, dated as likely oldest within the Gordon Group. The upper heavy mineral banded quartz sandstone of the maybe a Pioneer / Moina correlate (Corbett in Calver etal. 2014 & McCleneghan and Findlay, 1993). The Owen Group and particularly its contact with the NCV is a potentially favourable environment for Western Tharsis / North Lyell style mineralisation.

The Thomas Creek (Cu-Co-Au) Prospect is recognised as a significant occurrence of poorly outcropping low-grade copper, cobalt and gold mineralisation associated with hydrothermal alteration of an andesitic to dioritic intrusive-volcanic complex. Sulphide mineralisation occurs over a large area and is associated with micromonzodiorite intrusions, brecciation, veining and 'porphyry'-style K-feldspar-silica and magnetite-chlorite alteration. The combination of volcanic and intrusive

rock stratigraphic association, geochemical signature, alteration assemblages, sulphide assemblages, and geophysical expression has been used by previous explorers to draw analogies between the Thomas Creek Prospect and the Mount Lyell Cu-Au deposit (311Mt @ 1% Cu, 0.3g/t Au) of western Tasmania. However the addition of strong Co credits suggests it may also be similar to a Besshi-stlye VMS (i.e. Windy Craggy [Canada], 297 Mt @ 1.38% Cu, 0.2 g/t Au).

Previous Work and Exploration History

The lack of road access, absence of any permanent settlements, the difficult and scrubby nature of much of the country, have all served to inhibit exploration of the area. Knowledge and understanding of the geology has mostly come in the last four decades from several regional mineral exploration programs by large companies and by regional mapping surveys by Mineral Resources Tasmania through the 1990's.

Sporadic small-scale mining/prospecting was carried out around the beginning of the 20th century for asbestos at Asbestos Point, copper at Birthday Bay (where a few tonnes of chalcopyrite, bornite and copper carbonates were produced from near-shore workings and alluvial osmiridium, gold, and chrome along the Spero River south of Point Hibbs and on creeks along the north coast near Gravelly Beach and parts of Birch's Inlet.

1956–1962 Lyell-EZ Explorations (LEE)

A large helicopter-based exploration program was undertaken by Lyell-EZ Explorations (LEE) over an area stretching from Queenstown to Port Davey from 1956 to 1962. This ambitious program greatly expanded knowledge of the geology of South West Tasmania, which was largely unknown country at that time, but did not result in any commercial mineral discoveries. Airborne magnetics (the first over the southwest), EM and scintillometer surveys were flown over much of the area in 1958, and a variety of ground geophysical methods were used. The ultramafic belt between Point Hibbs and Macquarie Harbour was discovered (Hibbs Ultramafic Belt).

1964–1972 BHP Exploration

A second major helicopter-based exploration program, covering most of South West Tasmania (9,600 km^2), followed soon after, and was conducted by BHP between 1964 and 1972. The project resembled a geological survey in many ways, and much regional mapping was undertaken. BHP based their exploration on follow-up of the LEE aeromagnetics and EM surveys, with stream sediment geochemistry as their other main regional technique, however, Au and Sn were not assayed for.

BHP spent considerable resources cutting tracks and costeans along the northern part of the Hibbs Ultramafic Belt, concentrating on the nickel and chrysotile asbestos potential. Rock chip sampling from costeans across this contact returned up to 0.8% Cu and 0.15% Ni. In addition, a zone of disseminated pentlandite about 12 m wide occurring as small blebs up to 6 mm in slightly sheared olive-green serpentinite had been found along with specks of pentlandite in shear planes in a costean. One hole was drilled to 95m, testing a ground EM anomaly. No anomalous nickel was intersected with the anomaly being explained by an intersection of 3.4 meters of graphitic siltstone below the ultramafic contact. BHP recommended that EM traverses be run at 30 m intervals along strike but no further work was done on nickel. Towards the south of the belt an area of anomalous Zn and Ni was determined from stream sediment sampling in creeks between Hibbs Lagoon and Point Hibbs.

Asbestos was discovered in the northern part of the ultramafics and this became a major focus of further exploration by BHP in the area. This work culminated in the outlining of 8.5 million tonnes of 2.3% asbestos.

In 1971/72 BHP followed up an aeromagnetic anomaly southwest of Birch's Inlet with ground magnetics, soil sampling and rock chip sampling (Thomas Creek Prospect). The results are presented unprocessed with no discussion and it appears that there was no follow-up. Several samples from this work yielding up to 1000 ppm Cu, 1000 ppm Pb, 100 ppm Zn and up to 100 ppm Ag. The samples were taken from rocks with visible disseminated sulphides, some of the rocks being boulders. BHP's interest in the Sorell Peninsula was relinquished in 1972.

1983-88 Amoco Minerals Australia Company

(Later Cyprus Gold Australia Corp., in joint venture with Placer Development Ltd and Poseidon Minerals Ltd.)

Work initially comprised a detailed 150m line spaced airborne aeromagnetic and radiometric survey to assist geological mapping as well as to locate any tin replacement (i.e. Renison Style) deposits over the whole Sorrell Peninsula. In 1983-84 Amoco conducted reconnaissance mapping and sampling of the Noddy Creek Volcanics around Timbertops north to Briggs Creek and south to Thomas Creek to assess various aeromagnetic anomalies. The main target for exploration was a polymetallic volcanogenic massive sulphide orebody with minimum reserves of 15 million tonnes of 20% lead-zinc with gold plus silver credits similar to the Rosebery and Que River/Hellyer deposits 70 kilometres to the north.

A DigHEM survey was flown over the northern portion of the Hibbs Belt and Noddy Creek Volcanics in 1986 (Figure 3), which identified seven targets that were never followed up, as coincident DigHEM work to the south over the coeval Lucas Creek Volcanics at Elliot Bay located higher tenor anomalies which became the focus of later work.

Weak base metal veining was reported adjacent to diorite at Timbertops, and more significantly a Cu-Au (Ba) association with diorites and intermediate volcanics was recognised in the Warrens to Thomas Creek area. Here a peak value of 0.2% Cu, 0.1% Ba and 0.97 g/t Au was related to a sub-volcanic diorite intrusion south west of the anomalous Cu-Pb volcanics reported by BHP.

Follow-up bedrock soil surveys over a grid at Thomas Creek in 1984 followed and this outlined a zone of anomalous copper approximately 300 metres by 400 metres in size which was greater than 250 ppm Cu. Amoco had a polymetallic VMS focus and the absence of significant associated Pb-Zn with the copper or regularly repeatable high Au downgraded the prospect and no further exploration was conducted.

1992-1998 Plutonic Operations limited

Plutonic Operations Ltd were granted two licenses EL4/1992 and EL7/1992 which covered most of the ground currently held by Sherlock Minerals. In 1993-94 plutonic planned to carry out a 200m line space airborne GEOTEM survey over the Noddy Creek Volcanics (Figure 3) which are thought to be a direct equivalent of the fertile Mt Read Volcanics, but occur in a possible sub-rift immediately west of the main volcanic belt. Contractor delays meant this was not carried out until March 1996. The survey

identified approximately 20 targets that warranted follow up. This appears not to have occurred as ground operations had shifted by that time to Thomas Creek Prospect.

During the 1994-95 period a large program of gridding, soil sampling, and petrology over the Thomas Creek Prospect confirmed Amoco's results and indicated a significant zone of alteration with the characteristics of a porphyry Cu-Au system. The copper soil anomaly extended approximately 1000 m x 700 m, with other satellite anomalous zones also appearing. Many exceptional copper soil values were returned over 1000 ppm and includes 2 samples one recording 2.4% Cu and 1.04 g/t Au and another of 7.5 % Cu and 2.96 g/t Au in highly pyritic, chloritic and chalcopyrite bearing interpreted microdiorite. Elsewhere gold values were generally below detection, apart from where very high copper (>2000 ppm) were sampled. Panned concentrate from drainage areas fringing the eastern side of Thomas Creek plateau returned some visible gold with assays returning up to 3g/t.

In 1995 Zonge Engineering were contracted to conduct two gradient array surveys totalling 7-line km over the grid area and three dipole-dipole lines amounting to 1.25km within the detailed grid. These surveys were designed to outline the extent and relative intensity of disseminated or stockwork vein-controlled sulphide mineralisation in the Thomas Creek prospect area. The IP surveys successfully defined one major and three minor discrete chargeability zones. Zone A is a broad (600m x 400m) multi peaked, moderate to strong (3 times background) chargeability anomaly coincident with disseminated pyrite and copper anomalism in the detailed grid area.

In 1996 a light "Gopher" rig was used to test areas of high Cu soil geochemistry and corresponding IP chargeability. The program comprised 8 BQ sized holes angled 45 degrees to the South and 90 - 127m hole depth. Significant core loss (clays – highly altered/weathered) was encountered however more consolidated core sections showed intense K-feldspar–silicification, pyrite, chlorite, actinolite, magnetite, hematite, pyrite, chalcopyrite with late tourmaline, pyrite, smectite, and epidote alteration. The drilling revealed widespread copper anomalism, such as 58 m @ 0.08% Cu from 40 m in TCD2 and 15m @ 0.17% Cu from 32m in TCD5. Plutonic were disappointed that better copper grades were not intersected, given the high tenor of the soil geochemistry however did recognised that this was a large, probable porphyry style mineralised system, that required expanded exploration and deeper drilling. After failing to attract a joint venture partner, and due to other core business pressures occurring in the late 90's Plutonic relinquished the area in 1998.

1998-2001 Pacific-Nevada Mining Pty Ltd

The Hill 99 Prospect, located near the southern shores of Macquarie Harbour (Figure 2) was identified by Pacific-Nevada Mining Pty Ltd in 1999 after a reconnaissance sampling programme located an outcrop of massive pyrite-quartz mineralisation. A subsequent soil sample campaign identified a copper-zinc anomalous (150-511ppm Cu and 150-684ppm Zn) zone extending inland along strike from the coastal pyrite-quartz mineralisation. The zone trends north-east and is broadly coincident with a topographic high. Sampling of gossanous float material along the grid lines returned sporadic anomalous gold up to 50ppb with 92ppb Au also returned from a chlorite altered lithicwacke sample. A single panned concentrate stream sample returned 5.1 g/t Au.

A subsequent gradient array IP survey carried out over the Hill 99 grid identified a linear, moderate conductivity high coincident with the copper-zinc anomalous soil zone. A bullseye conductivity anomaly was also identified. A fixed loop ground EM survey failed to identify any conductive bodies

of probable economic importance, however it did show a strong conductor forming off the western edge of the survey coincident with a prominent magnetic feature. The thick vegetation precluded the survey being extended further west at that time and this target remains untested.

Pacific-Nevada drilled three diamond drill holes totalling 669 m. The first two drill holes H99-01 & 02 targeted the Cu-Zn soil anomalies/alteration and mapped gossanous float and intersected a highly altered chlorite-carbonate-fuchsite volcanic rock of mafic to felsic origin with minor Cu, Zn and Au (best result 0.3m @ 0.59% Cu). H99-03 tested the coincident high phase and resistivity low anomaly modelled at 150m depth. Localised narrow zones of pyrite-chalcopyrite (i.e. 36 cm @1.05% Cu) mineralisation and quartz-carbonate-sphalerite-galena veining (i.e. 30 cm @ 0.17% Pb & 0.25% Zn) with intense fuchsite alteration were intersected before drilling was stopped due to hole instability approximately 30m above the IP target.

2007 – 2012 MHM Metals

In 2010 MHM commissioned a detailed 100m line spaced helicopter borne VTEM surveys over 4 areas (Figure 3). The survey areas covered the Hibbs Ultramafic belt, an area along the north coast region, covering a portion of the Noddy Creek volcanics and over recognised VMS mineralisation at Hill 99 Prospect and over the Thomas Creek Prospect area. The surveys identified many intermediate to strong conductors, the best associated with the ultramafic in an area immediately north of BHP's asbestos work at Noddy Creek. Some of the conductors associated with the ultramafic rocks were followed up with a limited spot soil sampling campaign at EM target sites and returned highly anomalous Nickel up to 2500 ppm and gold up to 1 g/t. Other EM conductors in remote areas including some sites identified near Thomas Creek were not followed up.

At Hill 99 prospect MHM Metals drilled two further holes totalling 368m to follow up previous encouragement from Pacific Nevada's Drilling. Drill hole H99-04 tested strike persistency of mineralised intercepts from H99-01 and 2 and hole H99-05 tested the bulls eye IP anomaly identified by Pacific Nevada work. Geochemical results from hole H99-04 showed anomalous gold with peak values of 0.105, 0.182 and 0.105ppm Au associated with fuchsite-quartz-sericite alteration of andesites and basalts from 155 to 172m. Copper from a 30cm massive quartz-chalcopyrite vein intersected at 177.6m returned a grade of 10.55% Cu, and 0.244% Zn. Independent geochemical analysis of the core suggested the sequence is comparable to suite 1 of Crawford's (1992) stratigraphic proposal of the Mount Read Volcanics which hosts several major deposits including Mount Lyell (Cu- Au), Henty gold mine, and Rosebery (Pb-Zn-Ag).

At Thomas Creek MHM noted the circular magnetic high edging the intermediate intrusive body and undertook soil sampling around this feature at 50 m spacing. This work extended the copper anomalous areas further south at Thomas Creek, but also identified a new region of high copper anomalism (up to 500 ppm Cu) about 1.5 km northwest of the original prospect. This new site is unconstrained and occurs along the inner magnetic rim.

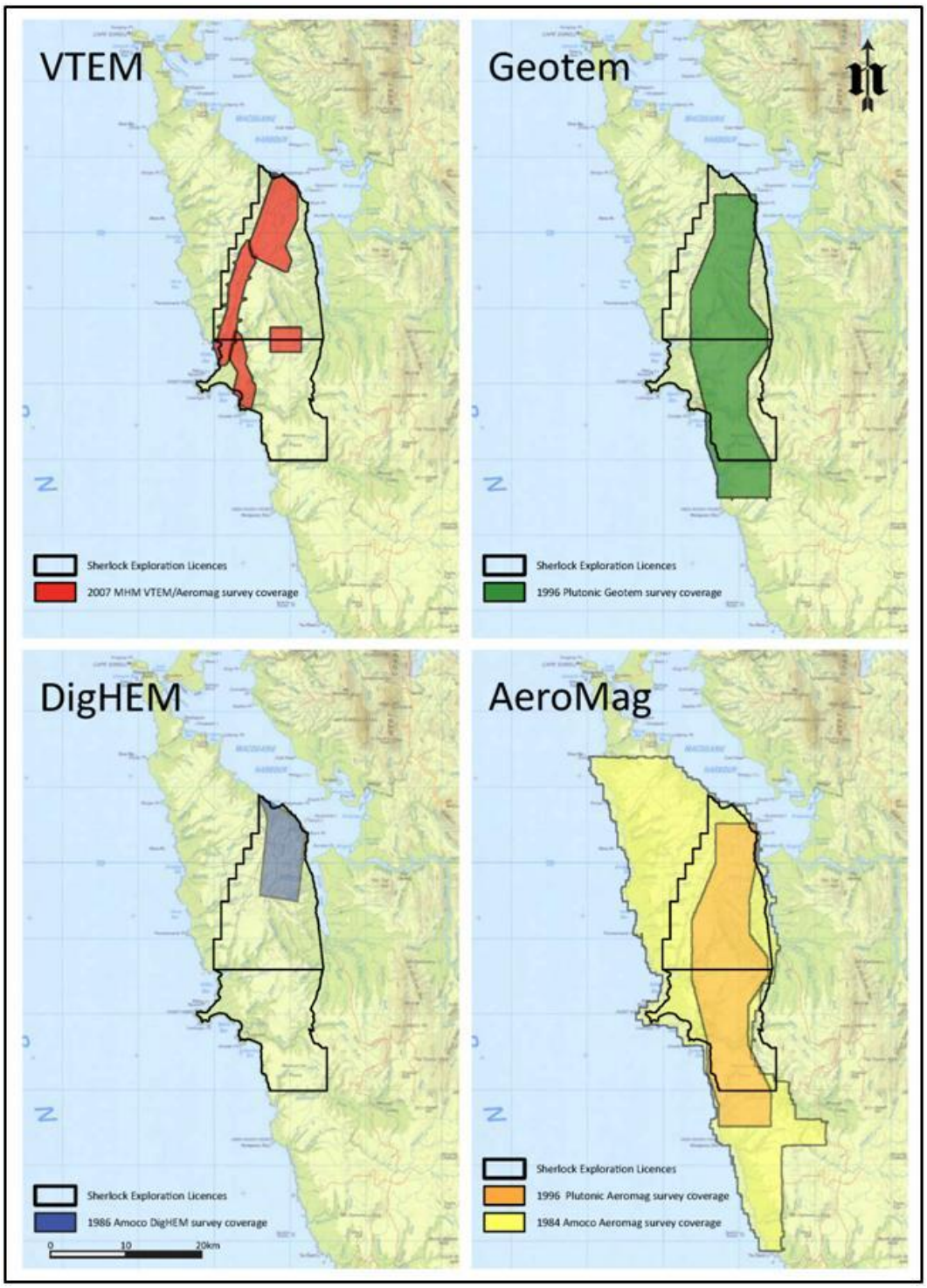

Figure 3: Summary Airborne geophysics surveys.

2013 to 2017 Sherlock

Sherlock undertook Dipole-Dipole induced polarization surveys, field reconnaissance and sampling, identifying Co potential. Geophysical modelling and interpretation of the historical drilling indicated the IP targets generated had not been previously drill tested.

In 2014, Sherlock Minerals conducted dipole-dipole induced polarisation (IP) surveys for a total of 7.3-line kilometres at the Thomas Creek Project. The IP surveys revealed the presence of a

chargeability anomaly approximately 300 m wide and 500 m long at 100 to 200m depth, that did not appear to have been tested by historical shallow exploration drill holes.

In 2015 at Thomas Creek, high-grade copper and gold mineralisation was redefined at surface, following up historic high-copper values in soils. The mineralisation comprised a massive pyrite zone approximately 5 metres wide containing abundant copper sulphides hosted within highly weathered saprolitic bedrock, beneath peaty soil cover. Geochemical analyses of the mineralised saprock zone returned values ranging between 0.8% to 3.8% copper, 0.7 g/t to 1.3 g/t gold, and 0.1% to 0.78% cobalt. The mineralisation occurs above the chargeability IP anomaly identified in 2014.

2017 to 2018 Accelerate Resources Ltd.

Accelerate Resources Ltd. undertook extensive exploration efforts on EL06/2013 targeting intrusion and vein related Cu-Co mineralisation at Thomas Creek, as well as Nickel-sulphide and platinum-group element mineralisation at the Young Henry Prospect.

During 2018, 212 field surface samples were collected from the Thomas Creek, Henrietta and Young Henry Prospect areas, comprising a total of 173 soil samples, 22 rock chips and 10 bulk stream sediment samples for -80# analysis. Soil sampling at Young Henry (No. 49) selectively covered the ultramafic rocks and surrounds, centred upon the targeted airborne EM. At Thomas Creek, the soil sampling (No. 124) rationale selectively covered previous un-sampled Sherlock 2014 IP grids and new Accelerate 2018 IP grids.

A ground IP survey at Thomas Creek was undertaken, extending the 2014 Sherlock IP survey. A total of 10.8 line kilometres was surveyed on five 150m spaced north-south and one east west oriented lines. The IP Survey was 2D dipole-dipole design with 75m dipole length using 1-14 separation. 3D IP modelling combining the 2014 Sherlock and 2018 Accelerate IP defined a large ~600 by 400m chargeable anomaly located along the eastern margin of an ovoid aeromagnetic body, below surface copper-cobalt soil anomalism (Figures 4 & 5).

Diamond drilling at Thomas Creek comprised three holes TCDD001 to TCDD003 for 831.7m, targeting strong chargeability highs and resistivity lows within the large 3D inversion modelled IP chargeability anomaly. The drilling intersected a fertile mineralised system bearing abundant disseminated and veined sulphides and several felsic-intermediate (micromonzodiorite) intrusions, with associated anomalous copper-cobalt grades. Best results included: 3m @ 2323ppm Co and 0.09% Cu in TCDD001; 46m @ 0.11% Cu in TCDD002; 22m @ 193ppm Co and 0.01% Cu in TCDD003 (Tables 3). All three holes intersected pervasive silica (+/– sericite) – pyrite alteration with overprinting magnetite-KFeldspar-actinolite-chlorite-pyrite-chalcopyrite veining. Zones of weak to moderate pervasive K-Feldspar-silicate alteration were also seen.

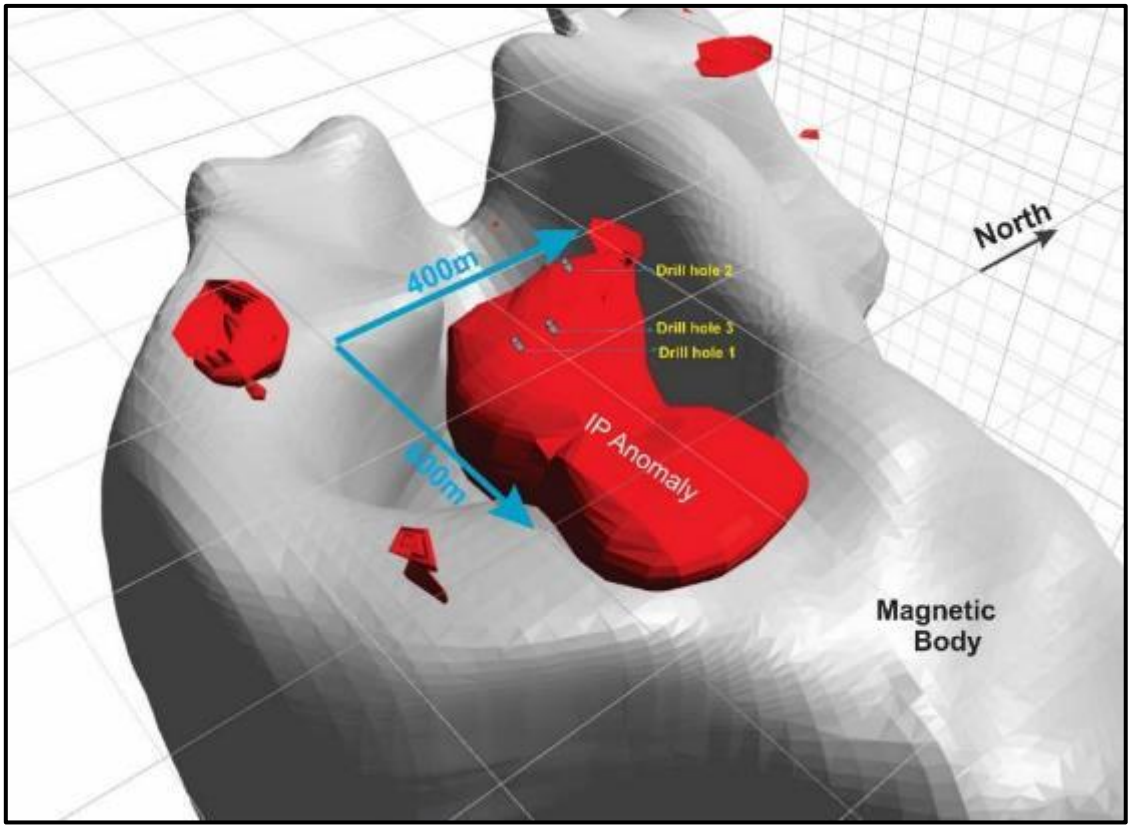

Figure 4: Thomas Creek - 3D Chargeable IP Anomalies with Drill Holes

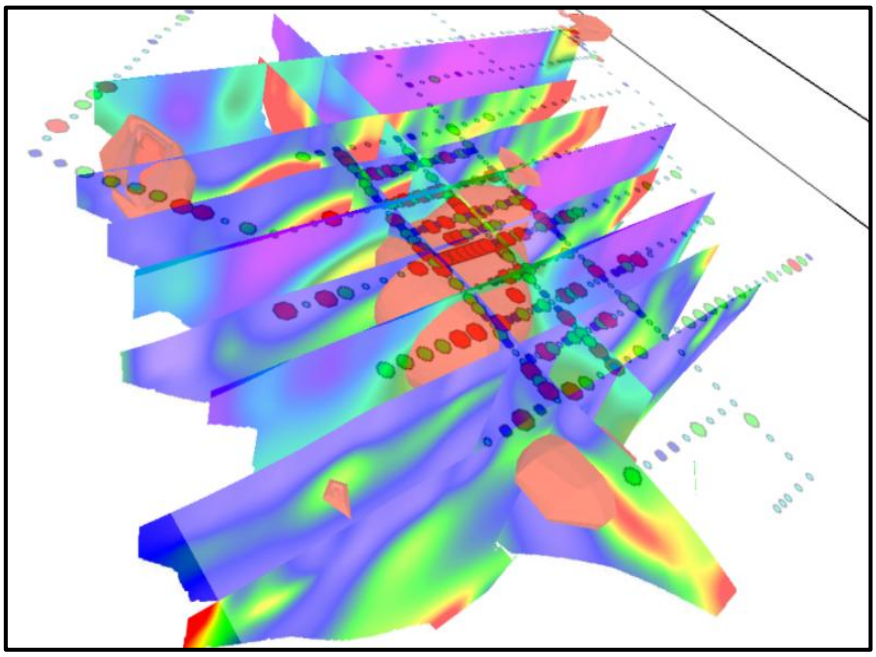

Figure 5: Thomas Creek, 3D IP modelling defines large chargeable body beneath Cu in soil anomalism

DHEM surveying of the three diamond holes facilitated by a further 1.5km of gridding for loops, indicated a number of in-hole and nearby conductors related to observed semi-massive sulphide mineralisation intersected by the drilling. The DHEM of hole TCDD003 identified a broad, distant and

unconstrained off-hole conductor to the southeast and located ~150m east of TCDD001. This conductor occurs within the shallower eastern parts of the IP chargeability anomaly, overlying the magnetic rim of the Thomas Creek intrusive complex.

SWIR data was collected for TCDD001 to 3, with a preliminary consultants report identifying strongest vectors to VHMS style alteration in TCDD003, which drilled at an acute angle to dominant structure and veining.

Exploration at the Young Henry Prospect targeted an Airborne EM conductor, potentially associated with Nickel-sulphide and platinum-group element mineralisation host within middle Cambrian mafic and ultramafic rocks of the Hibbs Ultramafic Belt. Mineralisation potential was clearly demonstrated with grid (3.6km) based sampling returning Ni, Co, Cu and Zn anomalous soils and gossan located up plunge from a modelled ground FLEM conductor. Drill targeting (YHDD001, 156m EOH) returned two significant intersections of 38.3m @ 0.23% Ni and 17.7m @ 0.19% Ni. Two zones with magmatic Nickel sulphide potential were identified at the base of both serpentinised ultramafics intersected.

Work Conducted

Exploration work during the year to 01/10/2019 continued to target the Thomas Creek Prospect, completing an ongoing field program, following on from last year's work which included IP and DHEM geophysical surveys, drilling (3 holes for 831.7m), soil sampling and field reconnaissance. One drill hole TCDD004 totalling 657m was completed at Thomas Creek with further associated field work. A 430line km Mobile Magnetotelurics airborne survey focused on the Thomas Creek area, but extended north encompassing the Timbertops area and south to Mt Lowran at the southern end of the Hibbs Ultramafic belt. GIS-based data compilation, planning and interpretation continued.

Logistics and field assistants were provided by Rogers Exploration Services. This followed on from their efforts last reporting year, involving grid cutting 10.8line km facilitating IP at Thomas Creek, as well as a further 1.5km for DHEM loops. At Young Henry 3.6km of line cutting was undertaken for FLEM and soil sampling.

Reporting of significant data compilation, interpretation, target generation and planning reliant on field data from the 2017-2019 program was undertaken. Reconnaissance geology targeted the Thomas Creek environs. -80# stream sediment sampling, panned concentrate and rock chips were collected during regional exploration with grid base soil sampling also undertaken at Thomas Creek. Analysis has not been undertaken on panned concentrate reference samples collected to-date. This reconnaissance clearly identified that access tracks need to cut to enable efficient exploration work in the area.

Two petrological studies were undertaken by MRT on Young Henry suspected Asbestos and a Thomas Creek Actinolite vein (EL062013_201910_15_LJN2018-130.pdf and EL062013_201910_16_LJN2018-143.docx, respectively).

Digital data is appended (see EL062013_201910_37_FileListing.xls) with data structure being further elucidated below.

Drilling

Drill hole TCDD004 was completed at 657m during the reporting year and was partly co-funded by the Tasmanian Government through MRT's Exploration Drilling Grant Initiative (EDGI) program. This completed an ongoing drilling program at Thomas Creek where to-date, Accelerate have completed four diamond drill holes totalling 1490.5m (Figure 6 & Table 1). A further hole YHDD001 for 156.1m at the Young Henry Prospect, resulting in a total of 1647m drilled during Accelerates' exploration program.

Table 1: Drill hole collar details; All Accelerate Drilling but highlighting TCDD004 from 2019.

Hole ID	East MGA94	North MGA94	RL	Azimuth	Dip	Depth	Date Commenced	Date Completed
TCDD001	369894	5285793	219	90	-60	272.9	6/04/2018	19/04/2018
TCDD002	369740	5286051	214	45	-60	200.9	27/04/2018	18/05/2018
TCDD003	369834	5285851	214	45	-55	359.7	29/05/2018	1/07/2018
TCDD004	**370114**	**5285822**	**215**	**135**	**-65**	**657**	**3/10/2018**	**16/12/2018**
YHDD001	368465	5304278	171	115	-65	156.1	24/08/2018	3/09/2018

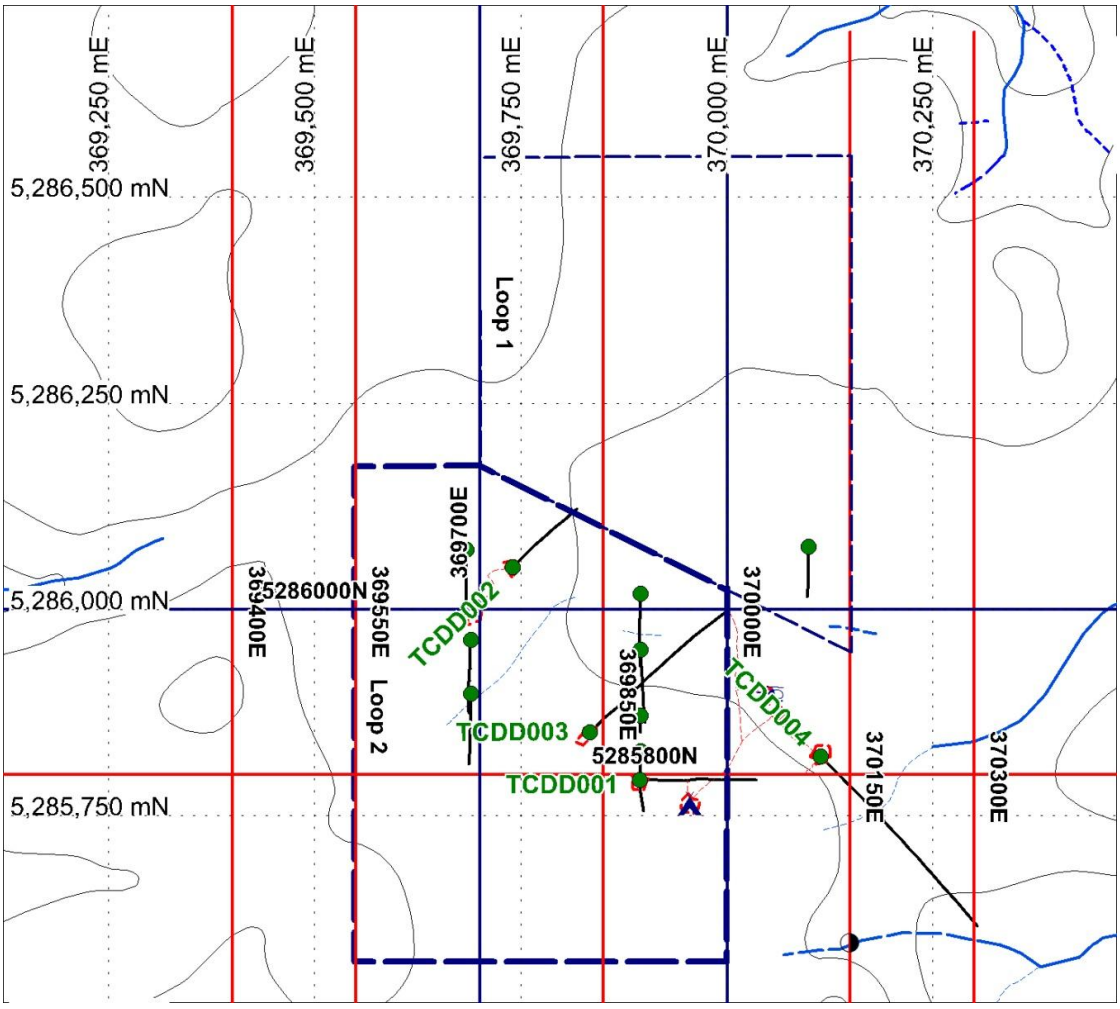

Figure 6: Thomas Creek Prospect drill collars, IP grids and DHEM Loops.

Drill hole TCDD004 targeted a coincident magnetic feature and IP anomaly (Figure 7) associated with a number of surface features, interpreted to indicate the presence of proximal potassic alteration and more distal propylitic alteration within a “classic” Porphyry alteration system. A further potential target was a broad, distant and unconstrained off-hole DHEM conductor located ~150m east of TCDD001, which was not explained. However, the possibility exists that the VHMS – like intersection in TCDD004 relates to a thin portion of a larger nearby VHMS body. Further characterisation of this VHMS – like intersection via thin section petrography and sulphur isotope work is required.

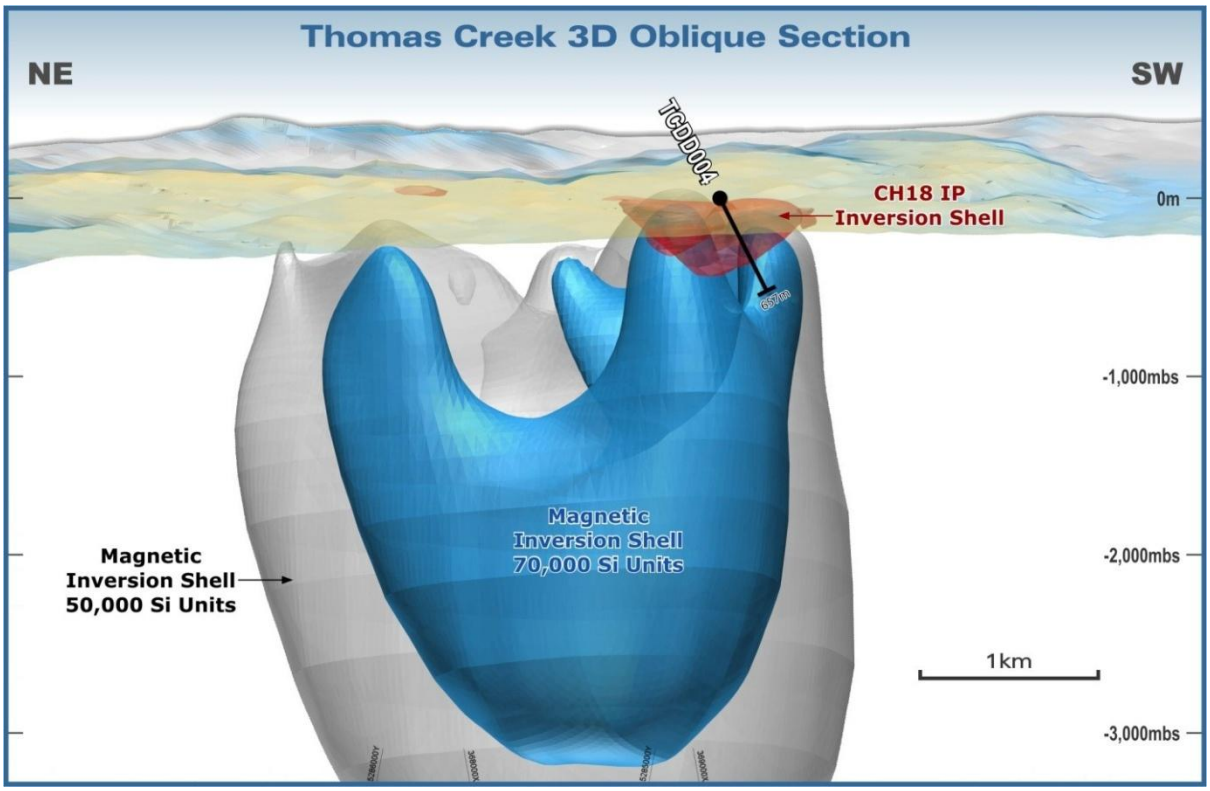

Figure 7. IP chargeability and magnetic inversion shells targeted by TCDD004

HQ and NQ diamond core drilling was undertaken using an LF70 helicopter portable diamond drill rig, supplied by Edrill Pty. Ltd. GPS averaging was undertaken over several days to confirm drill collar location. All coordinates are reported in GDA94, zone 55. A sighter line placed on ground prior to rig arrival. A drill rig fore and back site, to assess potential metal and magnetic disturbance, was undertaken to confirm collar azimuth. Future down hole electromagnetic surveys were facilitated with 40mm PVC run to the end of all holes.

Drilling related digital data are appended as various files for the 2019 tenure year; as per EL062013_201910_37_FileListing.xls. This includes orientated structures, surveys, core recovery and photos. Digital data for all Accelerate drill holes have been interpreted and formatted to match drill logging codes in EL062013_201910_05_Lithologycodes.xls. Lookups are a combination of a simple lithology lookup, with evolving prospect specific adaptations.

A drill core orientation (Orishot) tool from Borecam Asia Pty Ltd was utilized. Some spear with crayon orientations were undertaken towards the top of TCDD001. Bottom dead centre was marked and extended where possible. Structure data was collected from orientated and some un-orientated core. Down hole surveys utilised a standard Eastman Camera and were notably appeared erroneous where significant magnetite was present. Some surveys close to the dominant hole azimuth were estimated when calculating structure orientations. Data were classified according to various vein mineral contents and fracture types. Structure orientation was achieved using the Core Solutions Excel macro template, developed by CODES (Centre for Ore Deposit and Exploration Science). Data are listed in EL062013_201910_07_DStructure1.xls.

Use of HQ and NQ triple tube for Accelerates' drilling, despite common strongly broken ground, resulted in mostly very good core recovery, particularly when compared to the previous Plutonic BQ TK sized core (Table 2). Recovery from TCDD004 was good, averaging nearly 97%. In general, significant core loss associated with drilling poorly consolidated late stage sulphide veining was locally evident. Low RQD was encountered over broad broken zones within most drill holes, but mostly within mineralized breccias with late micromonzodiorites being relatively less broken. Core recovery was calculated each run by the driller and verified onsite during logging.

Table 2: Drill hole recovery statistics for Thomas Creek and Young Henry (YHDD001)

Hole_ID	Average of Recovery_%	Average of RQD_%
TCDD001	95.65	13.45
TCDD002	97.10	23.75
TCDD003	91.93	28.97
TCDD004	96.74	34.84
TCD1	85.90	
TCD2	91.87	
TCD3	92.69	
TCD4	33.72	
TCD5	79.13	
TCD6	86.83	
TCD7	85.64	
TCD8	88.22	
TC Total	91.34	26.56
YHDD001	95.48	49.74

Geochemistry

HQ/NQ sized core from holes TCDD004 was cut by Rogers Exploration Services utilising MRT's core facility in Mornington (TAS), with sample preparation at ALS Burnie prior to forwarding to ALS Perth for analysis. All remaining drill core is retained MRT's Mornington core library.

A total of 423 half core samples were collected from TCDD004. Sampling was at 1m intervals through the primary alteration zone from 198m to 302m, with the remainder of the hole sampled as a mix of 1 and 2m composite zones. All diamond core samples collected from the same side of the core to ensure consistent, representative sampling.

TCDD004 core samples were submitted to Independent certified laboratory ALS in Perth, for ore grade gold analysis by Fire Assay (30 gram charge) with AAS finish (Au-AA25 method) and multi-

element (48 element) analysis by 4-acid digest, ICP-MS (ME-MS61 method). Due to the early stage of exploration no external, additional standards, blanks or duplicates have been used. No verification or additional assaying has been undertaken to date. QC relies on the supplied laboratory report. Original lab results and QC data for the samples are attached as various pdf's.

TCDD004 Drilling Results

The hole intersected a sequence of altered andesitic lavas and volcanic breccias, cross-cut by a number of Potassium feldspar altered monzodiorites, with zones of magnetite – chalcopyrite - pyrite – potassium feldspar veining intersected in the upper 300m of the hole. The drilling returned a number of zones of anomalous copper and gold mineralisation (Table 3) associated with zones of visible copper sulphide (chalcopyrite) mineralisation and monzodiorite intrusions, including:-

- 292m to 296m, 4m at 0.19% copper, including 1m at 0.47% copper and 0.21 g/t gold from a zone of (290.60m to 298.43m) brecciated andesite containing between 5-10% disseminated to semi-massive pyrite and 0.3-0.5% chalcopyrite stringers, located immediately below a potassium feldspar altered micro-monzodiorite (288.50 to 290.60m) containing 0.5% disseminated chalcopyrite.
- 424m to 426m (2m sample), 2m at 1.65g/t gold associated with 30cm zone of pyrite (8%) and chalcopyrite (1%) veining and a 10cm semi-massive pyrite (20%) /magnetite vein, in a brecciated andesite located adjacent to a potassium feldspar altered micro-monzodiorite (429.78 to 440.0m) containing 0.5% disseminated pyrite and chalcopyrite.
- 458m to 460m, 2m at 0.41% copper associated with a zone of pyrite and chalcopyrite/epidote veining in a brecciated andesite, within a broader 6m zone (458m to 464m) averaging 0.18% copper.

A number of Potassium feldspar altered monzodiorites were also intersected in the lower half of TCDD004, within altered andesitic lavas and breccias. Some monzodiorites contained disseminated pyrite and chalcopyrite, including, 605.7m to 610m, which returned 4.3m at 0.11% copper and appears to represent a more mineralized intrusive phase when compared to other monzodiorites in the hole.

A series of thin volcaniclastic sedimentary horizons were intersected in the lower part of the hole. These include a fine to medium grained slightly hematitic andesitic volcaniclastic sandstone at 510.9m to 511.3m containing 0.5% disseminated chalcopyrite, which returned 0.4m at 0.15% copper. A 2cm thin volcaniclastic sandstone bearing rip up clasts is evident within the 519.25m to 519.46m interval containing 10% semi-massive to disseminated pyrite, locally reaching semi massive 25% pyrite with a very fine grained darker weakly banded pyrite form also present. This interval features VHMS-like characteristics with chemical precipitate like texture and locally massive to semi-massive pyrite replacement beneath a pervasively silicified-sericitised banding up hole (Photo 1); see log for more detail. Lower most is a volcaniclastic sandstone and siltstone horizon containing 0.1% disseminated pyrite and chalcopyrite, as well as featuring minor soft sediment fault deformation (possibly normal W?) at 627.50m to 629.0m.

Table 3: TCDD004 Significant Intersections

Hole ID	Interval (m)			Copper	Cobalt	Gold	Copper cut-off
	From	To	Width	%	ppm	g/t	
TCD004	**199**	**200**	**1m**	0.16	837		500ppm
TCD004	**210**	**215**	**5m**	0.09			500ppm
TCD004	**268**	**269**	**1m**	0.14			500ppm
TCD004	**292**	**296**	**4m**	0.20			500ppm
incl.	**294**	**295**	**1m**	0.47	638	0.21	1000ppm
TCD004	**424**	**426**	**2m**			1.65	
TCD004	**458**	**464**	**6m**	0.19			300ppm
incl.	**458**	**460**	**2m**	0.41			1000ppm
TCD004	**510.9**	**511.3**	**0.4m**	0.15			500ppm
TCD004	**605.7**	**610**	**4.3m**	0.11			500ppm

These sulphidic volcaniclastic horizons highlight the potential for exhalative VHMS seafloor horizons to occur within the project area. The up-dip potential for these horizons is indicated at surface by a zone of chargeability, in the south eastern part of the Thomas Creek survey grid, coincident with elevated potential VHMS Copper indicator elements (Bi, Te, Mo & Co; see below).

Both inferred VHMS exhalative horizons are underlain by irregular pyrite – chalcopyrite veining / stringer zoning strongest closest to the inferred horizon, within pervasively silicified andesite breccia. Sericite replacing feldspar is also evident closest beneath the horizons, whilst pervasive and semi pervasive K Feldspar overprint continues apparently more distal beneath pervasive silica. Late stage (porphyry related) magnetite-chalcopyrite veining are sparse and erratically distributed further down hole beneath these horizons in TCDD004.

These horizons lie at the top of andesite lava breccia flow facies, with external influence in the form of distal high density turbidite medium grained volcaniclastic sandstone. This likely represents distal input from WVS, interfingering with the NCV. i.e a time of relative local volcanic quiescence. There's interpreted potential for a stacked sequence of VHMS exhalative horizons being progressively buried by fresh andesite lava flows.

The hole was planned to go on to the resistivity boundary from 700m, which possibly represents a silicified top of the Western Volcansedimentary Sequence stratigraphically beneath the Noddy Creek Volcanics, where a VHMS mound may have had a longer time to develop. However, the basal volcaniclastic horizon was considerably less altered.

A proximal VHMS could be related to the off hole DHEM conductor located east of TCDD003 and 1, effectively towards TCDD004. A MobileMT conductor is modelled beneath and between TCDD002 and TCD2, north of this potential vector.

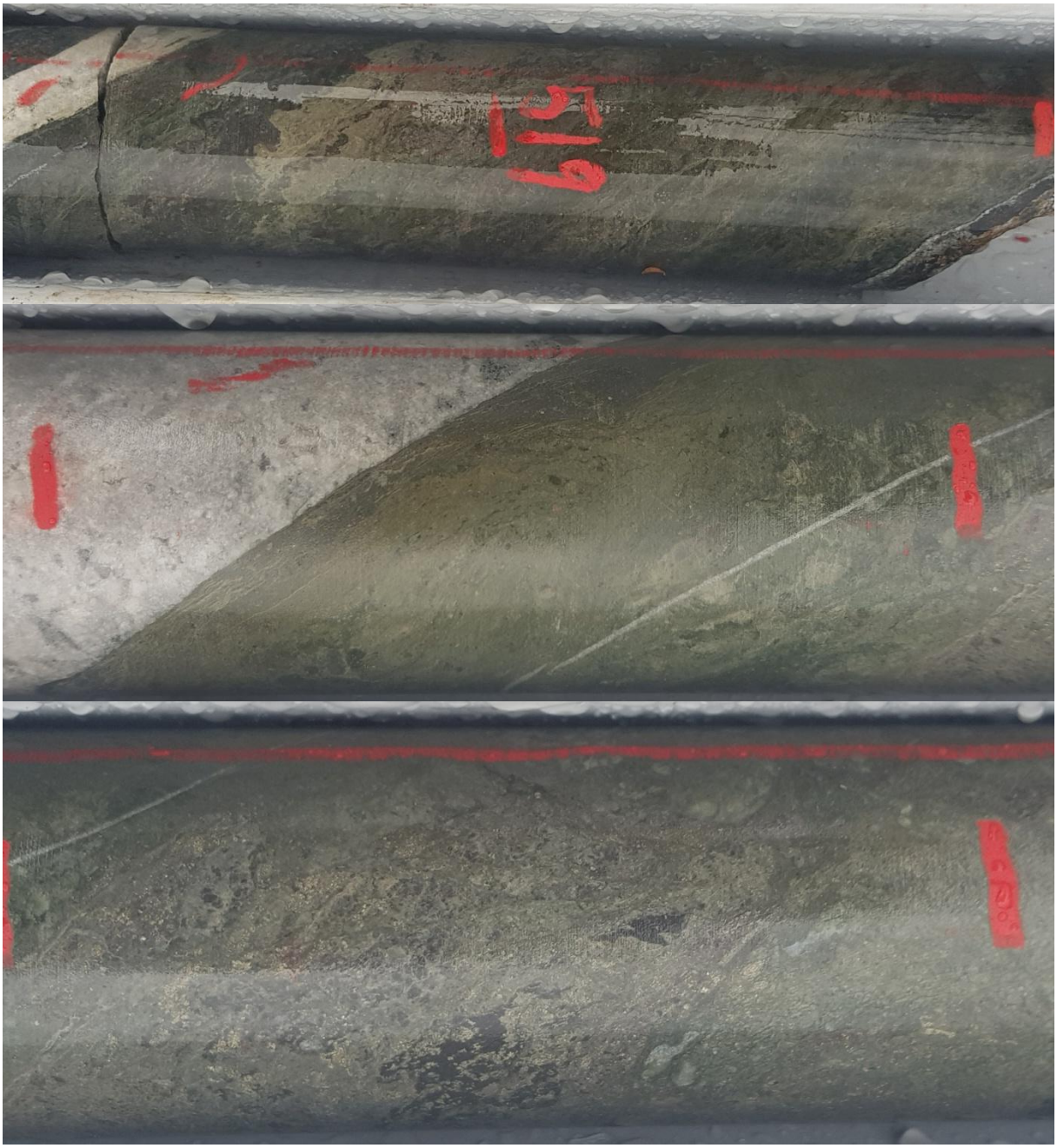

Photo 1: Top is TCDD004 upper part of inferred VHMS exhalative horizon 518.9m (left) to 519.1m (right), noting precipitate like growths in weakly banded pervasive silica-sericite. Middle is TCDD004 519.2m (left) to 519.3m (right) showing very fine grained darker sulphide band at quartz carbonate contact, marked by finely banded kaki green pervasive silica-sericite (which could include appreciable very fine grained pyrite?). Bottom is TCDD004 semi massive sulphide 519.3m (left) to 519.4m (right).

Geochemistry XRF

A portable/hand held Niton XRF, utilising standards for calibration, was used to establish qualitative/indicative presence of key metals (Co, Cu) in both drill holes and regional surface samples. Various mineralisation and alteration styles were also qualitatively assessed to identify potential element signatures. Drill core readings were taken in AllGeo mode (duration 90seconds), providing the most accurate and complete element suite. Results are presented in and EL062013_201910_09_DG_PortableXRF.xls.

XRF analysis readings were collected using a NITON XRF at 1m increments over most of drill hole TCDD004. A gap exists mid – upper hole and readings extend as 2m increments from ~350m. Scattered spot analyses were also taken from various salient alteration and mineralisation features. This included a number of Copper spot highs returning up to 13% Cu from obvious chalcopyrite bearing zones.

Some clear associations identified were:- Micromonzodiorite intrusions are readily reflected by high K. Ca distribution is generally high when K is low, whereas Ba and K highs are coincident. Cu, Ni, Co, S and Fe are a common elevated association, whilst K despite pink K-feldspar like occurrence in veins is low with these samples. Note the extent of Albitic (Na) alteration at Thomas Creek is little assessed at present. XRD analysis by Bottrill and Unwin (2019) determined that Albite was a significant component of a pink and green Amphibole vein from 226.5m in TCDD004. Weakly anomalous Sn to 140ppm is another portable XRF detected accessory of these veins.

Magnetic Susceptibility

Magnetic Susceptibility readings in SI units were collected using a magROCK magnetic susceptibility meter at 10cm increments down drill hole TCDD004 (Figure 8).

Distinct magnetic lows near 215 and 370m and 585 to 595m correspond to micromonzodiorite intrusions. Compositing magnetic susceptibility data down hole at 0.5m intervals results in a flatter profile that doesn't reflect local vein related variability as well.

A histogram of magnetic susceptibility (Figure 9) shows an apparently normal population peaking around 0.1SI, likely corresponding to primary magnetite in the andesites. Clearly anomalous values, commonly relating to magnetite bearing veins extend from ~0.25SI to ~0.7SI (Figure 8).

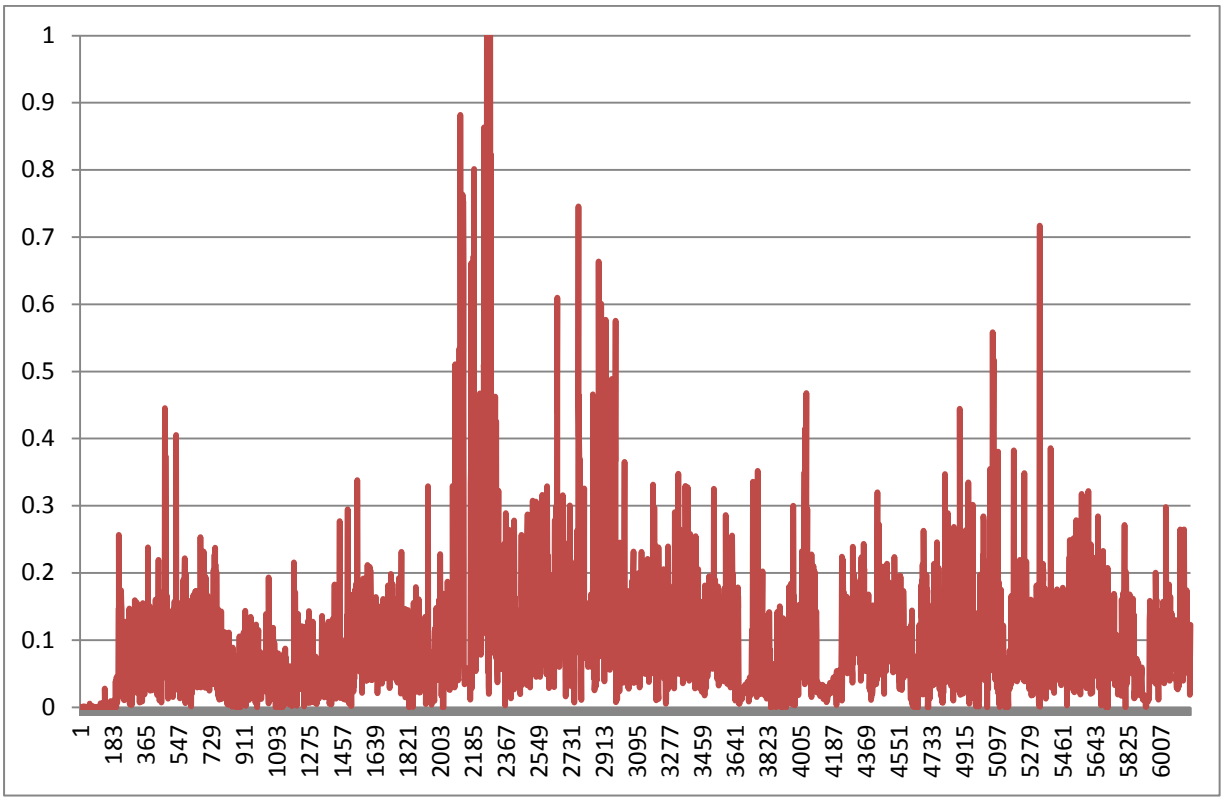

Figure 8: TCDD004 down hole magnetic susceptibility profile.

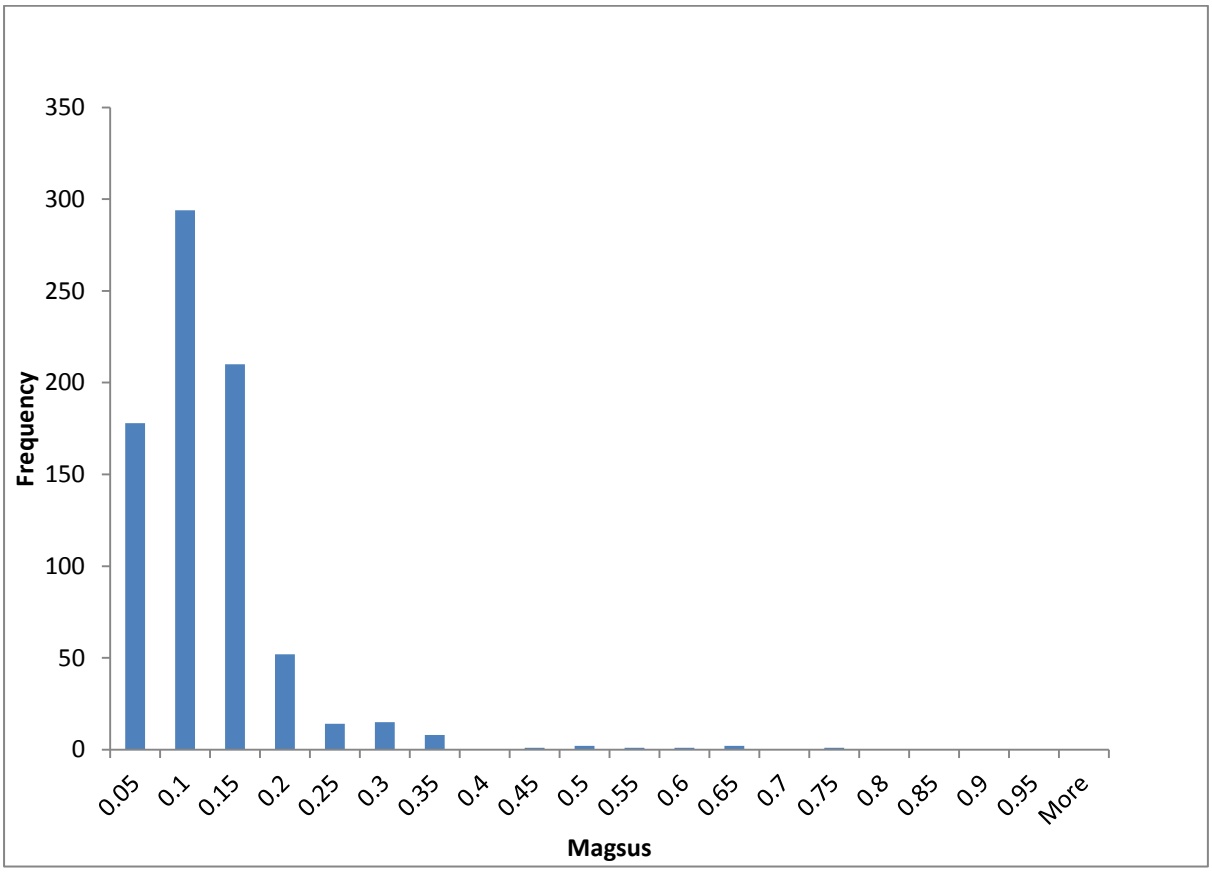

Figure 9: Magnetic Susceptibility histogram for TCDD004.

TCDD004 Structure

Orientated drill core structure measurements are reliant upon accurate down hole surveys, which in TCDD004/s case returned a number of spurious readings due to magnetite influence. Down hole surveys are fudged accordingly to reflect a relatively straight hole behaviour, as is reflected in most surveys from recent TCDD drill holes outside significant magnetic influences. Dip and Dip Direction is the common structural notation used for planes. All TCDD series drill hole structure data has been compiled to include fields reflecting common vein mineral types.

Bedding

Bedding in TCDD004 consistently dips ~30 to 315TN. Projecting the potential VHMS horizon up dip intersects a zone of key VHMS indicators Tl, Sb and Ba/Sr in soils in an as yet little known area. Zinc soils is also anomalous, whilst at very low <100ppm level in the far grids south. (Further discussion below with drill hole structure synthesis).

Laminar to thin bedded volcaniclastic siltstone and very fine grained volcaniclastic sandstone are evident from 627.5 to 629m, immediately up hole from strong pervasive K Feldspar alteration (11% K XRF). Beds are at low ~20LCA and are strongly disrupted by microfaults of <5cm throw. This likely represents soft sediment deformation, possibly indicative of a proximal Cambrian rift margin with graben located in an east to south east vector.

Faults

Table 4: Structural data from TCDD004 including faults and striated surfaces:-

dip	dip dirn	ID	depth	plunge	trend	lin pitch	displacement	Comment
44	194	15	218.25	39	160	-	-	striated chlorite on frac
47	186	18	220.93	28	126	-	-	planar smooth striated chlorite
29	162	26	236.22	29	164	-89	Reverse	planar frac wk sil mineral alignment wk ramps indicate top block to n
22	183	-	288.71	-	-	-	-	planar rough slickensided frac
45	275	-	314.85	-	-	-	-	very rough frac parallel to fault? zone
16	330	66	314.90	4	47	-13	Sinistral	slickensided with ramps top block to s. relativelly flat thrust? slicks in pgn and crm silicate.
50	20	44	288.76	50	34	-81	Reverse	undulating stepped frac weak steps top block to s

Veins

The main cluster of chalcopyrite bearing veins in TCDD004 on average dip ~-75 to 305TN. i.e the drilling azimuth is appropriate with the main strike being ~NE. Chalcopyrite veins commonly dip from 86 to 307TN to 60 to 295TN, as well as a small cluster at 67 to 337TN (Figure 10).

The common association of magnetite and chalcopyrite bearing veins is illustrated in Figure 11. Another clear association is K-Feldspar – Actinolite veining. Notably, at ~227m in TCDD004 apparent forceful actinolite vein intrusion follows fractures including Albite (identified by Bottrill and Unwin,

2019) fragments of mill rounded form, thus dating them to pre to early actinolite introduction. Many Epidote veins strike ENE.

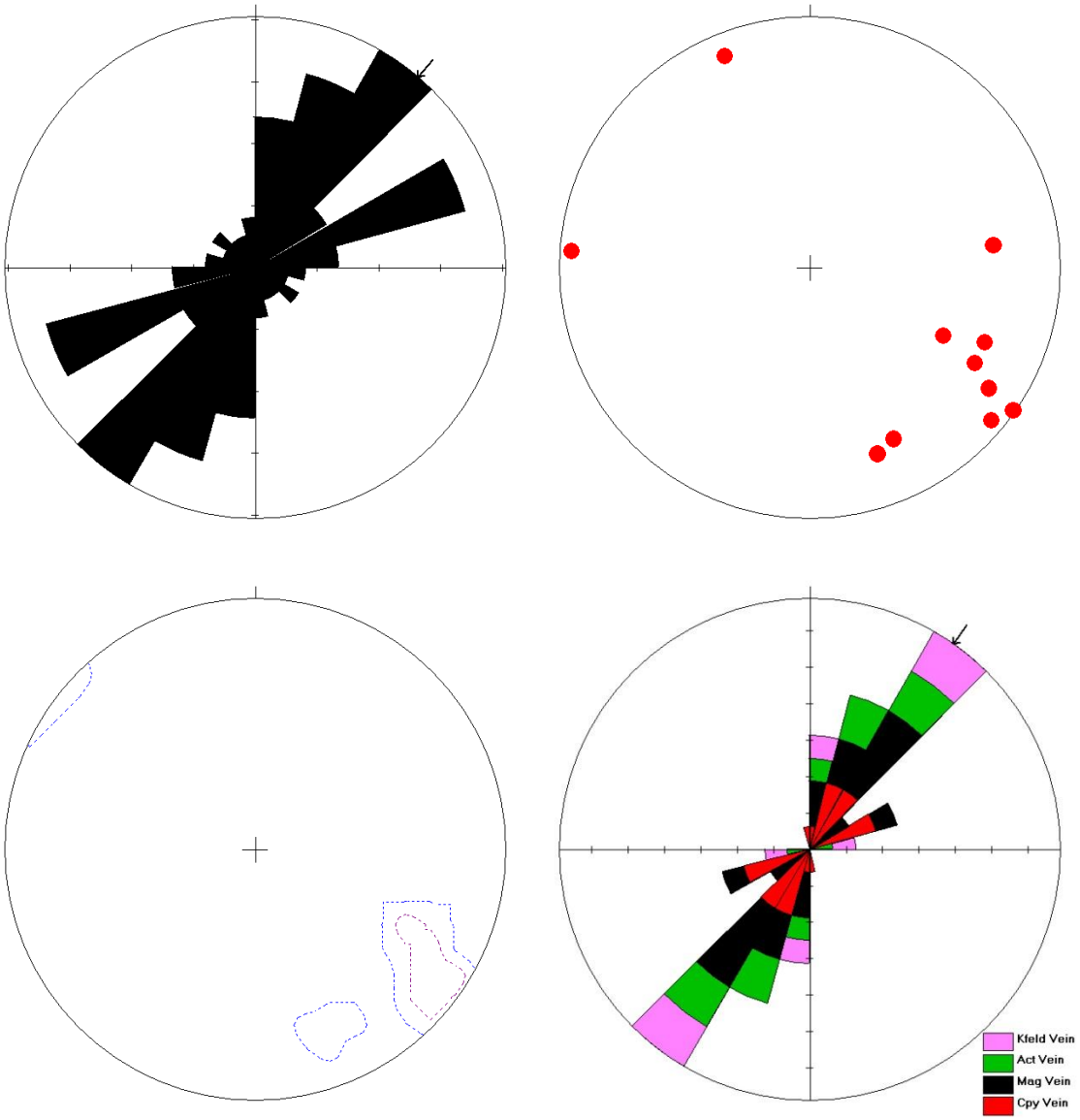

Figure 10: TCDD004 Rose Diagram All Veins (Top Left), Poles To Cpy Veins (Top Right), Cpy Vein contours (Bottom Left) and significant classified vein types ROSE (Bottom Right).

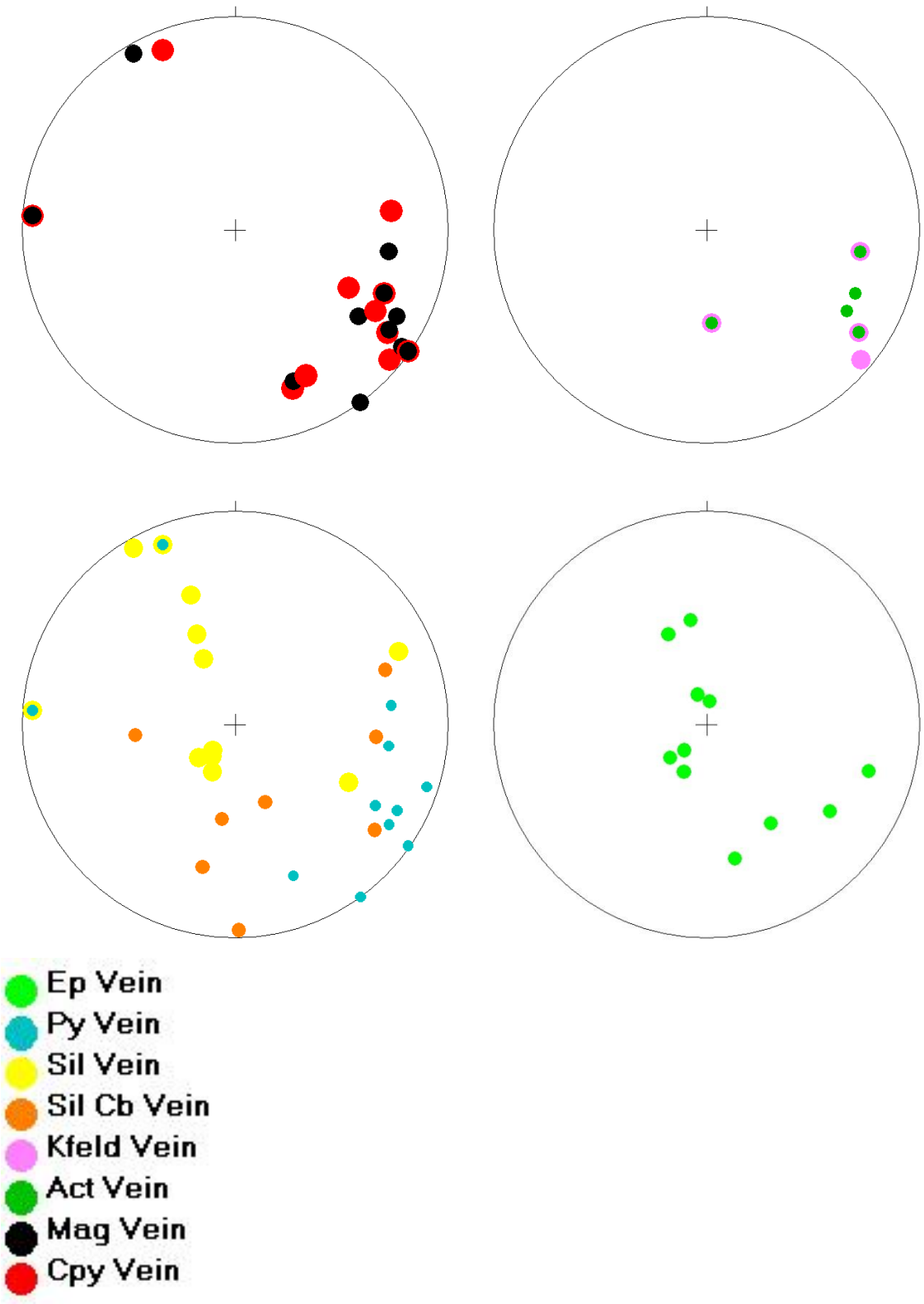

Figure 11: TCDD004 Stereographic Projection of poles to classified veins (No. 74).

Hylogger

MRT undertook Hylogger analysis of two intervals within TCDD004. These highlight zones of magnetite-actinolite-Kfeldspar chalcopyrite veining and disseminated chalcopyrite bearing micromonzodiorite intrusion with associated K-Feldspar alteration displayed in trays 56 to 62, versus a very interesting possible VHMS horizon and alteration study in trays 123 to 130. Data including photos are appended (EL062013_201910_14_TCDD004Hylogger.zip).

Surface Field Work

During 2019, 188 field surface samples were collected from the Thomas Creek (Figure 12), comprising a total of 152 soil samples, 25 rock chips and 11 bulk sample for -80# analysis (Table 5). Reconnaissance geological mapping, soil, rock and stream sediment sampling was extended near existing grid lines at Thomas Creek. Unsampled grid portions remain. No field work was undertaken at the Henrietta and Young Henry Prospects. Samples are listed with geological description and analysis in EL062013_201910_17_SG_1.xls (appended). The Sample_ID illustrates prospect, sample type and number within the sample type series. Further details include sample form, depth and a geological code classification, as per lithology lookups in EL062013_201910_05_Lithologycodes.xls. Surface sample Portable Niton XRF results are presented in EL062013_201910_18_SG_PortableXRF.xls.

Table 5: Surface Sampling totals for 2018/19; Total count 376.

Prospect	Thomas Creek	Young Henry	Henrietta	Grand Total
rock chip	36	7	4	47
comp rc	30	4	4	38
grab rc	6	3		9
soil	325	49		374
A/B horizon	2			2
B horizon	3			3
B/C horizon	11			11
C horizon	309	49		358
stream	15	6	8	29
80#	14	3	4	21
PC	1	3	4	8
Grand Total	376	62	12	450

Various GPS waypoint notes were recorded in spreadsheets. Waypoint averages were collected for significant points such as drill collars and grid intersections. These were taken over 1+ minute collection times to accurately define features. Key points such as collars had waypoint averages updated on 3 or more occasions to improve accuracy to potentially +/-2.5m. GPS recorded tracks were also used wherever possible to verify grid and feature locations.

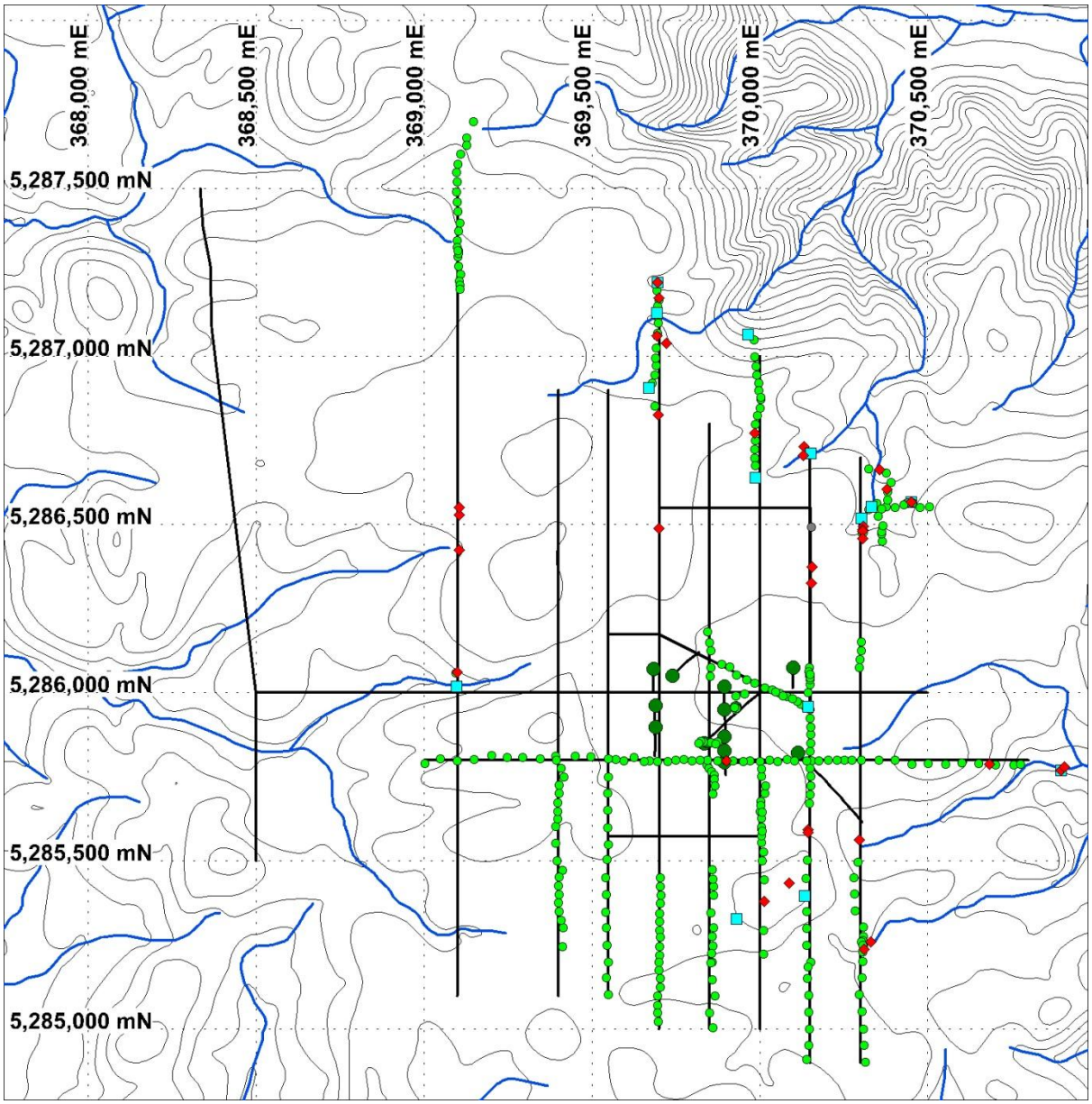

Figure 12: Surface Sample distribution 2019, Thomas Creek Grid (Drill holes green, soils green, rock red and stream sediments blue).

SUS Ground Magnetics

An Android smart phone (Rocklogger App) was utilised to conduct a SUS (**S**mart **U**se **S**martphone) ground magnetic survey. It's appreciated that whilst this is far from an accurate or precise instrument, high contrast differences in ground magnetics are readily detectable. GPS located survey readings were taken at ~2m intervals with most data in a realistic range of ~61000 to 69000nT. There was some apparent drift in response over repeated zones and levelling of lines was not undertaken. Drift in readings/base level is suspected to have occurred during survey as well. However, when lines/surveys are gridded individually clear anomalous responses that correlate well with a 1VD grid of past G856 ground magnetics are apparent.

The SUS technique proved positive with soil augering of highs returning gossanous, magnetic and chloritic sample in several instances (a potentially great aid to targeting soil sampling for magnetite).

Soil Sampling

Soil sampling was undertaken opportunistically, concurrent with drill operations at the Thomas Creek Prospect. Sampling aimed to cover existing open Sherlock and Accelerate grid lines. Soil sampling progress to date is shown in Figure 12. Note line 370000E, south of 5800N is selectively sampled at SUS magnetite highs. Historic data was added to an Access database.

C-Horizon soil samples from typically 30 to 100cm depth totalled 152, adding to last year's 173 samples and significantly extending soil sampling distribution around the prospect. The soil sampling rationale selectively covered previous un-sampled Sherlock 2014 IP grids and new Accelerate 2018 IP grids. Priorities were defined by various largely GIS interpretation driven criteria. Sample preparation and analysis was performed by ALS laboratories in Perth and Adelaide. Data are presented in EL062013_201910_17_SG_1.xls; digitally appended. Lithology codes are matched to drilling codes.

All data including Amoco, Plutonic, MHM, Sherlock and recent Accelerate data was compiled and gridded using a near search of 60m and far search of 150m, resulting in grids that still reflect gaps in the data distribution. Grids were commonly NW shaded with some having a 5 and 95% cuts applied to enhance strong features. Recent MHM, Sherlock and AX8 ICPMS soil data was gridded separately, whilst elements in common with earlier Amoco and Plutonic data sets enabled more wide reaching grids to be generated for interpretation.

Overall a number (~8) of soil samples returned Au >0.1ppm. A new Cu-Au prospective zone near Thomas Creek's northern magnetic rim was defined with TC402 to 404 returning an elevated (~0.1ppm) Au zone coincident with Cu (400 to 1400ppm, ~0.1% Cu; Figure 13, 369700mE, 5287150mN).

Rock Chip Sampling

Thomas Creek rock chip samples (No. 25 collected, 36 in total 2018/19) were typically collected as a composite comprising >6 fragments from a given area. Grab samples attempt to identify more specific sample character or stronger mineralisation and alteration. Further discussion is provided with interpretation below.

Two samples (TCR033 & 34) returned P > 10000ppm and >15% Fe, with 470ppm Cu and 134ppm Zn in the adjacent TCR032. These are strongly mineralised samples from the new Cu-Au prospective zone near Thomas Creek's northern magnetic rim mentioned in soil discussion above.

Best Au of 0.046ppm came from TCR028, an andesite breccia (Northern top waterfall) also bearing a rock chip survey high of 420ppm Cu and 137ppm Co. This sample contained significant Na at 3.85% suggesting that Albite was miss-identified as pink K feldspar-Silicate alteration. A similarly mineralised sample was returned from the southern grid area.

Gold in rock chip anomalism is generally outside K feldspar alteration influence. Interestingly, equigranular diorite bears low level background Au, commonly 0.01ppm. Diorite sampled in the west of the grid was very low in Cu.

Pb is ubiquitously absent, reaching a maximum of 22ppm. Scattered elevated magmatic elements W, Sn, Mo, U in rock chip samples are evidently coincident with best mineralised zones.

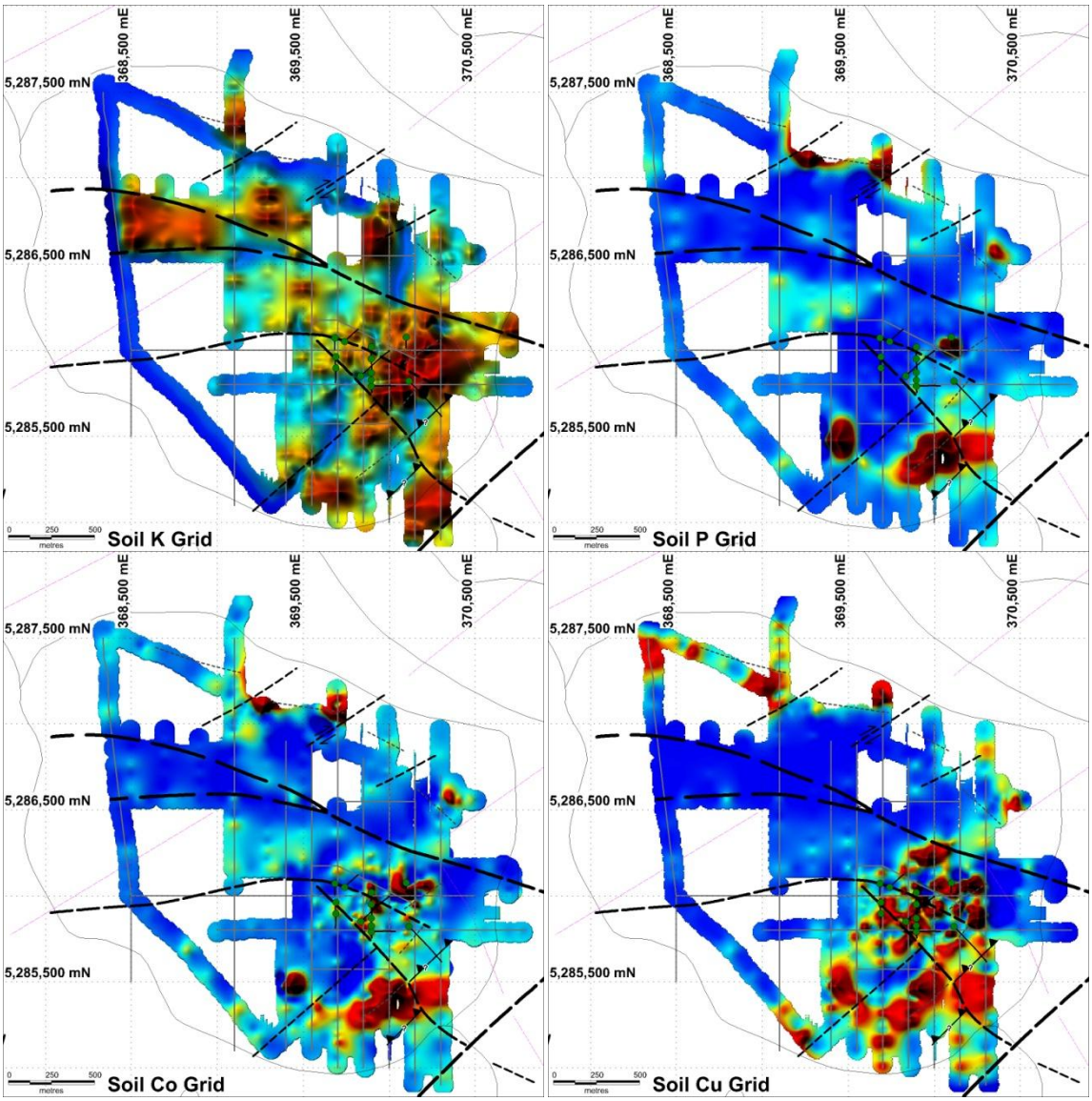

Figure 13: Soil grids for key elements K, P, Cu and Co

Stream Sediment Sampling

Thomas Creek stream sediment sampling for -80# analysis totalled 11, adding to last year's 10 samples from various prospects. A bulk approximately 1.5kg sample of active stream sediment was collected from each site for later drying and -80# sieving, prior to analysis. Panned concentrates comprise two 5 litre pan loads from the bottom of hole. No analysis has been undertaken on the panned concentrates collected this reporting year.

Appreciable Co at 60ppm drains past the water pump area ESE of Thomas Creek. Comparatively Co reached 240ppm in the Henrietta area were ultramafic rock is prevalent. Cu reached 97ppm from the top of a waterfall draining the northern magnetic rim of the Thomas Creek Prospect. Ni notably peaked at 889 and 1890ppm near the Henrietta Prospect. Zn elevated to 156ppm near the Henrietta Prospect may partly reflect input from shale dominated sediments. Pb in -80# sampling was remarkably low at <20ppm from all prospects / sites.

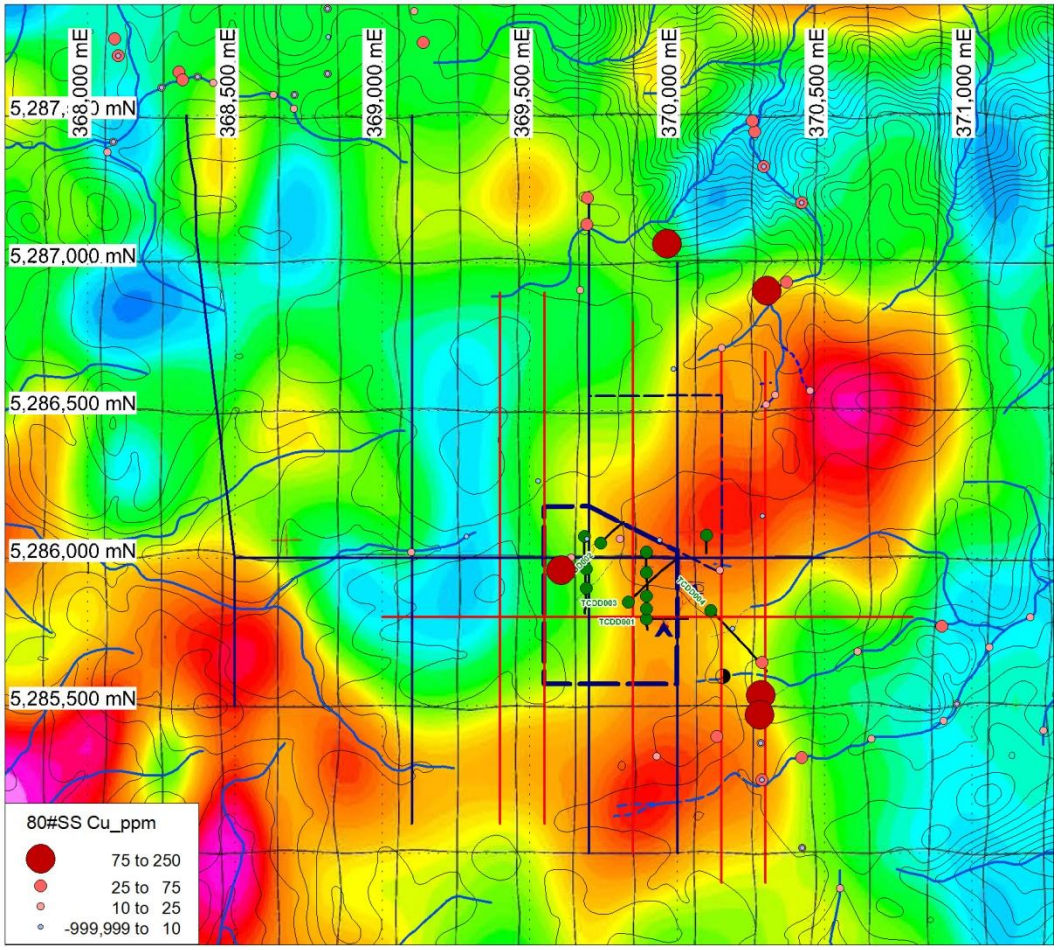

Figure 14: Thomas Creek -80# (incl. historic) sampling showing location of anomalous Cu over 224Hz MobeMT.

Geophysics

MobileMT

An airborne survey was completed during January 2019 by Expert Geophysics using its Mobile MagnetoTellurics (MobileMT) system (Photo 2), which is the latest innovation in airborne electromagnetics and the most advanced generation of airborne Audio-Frequency Magnetic Electromagnetic (AFMAG) technologies. A total of 430-line kilometres, covering ~104 km^2 were completed on 200m and 400m line spacings, in the immediate area over the ~13km^2 Thomas Creek copper-cobalt prospect and a smaller area in the southwest over the Mount Lowran prospect (Figure 15). A Data Aquisition and Processing Report from Expert Geophysics is appended (18014_AccelerateRes_report.pdf) within EL062013_201910_31_Expert_MobMtReport.zip, along with relevant survey files.

The final MobileMT data was inverted by Computational Geoscience Inc. to generate 3D results, mapping the conductivity spectrum to highlight absolute and relative discrete resistive and conductive anomalies. 3D inversion grids for various depth slices and sections, 3D dxf isosurfaces and a Voxel Model are included in EL062013_201910_32_CG_MobMT_3Dinv.zip and EL062013_201910_33_MobMt_model_final.zip appended).

Southern Geoscience Consultants (SGC) were used for additional geophysical data processing and preliminary interpretation (see EL062013_201910_34_SGC_MobMTprelimresults.docx and MapInfo files in EL062013_201910_35_SGC_MobMTpreltargets.zip appended). SGC further investigated the MobileMT inversion data extracting 3D DXF isosurfaces for the high resistivity end of the spectrum, aiming to identify strongest potentially alteration related resistors. These are included in the appended data (EL062013_201910_36 SGC_3DINVdxfmodels.zip) as the _0003 and _0005 surfaces (0.3mS/m and 0.5mS/m respectively).

The results of the MobileMT survey have enhanced the geological understanding of the Mount Read project and will enable targeting of further ground-based exploration and vectoring towards potential mineralisation. Further interpretation is provided in exploration planning discussion to follow. Geophysical consultant Russell Mortimer's comments and Expert Geophysics digital data are appended.

Photo 2: Mobile MagnetoTellurics system at the BHP Landing, Birches Inlet.

Key outcomes of 3D inversion of the survey data in the Thomas Creek area include defining a moderate relative conductor in the NE, a core highly resistive zone and a strong resistor near the Owen Group margin. The survey also confirmed a conductive zone associated with the initial Thomas Creek IP Chargeability and geochemical target area, where drilling by the Company (TCDD001-003) has intersected anomalous copper and cobalt mineralisation associated with semi-massive sulphide veins and broad zones of disseminated pyrite and chalcopyrite (Figure 16).

The newly discovered conductive anomaly in the north eastern part of Thomas Creek, is located on the eastern flank of the Thomas Creek magnetic complex, north of a major east-southeast striking regional fault, which separates the target area from the previously identified Thomas Creek mineralisation (Figure 16).

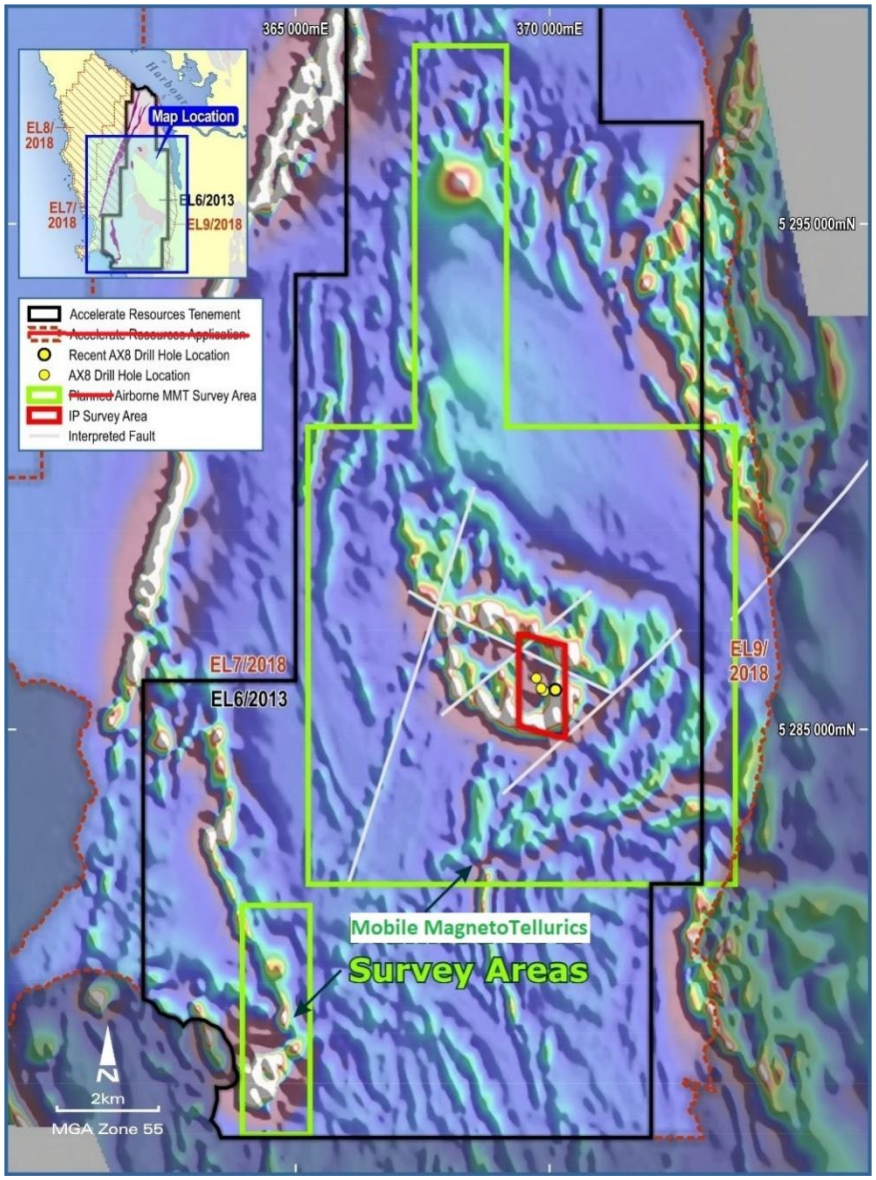

Figure 15: Mobile MagnetoTellurics Survey Areas on 1VD RTP Aeromagnetic Imagery

Field mapping undertaken by Accelerate during late 2018, discovered a 20m wide zone bearing gossanous subcrop associated with silica-magnetite altered diorite, proximal to the western side of the relatively shallow (>400m depth) conductive anomaly. The identification of gossanous material in association with the structural setting of the north eastern conductive anomaly and the correlation between MobileMT conductance and the previously identified copper-cobalt mineralisation at Thomas Creek, highlights the potential for the new anomaly to represent sulphide mineralisation.

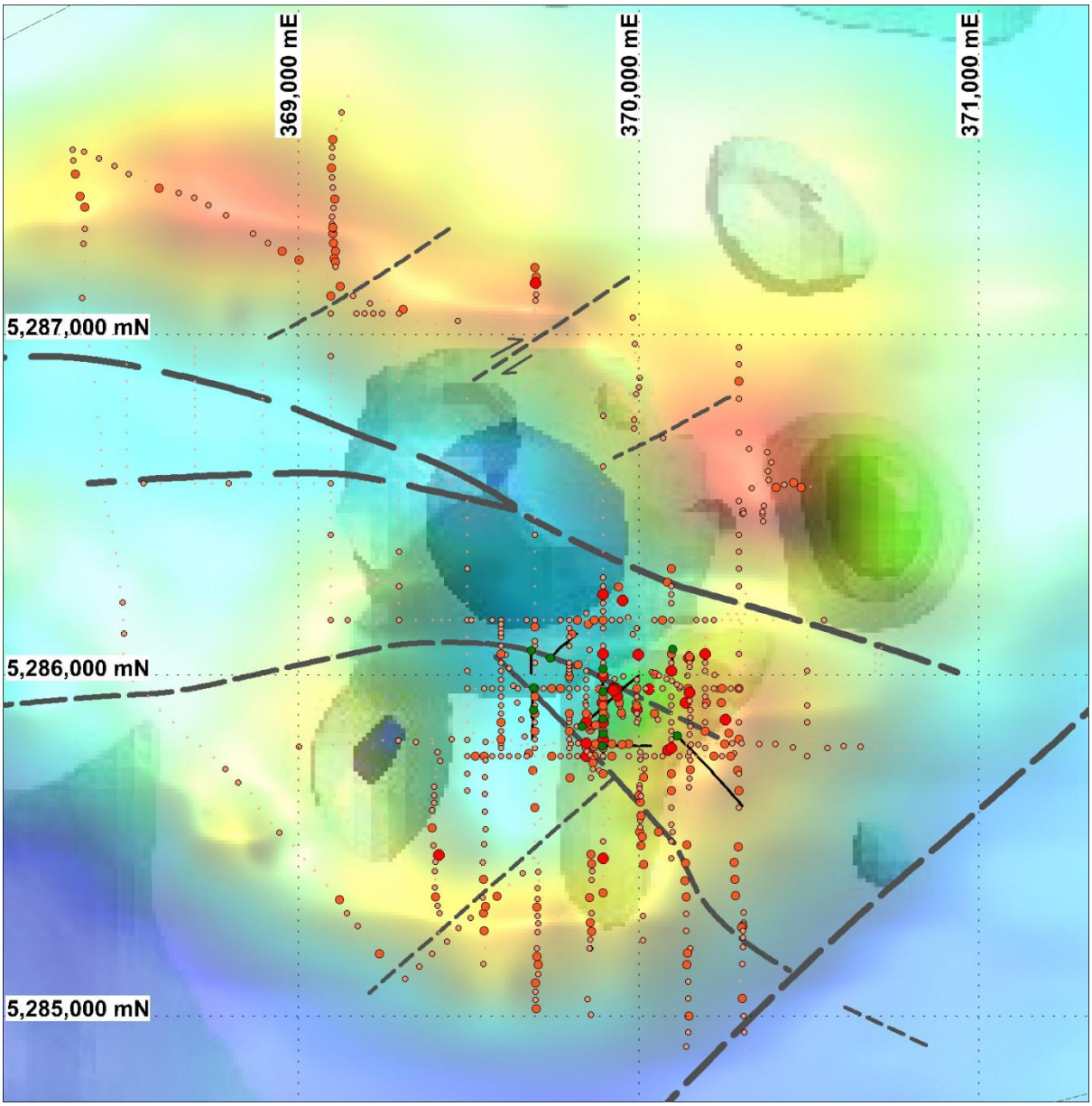

Figure 16: Prospective MobileMT anomalies identified in the Thomas Creek Prospect area (blue = resistivity & green = conductivity), overlain by aeromagnetics grid transparency highlighting anomalous magnetic highs (red), as well as structural interpretation and Copper in soil geochemistry thematic.

The 3D conductivity results also identified a number of high resistivity (very low conductivity) anomalies, including one in the central part of the Thomas Creek magnetic complex (Figure 16). Analysis and interpretation of soil geochemistry in conjunction with mapping, indicates that this resistive body possibly represents a silica-magnetite altered diorite intrusive core to the Thomas Creek complex.

Preliminary evaluation of the 3D inversion results, from the larger survey area have also identified a number of other potential target zones including a discrete conductive anomaly on the northern side

of the Timbertop magnetic high and another broader anomaly at Mount Lowran in the south of the project area. (Figure 15)

Discussion of Results

Much of the following discussion results from a compilation and re-interpretation of collated historic and new data. Notably little comment was made on surface samples in last year's 2018 annual report and is included herein.

Geology

The geology of the Thomas Creek Prospect is as yet poorly defined. Further historic data collection from Plutonic particularly soil sample logging) and MHM is required to complete the currently known geology. New traverses based upon both soil and rock chip sampling have loosely defined a significant extent of intrusive medium to coarse grained equigranular diorite in the western and central areas of the grid (Figure 17 & 18). Further diorite is evident in the far grid north and east.

Recent work has weakly defined micromonzodiorite intrusion distribution with SW strike at the Thomas Creek Prospect. Drill hole interpretation and structure indicate moderate NW dip to multiple dykes. The soil logging based geology of Close and Reid (1995) defined largely SW aligned micromonzodiorite intrusions in the immediate Thomas Creek Prospect vicinity, with a broad WNW zone identified in the NW. The micromonzodiorite trend defined by low Ti/Zr in the NW is apparently enclosed by inferred faults, extending NW from Thomas Creek, with elevated K and Ba in soils confirming likely rock composition. Andesites including phenocryst crowded varieties are evident throughout, with breccia notably identified near the northern magnetic margin. The Denison Group – NCV contact north of Thomas Creek is likely NE dipping, following the Timbertops synclinal fold.

Ti/Zr is a commonly used to reflect volcanic compositions and when applied at Thomas Creek delineates some key volcanic compositions (Figure 19). Histogram analysis of Ti/Zr ratio (Figure 20) from drill core analysis shows a weakly bimodal population indicative of Dacite (10-20) and more common andesitic volcanic (20 to 60). Gridded soil Ti/Zr shows that rock of rhyolite/dacite composition forms an E-W belt in the NW; previously soil mapped as medium grained microdiorite. Interestingly there's a general NE alignment of dacite Ti/Zr (12 to 20) in soils in the SE, whilst the preferred orientation is more WNW in northern portions of the grid (Figure 19). These trends in part define volcanic lithology (mostly NE trends) as well as micromonzodiorite distribution, ranging from 14 to 26 Ti/Zr (Figure 21). Further geochemical analysis including Ti/Zr with respect to lithology is likely to significantly improve geological mapping from soils.

Whilst volcanic composition is reflected by Ti/Zr, the effects of mobility of "immobile" elements Ti and Zr should also be considered as Ti (& P) is demonstrated to be mobile under high temperature pervasive K-feldspar alteration at Thomas Creek (Reid, 2001). Potential Ti mobility may be reflected in Ti/Zr ratio, with low values possibly being indicative of hotter alteration. Low Ti/Zr zones are evident in the Thomas Creek altered core zone and over the NW microdiorite (NB: high Zr, K & Ba internally, high mobilised? Mg & Ca at margins). High Ti/Zr zones possibly in part reflect hydrothermal Ti enrichment. Supporting is a spatial correlation between very high (>60) Ti/Zr and High P+Cu+Co zones.

Broad characters of the geology fit with a diorite intrusive complex beneath extrusive andesites (likely at a volcanic centre). Considering a Mt Lyell-like mineralisation model, the extensive resistive ground (MobileMT) to the SE of Thomas Creek could include silicification marginal to the andesitic intrusive complex. Ill constrained interpretation suggests possibility of a synclinal basin fold to the SE with a SE plunging anticlinal fold more proximal to the SE of Thomas Creek.

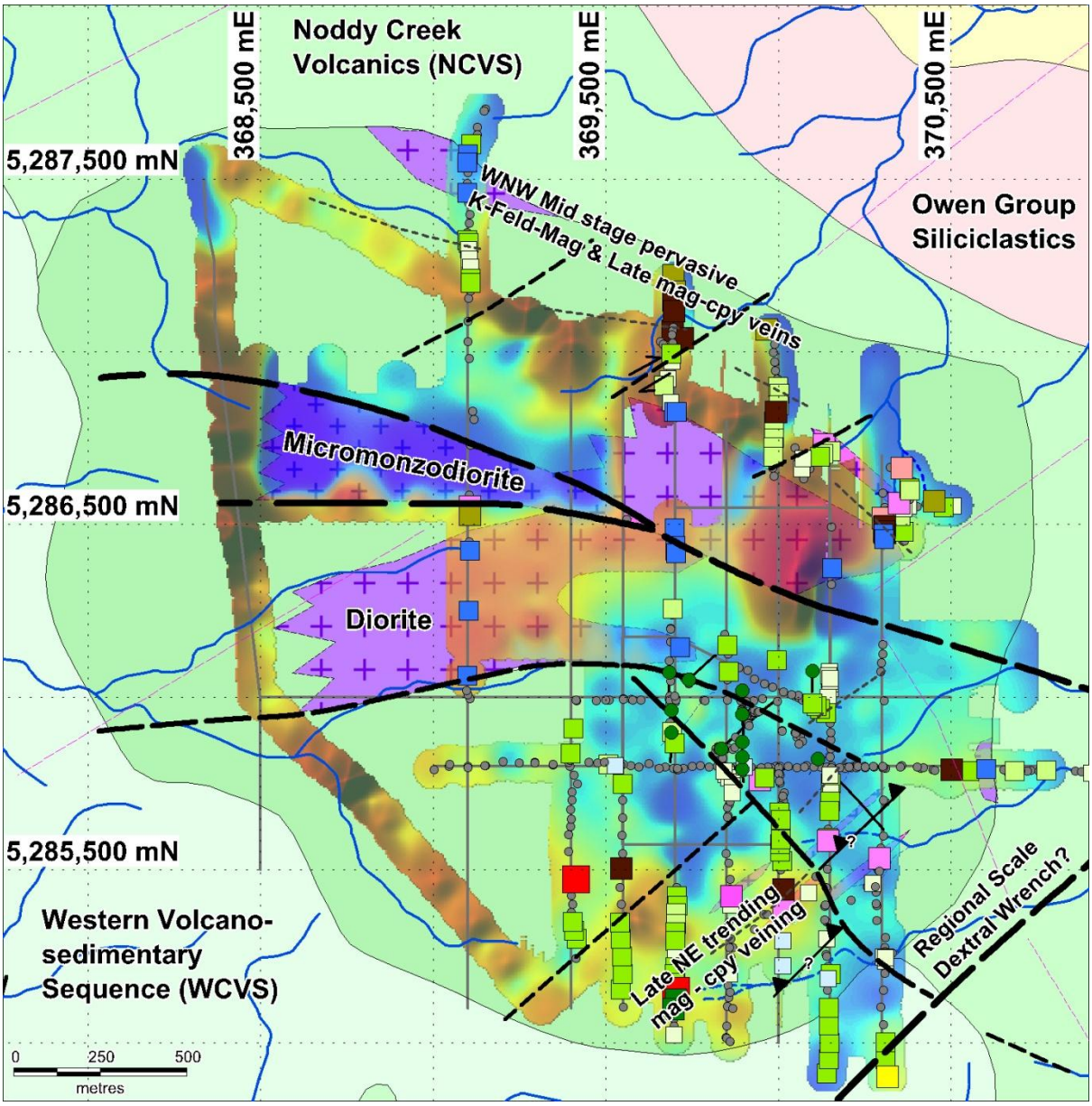

Figure 17: Thomas Creek Grid surface geological logging displaying the main rock type sites; being SMS Py = red square, magnetite/gossan = brown, chlorite = green, KFeld = pink, diorite = blue, andesite = green +breccia = dark green (drill holes green and 2018/19 soil sample circles), over Ti/Zr grid transparency and 1:250k digital geology (source MRT).

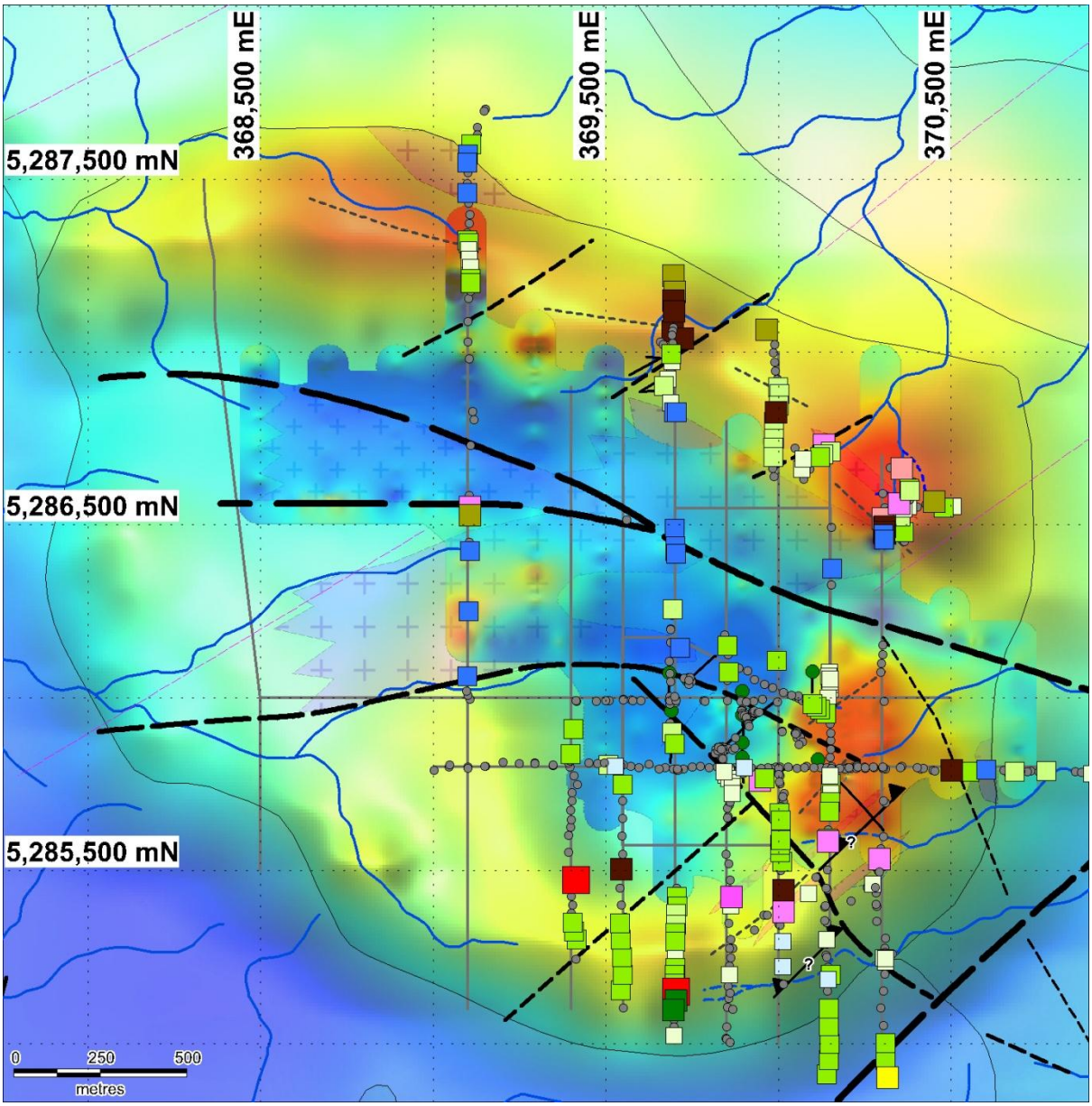

Figure 18: Thomas Creek Grid surface geological logging displaying the main rock types; being SMS Py = red, magnetite/gossan = brown, chlorite = green, KFeld = pink, diorite = blue, andesite = green +breccia = dark green (drill holes green and 2018/19 soil sample circles), over TMI ground magnetic grid, Aeromagnetics TMI transparency and 1:250k digital geology (source MRT).

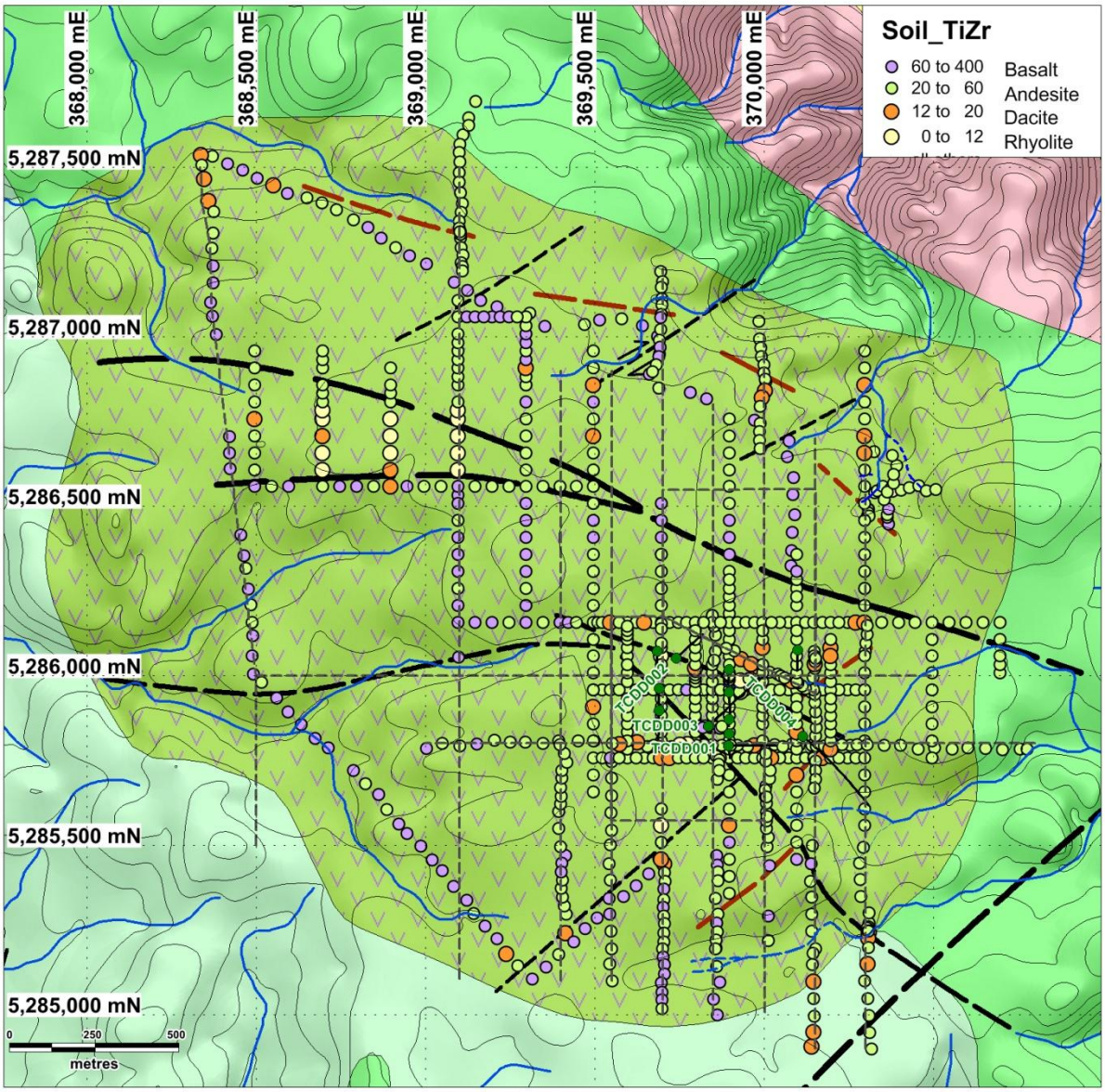

Figure 19: Ti/Zr in soils over 1:250k (MRT) digital geology.

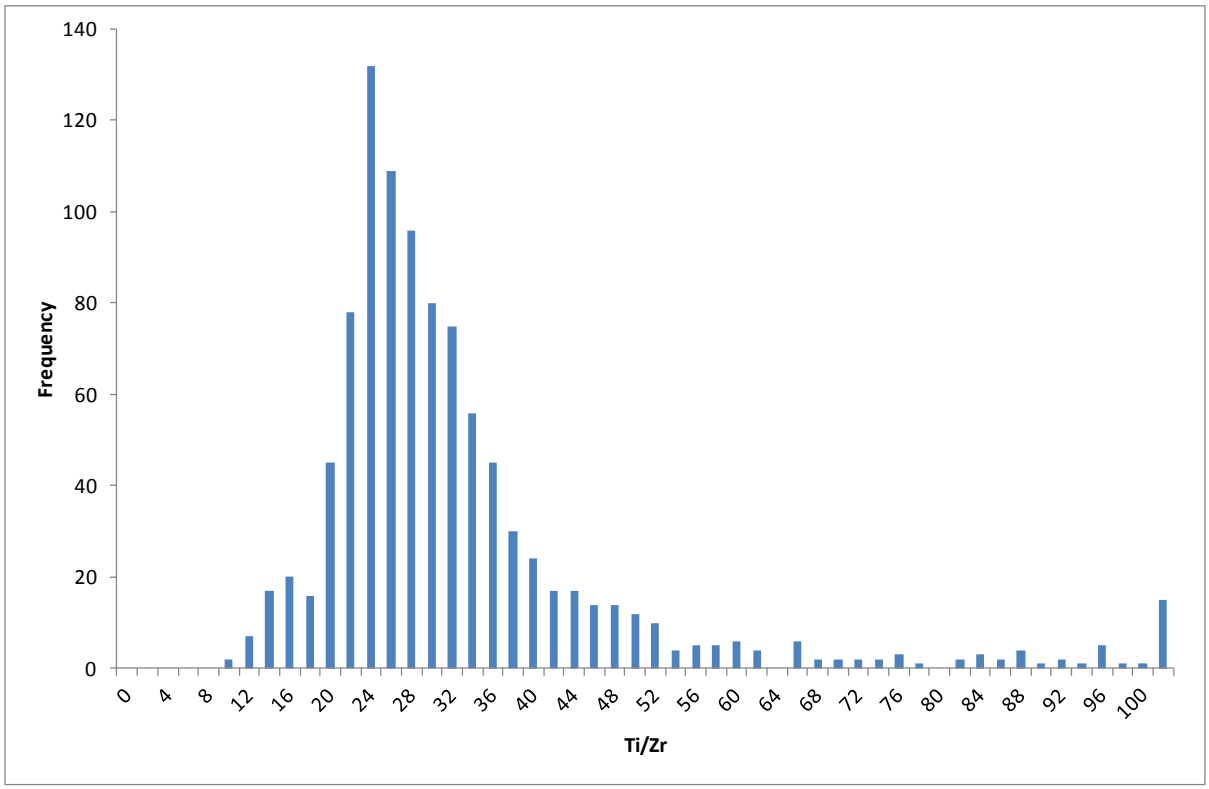

Figure 20: Ti/Zr frequency histogram for all Thomas Creek drill hole analysis

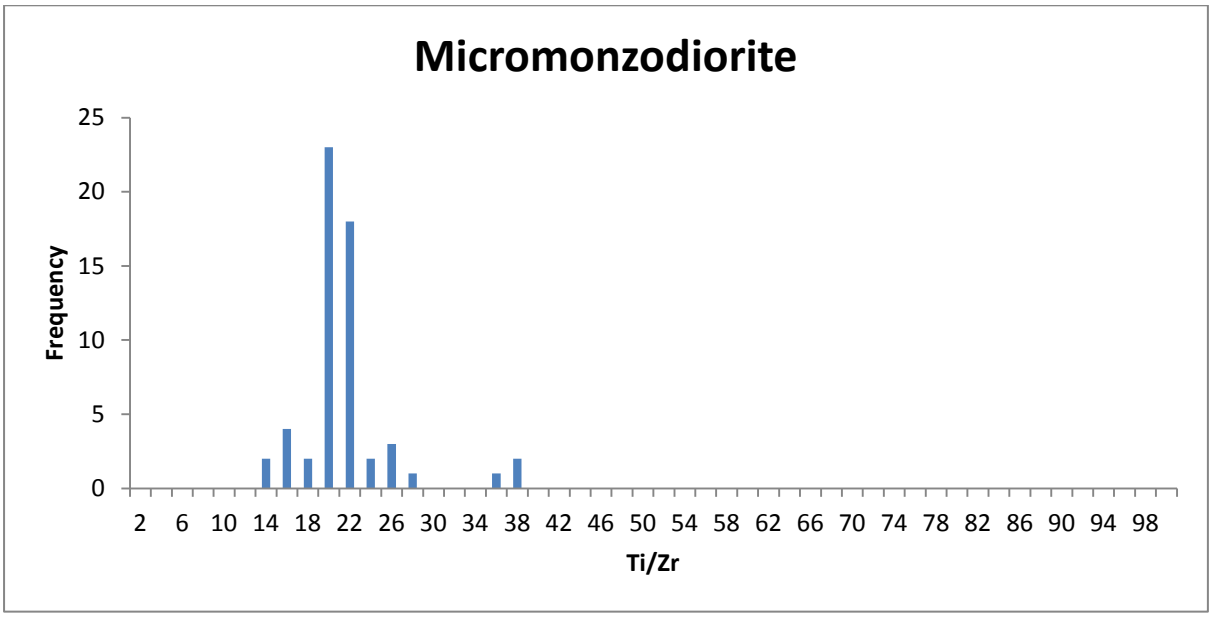

Figure 21: Ti/Zr frequency histogram for micromonzodiorite in Thomas Creek drill hole analysis

Structure

Thomas Creek Drill Hole Structure

Two principal SW and NW vein strikes are identified at Thomas Creek. Mineralised veins more commonly strike NE in TCDD001 and 4 in the south, with NW orientations more prevalent in TCDD002 to the north, but all holes reflect both orientations to a variable extent (Figure 22). i.e. N and S structural domains are defined with significant interplay in the more strongly brittle faulted zone between TCDD001 and 3. Comparison of Rose diagrams for classified vein type strike highlights some spatial vein associations:-

- No Tourmaline in TCDD004
- Possibly Pyrophyllite noted in TCDD002 & 4 only
- Intersection lineation -45 to 245TN of mineralised veins has ore shoot exploration potential
- Magnetite veining is more common to the south

Chalcopyrite and slightly more scattered pyrite vein orientations are broadly similar, with dominant ENE to NE strike (Figure 23). Chalcopyrite veins also commonly strike NW; this being prevalent in TCDD002. An exception is an additional cluster of pyrite veins with WNW strike, dipping around -45dip to 180TN. Both chalcopyrite and pyrite coincide with tourmaline vein distribution, as does pyrophyllite(?) which from a small sample size(10) plots on a Rose diagram with similar strike, but the main population is actually relatively flat lying, dipping -10 to 155TN and similarly to 35TN, suggesting a relationship to thrust fault planes. A small population of pyrite and tourmaline veins similarly dip, whilst chalcopyrite is rare on low dip veins. Importantly, late stage vein minerals including chlorite, K Feldspar, magnetite, hematite, sericite and epidote are all minerals evident on flat lying fractures, with apparent planes being -20 to 40TN and ~-15 to 165TN. This implies veining was syn to post reverse faulting and thrusting and late stage micromonzodiorite intrusion. Fault orientations are comparatively similar to micromonzodiorite and chalcopyrite bearing veins.

A potential mineralisation ore shoot plunge to model and consider for drill orientation is the intersection lineation for primary chalcopyrite vein sets (Table 6). The main SW and NW striking chalcopyrite vein orientations have an intersection lineation plunge of -43 to 254TN, whilst the NW and SW2 vein set (common in TCDD004) intersection is similarly -47 to 235TN (Figure 25). Consideration of features on this orientation during modelling would be worthwhile.

Stereographic projection of the various veins reveals the dominant orientations (Figure 23). Figure 24 illustrates the scatter in TCDD001 and 3 mineralised vein type orientations, inferred as fault proximal, relative to more consistent moderate SW and mod/steep NW dips in TCDD002, whilst TCDD004 dips are consistently NW and NE dipping.

Chlorite, K-Feldspar, magnetite, sericite, epidote are all minerals evident on flat lying (as well as other) fractures. This implies veining was syn to post reverse faulting and thrusting and the late stage micromonzodiorite intrusion. Noting that the micromonzodiorites are in large part un fractured and highly coherent compared to surrounding host rock.

Table 6: Significant/common orientations for chalcopyrite bearing veins.

Vein Type Orientations	dip	dip direction TN	strike TN
cpy veins main SW strike	63	315	225
cpy veins main SW2 strike	85	320	230
cpy veins main NW TCDD002 strike	47	225	315
cpy veins minor ENE strike	35	15	135
cpy veins minor TCDD004	65	345	255
cpy veins minor TCDD002	50	185	275
pyrite veins	55	290	200
Thrust? related Vein types	20	40	130
Thrust? related Vein types2	15	165	75

Overall orientations for intrusives, bedding and volcanic facies are sparse. A summary plot of all key structural aspects in Figure 25 illustrates the main strongest geological and structural features defined from stereographic analysis of Thomas Creek drill hole data.

Bedding (No = 4) in volcaniclastic sandstones from TCDD004 consistently dip -30 to 315TN. These more distally derived volcaniclastics likely reflect the surrounding regions seafloor with inferred volcaniclastic source derived from predominantly east, to south east. The potential exhalative horizon's lower contact dipping -75 to 285TN in TCDD004 (Figure 25) possibly mimics local volcanic facies dip. Andesite and related breccia contacts variably dip -30 (TCDD004) to -80 (TCDD002), mostly to the south and southwest. Other examples include, an intrusive chilled margin contact of -55 to 220TN (TCDD001), being similar dip direction to a -76 to 223TN andesite contact in TCDD002. Whilst andesite volcanic contacts could be expected to be highly variable, the differences could be weakly interpreted as steeper andesitic volcanic centre proximal flanks in the prospects north, grading to shallower distal volcanic slopes to the south, with distal turbiditic influence.

Most micromonzodiorites (No=3) dip approximately -70 to 325TN / SW strike (~-70 to 315TN TCDD004). This orientation is similar to that of NW dipping chalcopyrite / mineralised veining (Figure 25). Some recorded fault orientations are also of similar strike to principal chalcopyrite veins and the micromonzodiorite intrusions (including -47 to 336TN), however their shallow to moderate dips are less steep.

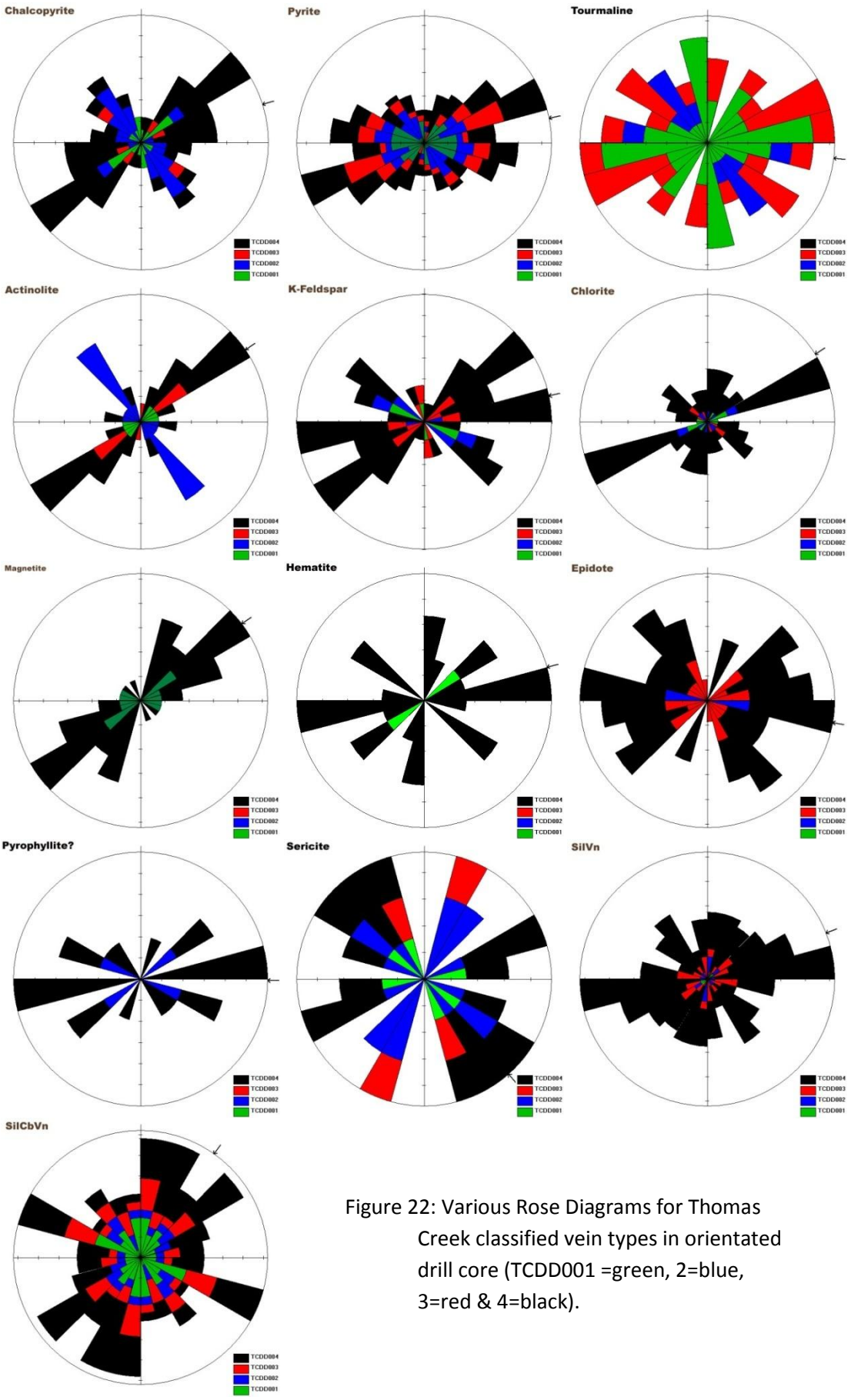

Figure 22: Various Rose Diagrams for Thomas Creek classified vein types in orientated drill core (TCDD001 =green, 2=blue, 3=red & 4=black).

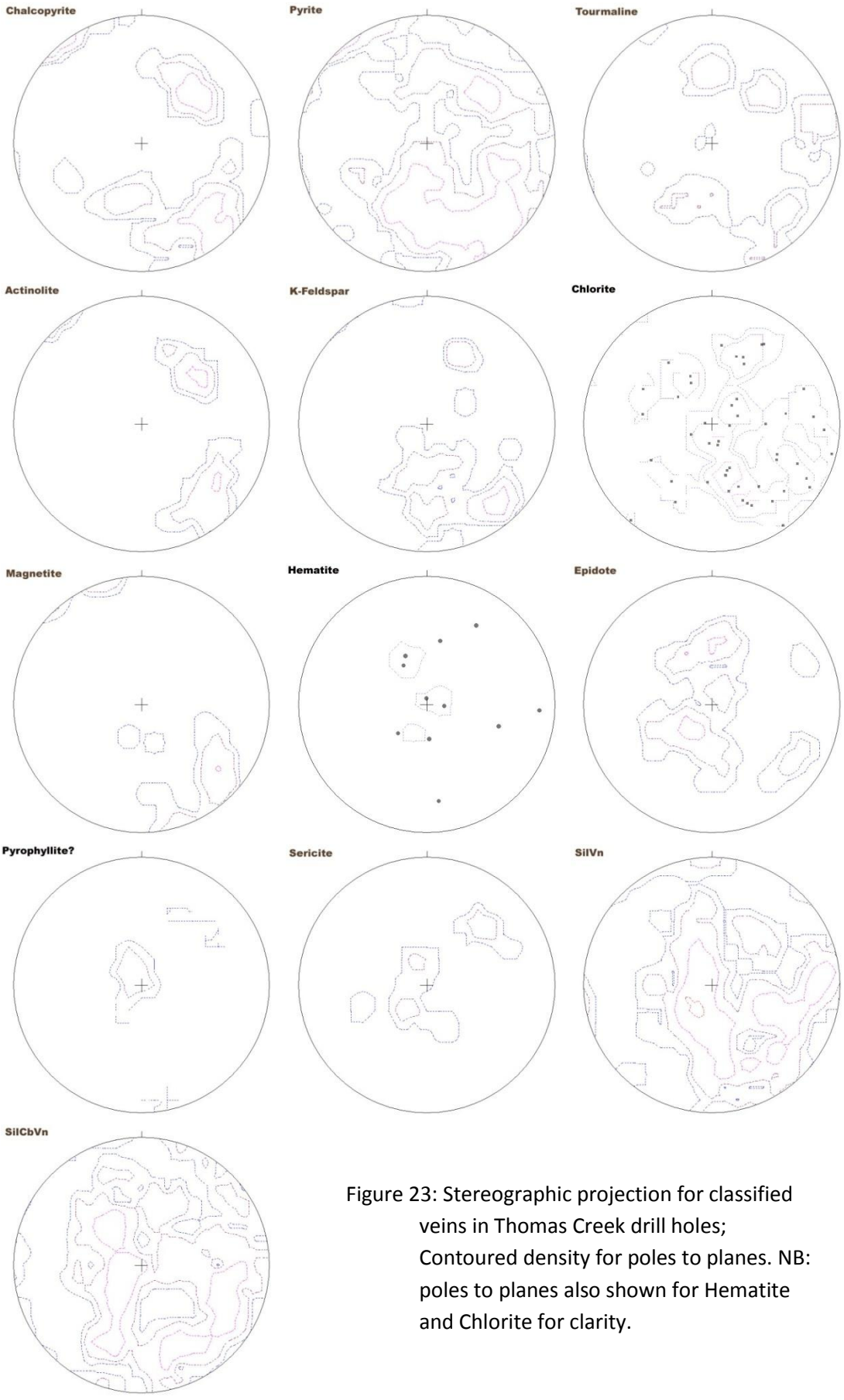

Figure 23: Stereographic projection for classified veins in Thomas Creek drill holes; Contoured density for poles to planes. NB: poles to planes also shown for Hematite and Chlorite for clarity.

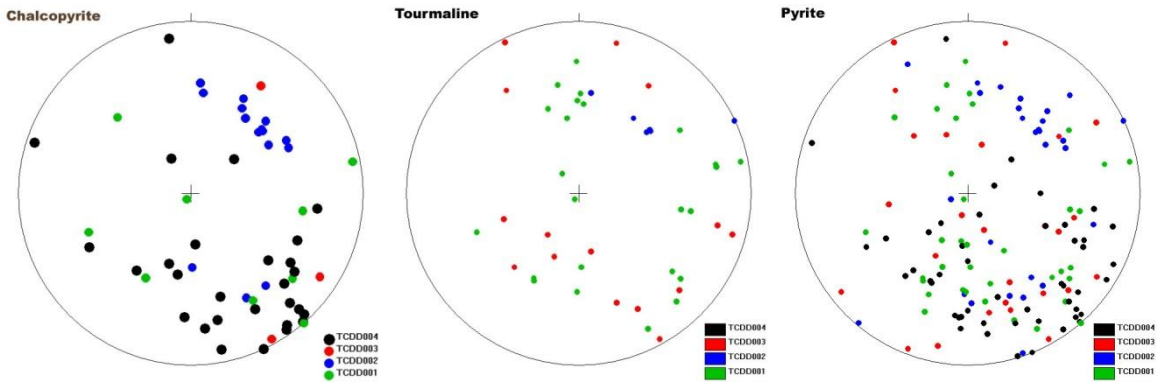

Figure 24: Stereographic projection for classified veins in Thomas Creek drill holes; Contoured poles to planes Cpy (clockwise from top Left) & Py density, Poles to planes by drill hole and Rose diagram.

Three principal fault orientations, -16 to 340TN (including 3 faults from disparate drill holes; the Thomas Creek Thrust), -45 to 340TN and -62 to 215TN are defined from analysis of poles to faults and contoured poles to slickensided planes (Figure 25). Another flat fault dips -30 to 80TN, both in concert with potential thrust fault observations from flatter lying vein sets. (Figure 25)

Fault orientations are confirmed with comparison of poles to lineations on slickensided planes, shown in Figure 25. Numerous recordings from TCDD004 cloud the stereonet, but a density plot compared to patterns from other drill holes finds mostly shallow to moderate plunges with principal lineation plunges of -20 to 300TN, -30 to 265TN, -45 to 215TN, -40 to 180TN and -5 to 55TN. These lineations when further resolved with movement sense indicators highlight a number of different movements on the various slickensided planes (Figure 26). Movement indicators for the -16 to 340TN thrust are all reverse. The steeper -45 to 340TN fault orientation may have had both normal and reverse movement. The -62 to 215TN is a clear fault orientation defined largely by TCDD003 slickenside lineation data and in common with an observed dextral fault in TCDD002 (Figure 25). The orientation of the significant fault to the north of TCDD002, bisecting the Thomas Creek Intrusive complex, possibly mimics this fault. Both reverse and normal sense movements are possible (Figure 26). A further weakly defined NE (-50 to 50TN) dipping fault orientation of reverse movement could be inferred from the lineation data.

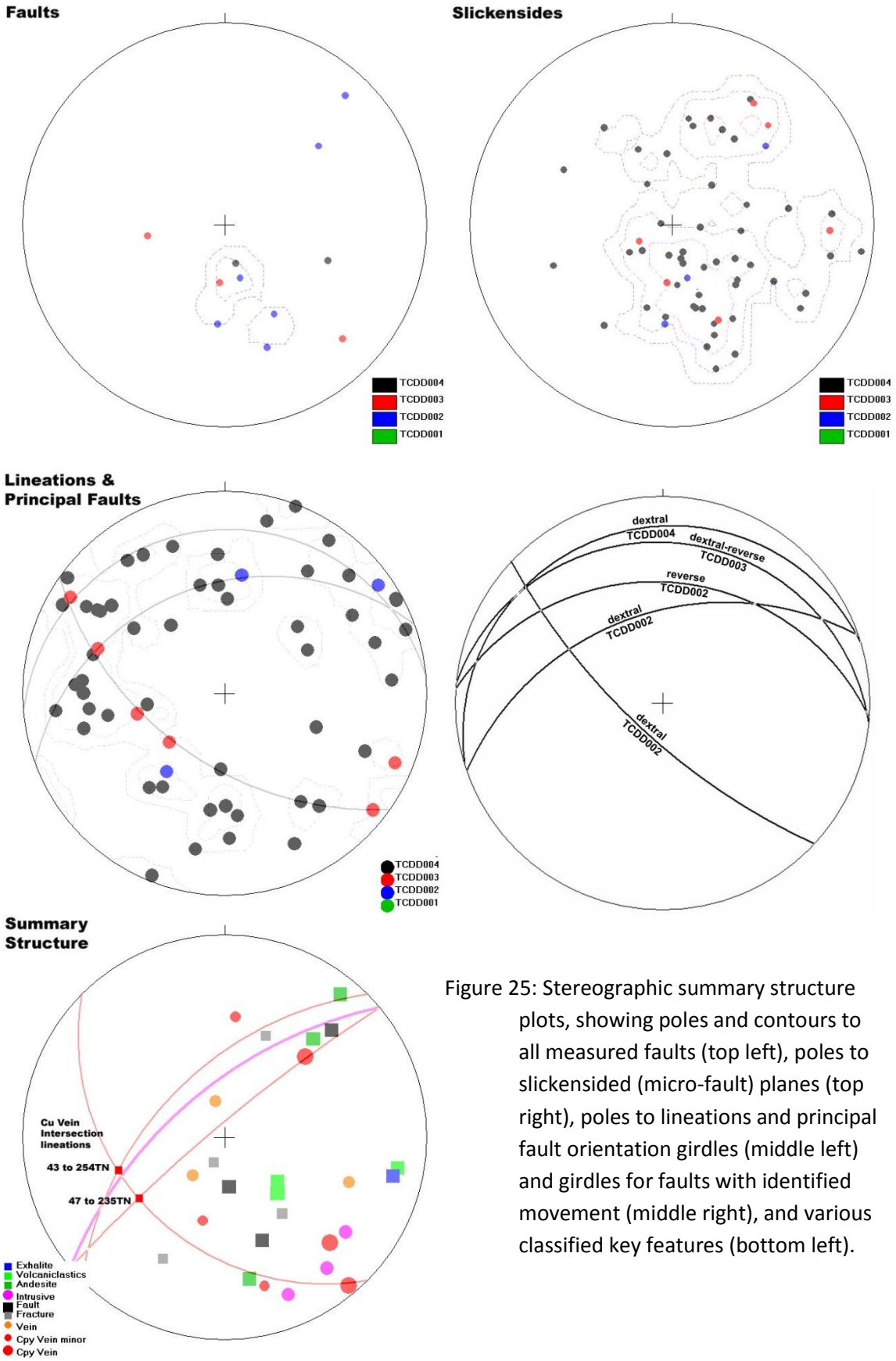

Figure 25: Stereographic summary structure plots, showing poles and contours to all measured faults (top left), poles to slickensided (micro-fault) planes (top right), poles to lineations and principal fault orientation girdles (middle left) and girdles for faults with identified movement (middle right), and various classified key features (bottom left).

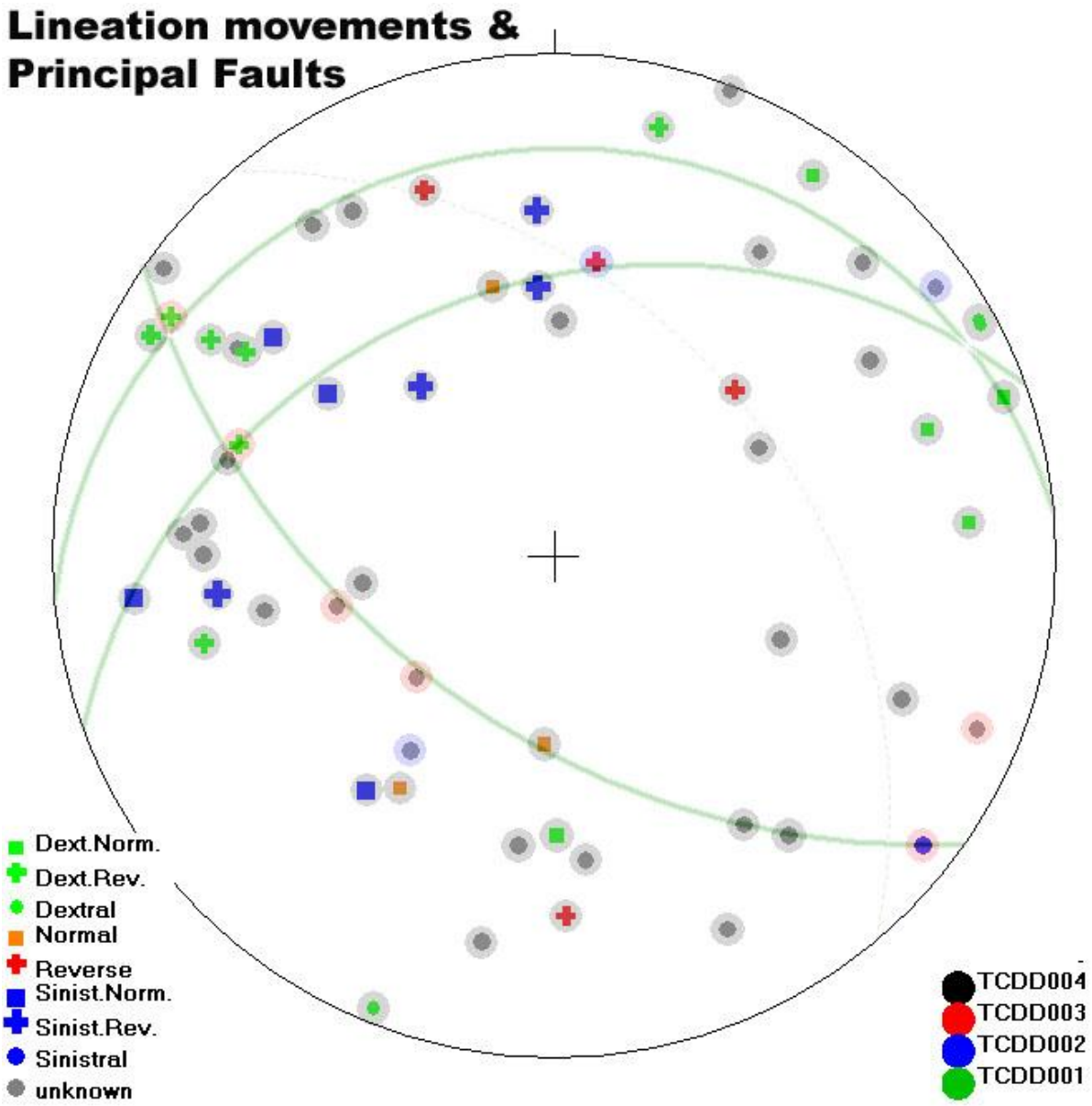

Figure 26: Principal movements on slickenside lineations classified by drill hole. NB: No TCDD001 results.

Discussion

In a regional context, Thomas Creek possibly lies near the interface between the southern end of the Dundas Trough and the more deformed Cambrian terrains to the south. The west coast Dundas Trough is thought to be a south propagating extensional tear forming a graben with the eastern margin under N-S principal stress, forming SW and hypothetically NE directed thrusting either side of the Tyennan Block at the core of Tasmania. Berry (2014) notes E-W trending folds of probable Middle Cambrian age are prevalent to the east of the Dundas Trough, although equivalents are absent in the trough. For example, on Tasmania's south coast are folds overturned to the northeast with major NE striking shear zones. Similar folding at Adamsfield pre-dates Late Cambrian. Folds of NNW to N upright trend near Port Davey are another Cambrian fold event. Whilst, in northern

Tasmania, similar E-W folds have been attributed to major SW directed thrusting during the late Cambrian.

Berry (2014) makes the following summary observations regarding Cambrian deformation.

- An early fold phase likely predates the unconformities at the base of the Owen Group
- Bulk of existing evidence is that the Late Cambrian was a period of compressional tectonics with open upright folds and west dipping thrusts.
- Deformation is thought to continue during and after Owen Group deposition.

Clearly, a number of structural movements are reflected in the Thomas Creek data collected, although timing is not clear; be they Cambrian, Late Cambrian, Devonian through possibly brittle Tertiary events? Complicating is the strong Devonian structural overprint commonly masking earlier Cambrian structures. The observed lineation orientations, movement indicators and observed fault offsets at Thomas Creek are partly consistent with principal NW-SE stress, with thrust ramping to the SE. A likely thrust surface interpreted from drill sections (Figure ?longProj) fits this model. This supports observation that the NW strike of the Hibbs Ultramafic Belt is consistent with emplacement during NW-SE compression during the Cambrian (Berry, 2014).

However, a number of Thomas Creek area features also fit with a dextral fault regime model, most likely related to a large NE striking fault mapped regionally to the south of Thomas Creek. This fault may have been a thrust / reverse fault during the earlier Cambrian NW-SE compression, then possibly reactivated with dextral movement during the late Cambrian, and was possibly again sinistrally active in the Devonian. Hypothetically NW striking chalcopyrite and magnetite veining, as well as the enigmatic monzodiorite intrusion in the NW formed in extensional orientations related to sinistral movement during the earlier NW-SE Cambrian compression. Continued syndeformational magmatism and NE striking chalcopyrite and magnetite veining were possibly related to Late Cambrian reversal to a dextral wrench regime. The NW dipping micromonzodiorites and postulated NE dipping (-50 to 50TN) reverse fault fit with a dextral rebound compression model for the late Cambrian.

Favourable comparison can be made to the current structural model for Mt Lyell, outlined in Corbett (et al., 2014), whereby rising diapirism and compressional tectonism likely correlated with North Lyell mineralisation. At Thomas Creek there are two differing alteration and mineralisation styles. The earlier more pervasive style possibly involved an extensional setting with significant sea water interaction within an active volcanic environment driven by diorite intrusion. A Late Cambrian compressional change possibly lifted the volcanic pile into a more subaerial environment with veining, meteoric water influence and forceful micromonzodiorite intrusion being more prevalent. In this scenario, oxidation of the Middle Owen Sandstone near Mt Lyell and the North Lyell deposit possibly represents Fe devolatilisation from late intrusives, surface exhalation and / or interaction with more meteoric dominated pore waters at the faulted contact.

The protracted tectonic history is also supported by slight differences in Co (+/-Ni) versus Cu in soil trends, suggesting they are intruded at different stages. Cu introduction is interpreted as initially early with diorite intrusion, followed by Cu associated with micromonzodioirite and latest Cu bearing magnetite, Co and Ni sulphide veins. Vein mineralisation is apparently more Co and Ni rich at later

stages, which is possibly related to longer term partial melting of the early Cambrian ultramafic crust beneath.

The significant volume of sub volcanic intrusions beneath Thomas Creek likely led to rheological contrasts providing a focus for associated dilation and brittle faulting related to interpreted regional dextral transverse movement, during Late Cambrian compression.

As noted, structure at Thomas Creek likely resulted from interplay of at least a Devonian and possibly two Cambrian tectonic events. Interestingly, the Timbertops Syncline is mapped with a basin like folded form and correspondingly adjacent to the SW is the Thomas Creek Intrusive complex which has somewhat dome–like form. Thus there may be as yet undefined dome and basin fold interference in the regional resulting from interplay of Cambrian and Devonian deformation events. Such hypothetical fold interference is possible given recognised E-W and NNW Middle Cambrian fold trends to the south near Port Davey (Berry, 2014). Further, a significant plug/root of diorite beneath the Thomas Creek intrusive complex could act as a high rheology block over/around which an anticlinal fold or dome is more likely to form. An hypothesised diorite plug beneath Thomas Creek could also provide a block, initiating over thrusting. Thus, possibly only the top of the complex has been significantly affected by thrust faulting.

Mineralisation

Study of the geochemical character of mineralisation and alteration at Thomas Creek was undertaken, with further benefits generated from comparison with Mt Lyell and VHMS in general. Related literature review focused upon developing ore vectors / index's. Complicating interpretation at Thomas Creek is the interplay/overprinting of hybrid VHMS / high sulphidation equivalent mineralisation by more directly intrusion related element suites.

Geochemical Correlation Trends

Correlation trends were generally similar comparing drill core and soil analysis, whilst potentially weathering depleted soils reflect a broader view of the geochemical environment. Analysis of correlation trends for Thomas Creek resulted in definition of two clear key element associations for intrusion / K Feldspar silicate/ potassic alteration (K, Ba, Rb & Tl) and vein related styles (Cu, Co, P, W, Ni & Re). The vein related association is partly reflected in literature for the Prince Lyell deposit (Cu, Co & P).

The total number of soil analysis in the Thomas Creek Prospect database is 948. Of these major elements are well covered at 876 samples, including the Plutonic sampling over the core of the grid. Larger multielement (including trace element) analysis totalling 434 are mostly from more recent times (MHM, Sherlock and Accelerate), covering both peripheral and some core areas. 581 analysis include Au, but not all are multielement. Interpretation should consider the spatially incomplete ICPMS data coverage, which leaves plenty of hints of various anomalous elements and indices, with mineralisation potential commonly left open; notably at the northern magnetic rim and MobileMT conductive zone in the northeast.

Note there is some concern over comparative element levels between MHM and other data. The MHM survey commonly reported low for a number of majors and trace elements and consequently interpretation should be undertaken with some caution; although relative anomalies are still apparent. Another consideration is that the MHM survey largely covered the magnetic rim, where

alteration induced element mobility is possible. The southernmost NE trending MHM sampling is a good example where gridding differences are reflected, but a caveat being potential to be structure parallel through this area.

Element and ratio trends were investigated via correlation analysis on soils and drilling analysis data. Amoco soil data was not utilised due to a relative lack of comparative elements. Similarly, Plutonic soil data was only utilised for common majors and base metals. Observed patterns in likely magmatic, mineralisation versus lithology related trends from soils are:-

Investigation of alteration elements trends:-

Base metals and major element soil correlation trends (See table in Appendix 2; Thomas Creek Soil Geochemistry Correlation):-

- Co and Cu correlate well at 0.82, with both moderately correlated with P indicating a strong association.
- K and Ba correlate well at 0.82, but correlate poorly with Cu and Co (+base metals), indicating a strong association separate from Co-Cu mineralisation; evident in spatial distribution as well.
- Zn correlates weakly with Mg and Pb.
- All Au correlations were poor (<0.15)

ICP-MS correlation trends from drill core appear to define more clearly separate vein and intrusive/K Feldspar – silicate alteration (See table in Appendix 3; Thomas Creek Drill Hole Geochemistry Correlation):-

- Vein Association:- Cu, Co, P, W, Ni, Re. Co and Cu strongly correlate, as well as with U and S. Other well correlated potentially magmatic related elements Se, Sc, P, W, Hg, Ni and Sn.
- Interestingly Mo correlates poorly with all elements, an exception being very weakly with Cu.
- Intrusive association:- K, Ba, Rb & Tl. Tl correlated well with Zr and Al suggesting it's distribution is in part lithology related. An association with intrusives is likely given good Ba, and strong K and Rb correlations. Thus Tl in the grid SE zone is possibly largely intrusive related. VHMS potential is also good at the very strongest Tl anomaly (0.45ppm) here being a Zn VHMS vector.

Comparison to Mt Lyell

It's increasingly apparent that there are many facets of the alteration and mineralisation at Thomas Creek in common with Mt Lyell. Thomas Creek is an intrusive porphyry related volcanic environment that differs from traditional porphyry settings in being submarine at early mineralisation stages with hydrothermal fluids potentially influenced by sea water. Thus more pervasive rather than brittle fracture vein fill style alteration is locally prevalent with potential for Prince Lyell style stringer and disseminated mineralisation. At Thomas Creek early chalcopyrite may have zoned ahead of intrusion driven K Feldspar – Silicate alteration. Later stage magnetite-hematite-chalcopyrite veining, likely related to devolatilisation of forcefully intruded micromonzodiorite is evidently Late Cambrian deformation coincident and potentially contributed to North Lyell/Western Tharsis style mineralisation in a less seawater dominated, near sub aerial environment. Historical summary and

significant recent advances in the understanding of the Mt Lyell system are detailed in the "Geological Evolution of Tasmania" book sections by Corbett in Calver (etal., 2014) and illustrated as a model in Figure 27.

The Mt Lyell mineral field covers volcanic environments from seafloor to up to ~1.5km subsurface. A Thomas Creek like equivalent likely drove the system from depth. Although some high level andesitic intrusions are known at Mt Lyell. Table 7 lists various volcanic environments, their ore deposits, target character and exploration vectors focuses strongly on comparative Thomas Creek and Mt Lyell analogies.

Exhalative zone:- A relatively recent discovery is the Comstock chert body where prominent hematite jasper barite veining is known with mineralisation showing transitional features between Zn-Pb rich upper exhalative closer to seafloor and a deeper bornite rich lower. The Iron Blow was a similar hematite – barite body forming a bonanza shoot (850t @ 21% Cu & 31,000g/t Ag; Corbett, 2014) in contact with the middle and upper Owen Formations; opening potential of the Timbertops Syncline hosted Upper Owen or at least proximity to its basal contact.

Higher grade but smaller 1Mt+ ore bodies formed in the sub seafloor silica cap zone at Mt Lyell (eg. N Lyell 4.57Mt @5.5%Cu, 39.48g/t Ag and 0.4g/t Au) as well as deeper to Western Tharsis (<500m to 800m) levels are argued by some as single origin for chalcopyrite and bornite rich ores formed in the same area (Huston and Kamprad, 2000). However Solomon et al. (1987) argue a later stage more oxidising fluid is responsible for the N Lyell ores. Thomas Creek interpretation is in agreement with the later; late stage micromonzodiorites being likely sources for oxidised magmatic fluids. The Sulphur isotope comparison between N Lyell, Prince Lyell and Thomas Creek ores is close (Reid, 2001) with both areas having late magmatic -6 to 2 del34S and Prince Lyell like 3 to 12 del34S values.

Bornite rich ore bodies such as at North Lyell were "plastered "against the base of silica caps. The oxidised ores are accompanied by high sulphidation minerals. The presence of pyrophyllite, topaz, zunyite and woodhousite in the alteration assemblages suggests that the Western Tharsis is a deep-level 'high sulphidation' Cu–Au deposit (Huston and Kamprad, 2000). Strong spot highs for Al are possibly indicative of Pyrophyllite ($Al_2Si_4O_{10}(OH)_2$) and Woodhouseite ($CaAl_3(PO_4)(SO_4)(OH)_6$, considering a model targeting potentially high sulphidation related bornite rich North Lyell and Western Tharsis style mineralisation. Notably these spot highs lie adjacent to P + Co + Cu additive anomalies at Thomas Creek (Figure 28 & 29).

The Western Tharsis study of Huston and Kamprad (2000) represents the only multielement study located from the Mt Lyell area. Key findings were:-

1. elements As, Bi, Cu, Mo, Ni, S and Se are strongly enriched in the ore zone, and in the pyrite-bearing alteration zones, but depleted in the marginal carbonate-bearing alteration zone;
2. elements K and Cs are characterised by uniform values except for extreme depletion within the pyrophyllite-bearing zone that forms a shell around the orebody; and
3. elements C, Mn, Ca, Zn and Tl are enriched in the carbonate halo but depleted in the pyrite halo."

They further note that "extreme alteration in the Western Tharsis deposit has resulted in the mobility of REE and some HFSE. Rare earth element mobility, in particular Ce and Eu may be useful

as pathfinders in this and other 'high sulphidation' Cu–Au deposits", with positive Ce anomalies developed within and adjacent to the orebody.

Deeper below silica heads level are low grade and high tonnage Prince Lyell ores (311Mt @0.97% Cu & 0.31g/t Au). Prince Lyell style ore is pyrite, chalcopyrite, magnetite, apatite bearing, (Cu, Co, P association) similar to the vein index developed for Thomas Creek. This index targeting late stage veined zones is shown to be locally coincident with the Western Tharsis Cu vector. Regionally, the Darwin and Murchison Granites are flanked by chlorite – magnetite+/-apatite – pyrite and an outer zone of sericite alteration. Key mineralisation related mineral occurrences are from the deeper parts of Prince Lyell (Large, 1996), Jukes Pty and the Garfield Prospect. Such mineralisation is likely transitional to the more directly intrusion related Thomas Creek.

VHMS

Exhalative VHMS style mineralisation is possible at all palaeo seawater interfaces. The possibility is demonstrated deep (~520m) in TCDD004. This horizon projects south to surface at shallow to moderate angle. VHMS exhalative styles could include Cu and / or Zn rich varieties, as per comparison with Comstock and the Iron Blow at Mt Lyell. Cu-rich Besshi style is also an applicable exhalative VHMS model.

Two main models are explored in the literature; Zn rich VHMS are relatively well understood, with Cu-rich VHMS systems a little less known. Cu rich ores are more prevalent close to volcanic centres, where key trace elements are Bi, Te, Mo and Co, whilst As, Sb, Hg and Tl are identified trace element vectors to Zn rich more distal ores (Gemmell, Large and Zaw, 1998). Gossan trace elements identified in relation to VHMS include Au, Se, Te, As, Sb, Bi, Cd, In, Tl, Hg, Sn and Ba. Tl and Sb are known to increase towards Zn rich VHMS ore (Large, 2001), but Tl maybe depleted in Cu rich VHMS ores (ref?).

Aside from Prince Lyell stringer type, Cu rich VHMS ores are known to have a strong EM response. A mound deposit with high aspect ratio is a likely target, similar to the Iron Blow deposit at Mt Lyell. Deposits are commonly located adjacent to major rift faults. Large 2001 hint that Cu rich VHMS may behave differently to Zn rich systems in regard to Sb and Tl, with Tl interpreted as zoned proximal to ores.

Table 7: Volcanic environments, their ore deposits, character and exploration vectors focused strongly on Mt Lyell analogies.

Ore Type	Character	Size / Resource	Minerals	Pathfinders
Exhalative. Comstock, Mt Lyell	Seafloor exhalative VHMS	small at Mt Lyell but 1Mt+ potential; eg Tasman Crown 90 by 50 by 8m @ 28% PB, 20% Zn, 0.5% Cu, 500ppm Ag, 0.3g/t Au; Comstock steep dipping irregular 60 by 20 by 300m		Cu, Pb, Zn, Ag, Au. Resistor with adjacent IP chargeability or Cu sulphide rich conductor, particularly if Cu rich; Zn rich are poor conductors, chargeable footwall and potentialy hangingwall in a stacked system.
Exhalative. Iron Blow Sulphide Orebody	Cu rich VHMS, ser-py-chl schist host. Bornite rich ore bodies such as at North Lyell were "plastered "against the base of silica caps.	200 by 50 by 250m deep. Massive to banded py cpy, exhalative. Promounced hematite - barite body forming a bonanza shoot (850t @ 21% Cu & 31,000g/t Ag; Corbett, 2014) in contact with the middle and upper Owen Formations		Ba, Fe, Cu, Pb, Zn, As, Mo, Sn, Sb, S from a variety of sulphides. resistor adjacent to ore; IP chargeability or conductor
Silica Head Zone. Western Tharsis	sub seafloor, includes extension of N Lyell like with progressively smaller silica heads extending 500 to 800m below the silica cap. Host in sericite pyrite schists and chert. Adjacent North Lyell Fault and Owen Group sediments up to upper Owen in age.	eg. N Lyell 4.57Mt @5.5%Cu, 39.48g/t Ag and 0.4g/t Au. Western Tharsis 7.3Mt @ 1.3Mt, 300 by 30 by 800m deep.	pyrophyllite, bornite, chalcocite, covellite,	As, Bi, Cu, Mo, Ni, S & Se. Al highs (Pyrophyllite), pathfinders. resistor adjacent to ore; IP chargeability or conductor. MobMT resistive anomalous zones coincident with andesites and associated breccias (not Diorites/intrusions) are targets. Silica heads similar to the top of the Mt Lyell system, if present should be resistive and potentially increase approaching Owen Group siliciclastics
Low grade below silica heads zone. Prince Lyell, Cape Horn	sub sea floor. sericite, pyrite, chlorite schists with chlorite more common in the outer halo. Magnetite and apatite are known from the deeper parts of Prince Lyell	Prince Lyell ores (311Mt @0.97% Cu & 0.31g/t Au)	sericite, pyrite, chlorite, magnetite, apatite	Cu, Co, P, high CCPI halo, Al, Spitz-Darling (Sericite) index . IP chargeability, magnetics
Thomas Creek Veining. sub to volcanic levels; seafloor / surface extension potential	Deformation coincident veining associated with Micromonzodiorite intrusion. Analogus to deep level N Lyell style.	?	magnetite, actinolite, K Feldspar, tourmaline, hematite, chalcopyrite, pyrite+/- epidote	Cu, Co, P, W, Ni & Re zoned proximal from K, Ba, Rb, Tl & K radiometrics; Proximal to coincident with K lows, rare earth mobility incl marginal +ve Ce (& Eu). structural intersections, IP chargeability, magnetics
Thomas Creek Early? Pervasive K Feldspar. sub volcanic / intrusive.	pervasive silica sericite chalcopyrite, pyrite +/- biotite, magnetite (aka TCDD002), Demonstrated high field strength element mobility (Zr) at Thomas Creek	?	magnetite, chalcopyrite, pyrite, apatite? pervasive Silica magnetite - biotite? zoned distal to K Feldspar silicate alteration.	Cu, Co, P, zoned away from intrusive K Feldspar index. chargeable, locally conductive?, locally resistive, magnetic
Exhalite. VHMS Zn & Cu	eg. See Gemmell et al. (1998)		chalcopyrite, sphalerite, galena, arsenopyrite. Footwall chlorite and stringer.	Elevated Pb, Zn, Cu, Au, Ag. Zn VHMS:- As, Sb, Hg and Tl. AI, CCPI, Ba/Sr, Na –ve. Tl and Sb are known to increase towards Zn rich VHMS (Ore values ~>1ppm Tl). Cu VHMS:- Bi, Te, Mo and Co. Tl maybe depleted in Cu rich VHMS ores. AI, CCPI, S/Na2O, Na –ve. Conductive ore body (particularly if Cu rich); Chargeable ore and chlorite footwall stringer and possibly hangingwall if a stacked system.

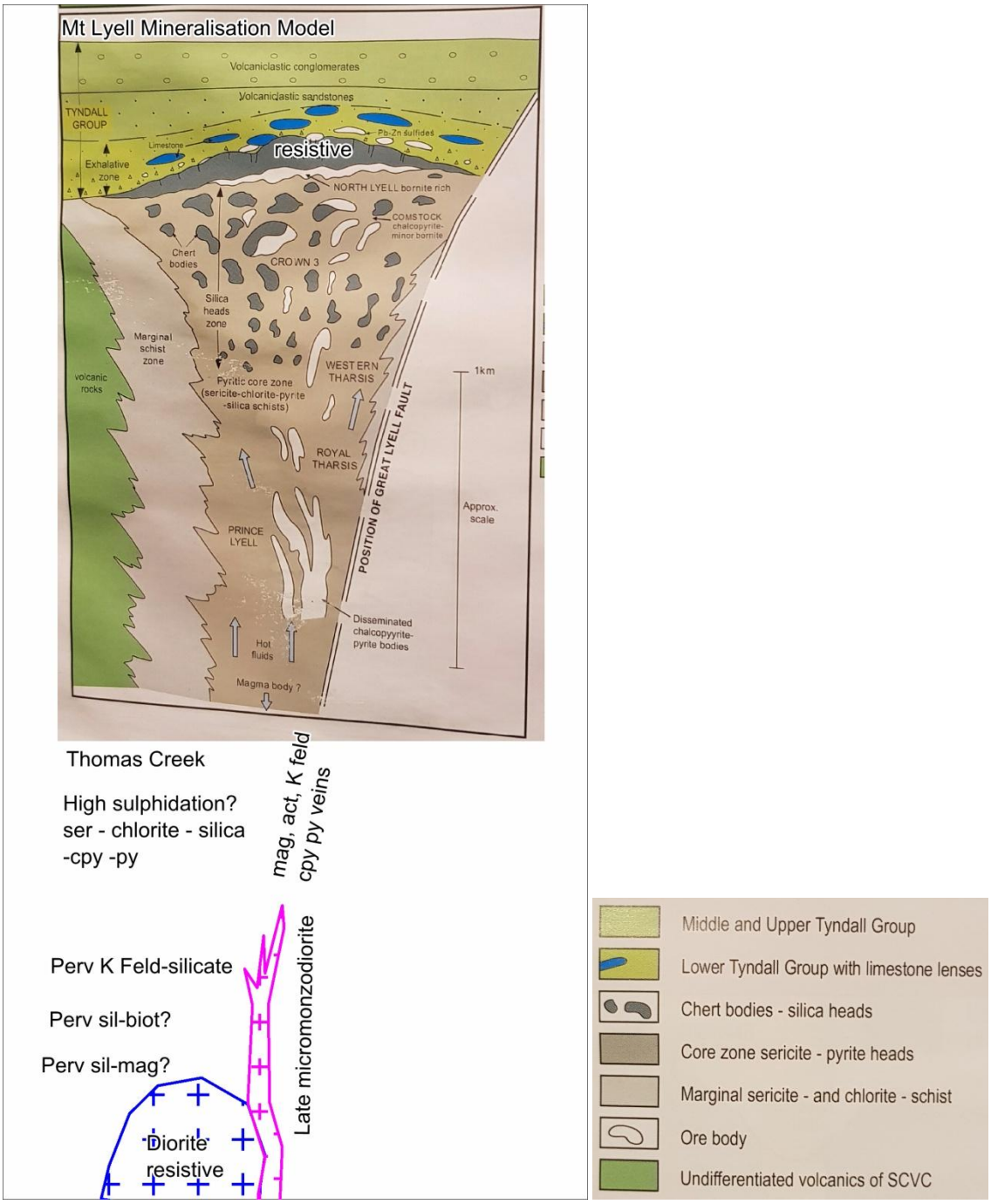

Figure 27: Model for formation of Mt Lyell Ore bodies (after Corbett, 2014), modified to roughly reflect the Thomas Creek model.

Key differences to Mt Lyell are the lack of a CVC pile underlying the exhalative expression of the NCV and the late stage high level micromonzodiorite intrusions and magnetite bearing veins overprinting at Thomas Creek. Comparison to Mt Lyell genesis diagram of Corbett (2014) can readily be made, with the key lacking CVC in mind (Figure 27). Salient points describing and comparing Thomas Creek and Mt Lyell follow:-

- Lack of a thick CVC sequence at Thomas Creek; NCV & underlying WVS. Possibility to develop Cu – rich exhalative VHMS with possibly closer proximity to seawater influence partly via "compressed" stratigraphy?
- Thick Lower Owen conglomerate sequences missing
- Less foliation and more brittle structure at Thomas Creek
- Earlier disseminated and stringer pyrite +/-magnetite-apatite (P; Prince Lyell equivalent).
- Cu and/or Zn rich VHMS potential (Iron Blow & Comstock equivalents) at local seafloor (eg. TCDD004 horizons), potential as late as upper Owen times.
- Thomas Creek late magnetite-actinolite-tourmaline-chalcopyrite-hematite veining; structure hosted / intersection lineation targets at depth (eg. NE Thomas Creek) and likely North Lyell and Western Tharsis equivalents near the Owen Group contact.
- Thomas Creek late stage high level intrusives telescope over earlier alteration and mineralisation. Some andesite intrusives are known from Mt Lyell.
- The inferred volume increase driving the formation of a lobe of volcanics at North Lyell (Corbett, 2014) may have in part been driven by forceful intrusion of micromonzodiorites at depth?
- The extensive and intense silica pyrite in the central core of the Thomas Creek intrusive complex could be a relatively barren Glen Lyell like occurrence (Pyrophyllite is potentially identified), possibly located near a volcanic vent.

Thomas Creek Mineralisation Model

- Early diorite intrusion beneath an andesitic volcanic centre; high level Prince Lyell like hybrid VHMS / high sulphidation system (seawater influenced, more pervasive alteration styles).
- Late stage devolatilisation of Fe, Cu, P, Zn, S from micromonzodiorites, likely forming mag-act-KFeld cpy veins; upgrading Prince Lyell style (Mt Lyell model targeting potentially high sulphidation related bornite rich North Lyell and Western Tharsis style mineralisation; partly sub aerial with some meteoric water influence?, more brittle vein styles).
- P+Co+Cu (Thomas Creek / Prince Lyell metals) and Western Tharsis index proximal vectors
- K, Ba, Rb, Tl highs reflect strongest intrusion related alteration and mineralisation; Cu likely zoned away.
- Prince Lyell level:- IP chargeability highs; Weakly conductive locally? (Including incl. Magnetic highs at deep level / Thomas Creek), Proximal chlorite alteration, high CCPI, AI?
- At high level:- IP chargeability highs adjacent to or within resistivity zones (aka Comstock & N Lyell Chert's). Late silica and oxide overprint near surface water interface. The Owen Group and particularly its contact with the NCV is a potentially favourable environment for Western Tharsis / North Lyell style mineralisation.

Alteration at Thomas Creek possibly zoned from a deep devolatilising intrusive source (diorite?), to residual silica-magnetite, generating Ti mobility re-depositing adjacent to outward zoned pervasive Feldspar-Silicate, driving chlorite-sericite-pyrite-chalcopyrite Prince Lyell-like stringer mineralisation to shallower levels.

Prince Lyell-like disseminated and stringer mineralisation likely formed early, zoned (higher and laterally) away from Fe, Cu, S, Zn and P mobilising(?) Feldspar-silicate alteration. Supporting is prevalent silica alteration in the TCDD002 area, bearing the best significant Cu intersection from

Thomas Creek to-date (56m @ 0.1% Cu), whilst potentially Cu and P mobilising K feldspar silicate alteration is absent here. Spiky soil Cu geochemistry noted in the core of the Thomas Creek grid may mostly relate to late stage magnetite-chalcopyrite bearing veins, overprinting earlier broadly pervasive K Feldspar – silicate alteration. This late event is overprinted by high level likely coeval forcefully intruded (syn deformational) micromonzodiorite intrusion, which likely sourced low del34S chalcopyrite in more magmatic influenced Cu, Hematite, Magnetite, Apatite(?) and semi-pervasive K feldspar veins via devolatilisation. These veins are most common in drill holes TCDD004 and 1. More regionally, local vein occurrences are found in the grids south, with a significant WNW alignment of magnetite veining coincident with the aeromagnetic high's northern margin. A significant >20m wide gossan zone was located in the grids NE, likely at a structural intersection, adjacent to the significant identified MobileMT conductor.

Geochemical Exploration Vectors

Various observations from Thomas Creek, Mt Lyell and VHMS research were utilised to derive indices for exploration targeting (Table 8). These are reviewed below in a Thomas Creek and broadly western Tasmanian context. Key trace elements for VHMS ore types and indices are discussed by Large (et al., 2003), Gemmell et al (1998) and Huston and Kamprad (2000). Thomas Creek analysis data ranges for some Index defining potential element associations were normalised to 100 to reflect proportionate input from each element. The resulting grids of various indices were applied to soils and drilling data, with surface projected plan views allowing comparison to soils.

Additive element indices were derived from Gemmell (et al., 1998) for key trace elements related to more volcanic vent proximal Cu and relatively more distal Zn rich VHMS ores. Unfortunately a Zn rich VHMS index could not be calculated for drill holes, as Hg was mostly un-reported. Instead an As+Sb+Tl ratio was calculated, essentially similar to the Tl+Sb correlation noted by Large (2001) for Zn VHMS ore proximity. Large (2001) lists Cu rich VHMS ore pathfinders as AI, CCPI, S/Na2O and Na –ve, whilst Zn rich VHMS ore vectors are AI, CCPI, Tl, Sb, Ba/Sr and Na –ve.

Sb, Hg and Tl are known as haloes to Pb-Zn rich VHMS, but are thought to be more soluble in more Cu rich systems (Large, 2001). At Thomas Creek, strongest Sb and Tl anomalism forms clear highs in the SE, with further elevated Tl extending into the Thomas Creek core grid. Sb is zoned proximal to Ni highs indicating Sb is possibly partly vein related. Tl may in fact be a better indicator of proximity to Cu rich VHMS at Thomas Creek.

The use of VHMS indices is considered less reliable given the over printing intrusion related alteration. K, Ba and Sr have been shown to be associated with pervasive K-Feldspar silicate alteration (Reid, 2001), but Ba also potentially reflects exhalative alteration. Thus whilst Ba/Sr (VHMS hanging wall indicator) ratio reflects a very strong high in the grids SE, the result is circumspect as it's coincident with the Tl and Sb anomalies. Although there is a weak indication of increased Zn VHMS index at the grids southern end.

Similar methodology was applied to Western Tharsis and Thomas Creek intrusive and veining indices derived from correlation analysis. Elements used were normalised to reflect equally weighted proportionate influence. Interestingly, the peak anomaly distribution of both VHMS indices is roughly coincident in the grid south, excepting that the Zn index not unexpectedly appears a little more strataform as compared to possibly structure focused Cu trace elements. Potential indicated by these indices is good and open in the north and east.

Given the overprinting nature of various mineralisation and alteration events, Index's relying upon major element analysis are potentially weathering influenced. Generic VHMS indices are similarly hard to convincingly apply, given the intrusion related overprint. Whereas, trace element indices specific to identified element associations, such as those specified for Western Tharsis and Thomas Creek veining, are better vectoring indicators. The more generalised P+Cu+Co Prince Lyell like index appears to have focused application too (Figure 29).

WT indices developed from Huston and Kampard (2000) for Cu mineralisation at Western Tharsis are derived from the only currently known published multielement data, whereas data from Raymond's (1996) study of North Lyell, are thought to be available but were unknown at the time of writing. Identified element correlations from Thomas Creek compare closely with those defined for Western Tharsis (Huston and Kamprad, 2000). Good drill core Ni v S & Se correlation favourably compares to key Western Tharsis indicator elements (As, Bi, Cu, Mo, Ni, S & Se; Figure 28 & 29).
Key indices for vectoring to Western Tharsis style mineralisation (Figure 28) are aluminium potentially detecting associated pyrophyllite, K multiplied by Cs to show peripheral to ore zones, MnCaZn? for proximal alteration and WT Cu targeting mineralisation.

Huston and Kamprad (2000) found "The distribution of K is characterised by extreme depletion (0.06–0.9% K2O; figure 3C) in narrow (20–30 m) zones that flank the orebodies both in the footwall and the hanging wall and enveloping the orebody at surface. The K and Cs depletion anomalies correlate spatially with the pyrophyllite bearing alteration zone that wraps around the orebody". An A multiply grid for K and Cs applied to Thomas Creek in Figure 28 shows a low zone adjacent to the southern anomaly.

Demonstrated high field strength element mobility at Thomas Creek is discussed with geology above. Potential Ti mobility may be reflected in Ti/Zr ratio, with low values possibly being indicative of hotter alteration. Low Ti/Zr zones are evident in the Thomas Creek altered core zone and over the NW microdiorite. High Ti/Zr zones possibly in part reflect hydrothermal Ti enrichment. Supporting is a spatial correlation between very high (>60) Ti/Zr and High P+Cu+Co zones in soils (Figure 29).

Alteration index (AI) >90 is considered to be closely related to both exhalative VHMS and hybrid Cu mineralisation. An extensive zone of high AI extends on NE trend from south of TCDD001 through TCDD004, being open to the NE. This zone also correlates well with conductive zones form the MobileMT. CCPI agrees with the NE trend reflected in AI, with a focus in the SW half of the AI trend. Notably a weak AI zone links through Thomas Creek drilling, west over mapped diorite (Figure 30).

Carbonate – chlorite – pyrite Index (CCPI) is applicable to define chlorite haloes to Prince Lyell style mineralisation. Strongest combined Alteration Index and Carbonate – chlorite – pyrite Index is focused at several locations, among them being in the SE of the Thomas Creek Drilling (Figure 30). These are commonly mutually exclusive with K and Ba grids, which are indicative of K feldspar alteration and micromonzodiorite intrusions.

Tl is a potential Zn VHMS ore indicator, with >1ppm recorded in many VHMS examples (Large, 2003). Interestingly at Thomas Creek, Tl exhibits similar distribution to apparently intrusion related elements, although a distinct 0.45ppm+ high is NE aligned across two grids in the far SE of the grid. However, in this case the Tl – Ba association reflects a more likely intrusive related input. High Ba/Sr,

a potential hanging wall indicator also focuses in the SW, as does Na depletion; Problematic as discussed above.

The Na grid (Figure 30) has a strong 50% top cut applied to accentuate low Na potential VHMS footwall zones. Low Na zones are clearly PCuCo and WT index coincident.

Table 8: Various alteration indices applied to VHMS exploration and developed from Thomas Creek element correlations from both drill core and soil analyses.

Indice	Formula	Comment
TC_Veining	Cu+Co+P+W+Ni+Re	Vein related association. normalised, determined from correlation analysis
TC_PCuCo	P+Cu+Co	TC mineralisation element correlation. Normalised. Prince Lyell assemblage (apatite association)
TC_Intrusive	K+Ba+Tl+Rb	Intrusive related association. Normalised. determined from correlation analysis
WTharsisCu	As+Bi+Cu+Mo+Ni+S+Se	Western Tharsis Ore Vectors
Wtharsis Proximal alteration	Mn+Ca+Zn+Tl	Western Tharsis Cb haloe enrichment and py halo depletion Vectors
K_Cs	K*Cs	Western Tharsis extreme depletion in pyrophyllite orebody shell
VHMS_Cu	Bi+Te+Mo+Co	Cu - rich VHMS ores
VHMS_Zn	As+Sb+Hg+Tl	Zn - rich VHMS ores
SpitzDarlingIndex	Al2O3/Na2O	
Sericite Index	K2O/(K2O+Na2O)	reflects KFeldspar at TC
AlterationIndex (AI)	100*(MgO+K2O)/(MgO +K2O+CaO+NaO)	VHMS vector
Carbonate Chlorite Pyrite Index (CCPI)	100*(MgO+FeO)/(MgO +FeO+NaO+K2O)	Enables separation of chlorite, sericite and carbonate alteration
AI_CCPI	AI_CCPI	Both increasing to VHMS ore
Mn	Mn	
S/Na2O	S/Na2O	
Ba/Sr	Ba/Sr	Hangingwall VHMS
Tl+Sb	Tl+Sb	Tl and Sb are known to increase towards Zn rich VHMS ore (Large, 2001), may extend into footwall and hangingwall (Ore ~>1ppm Tl)

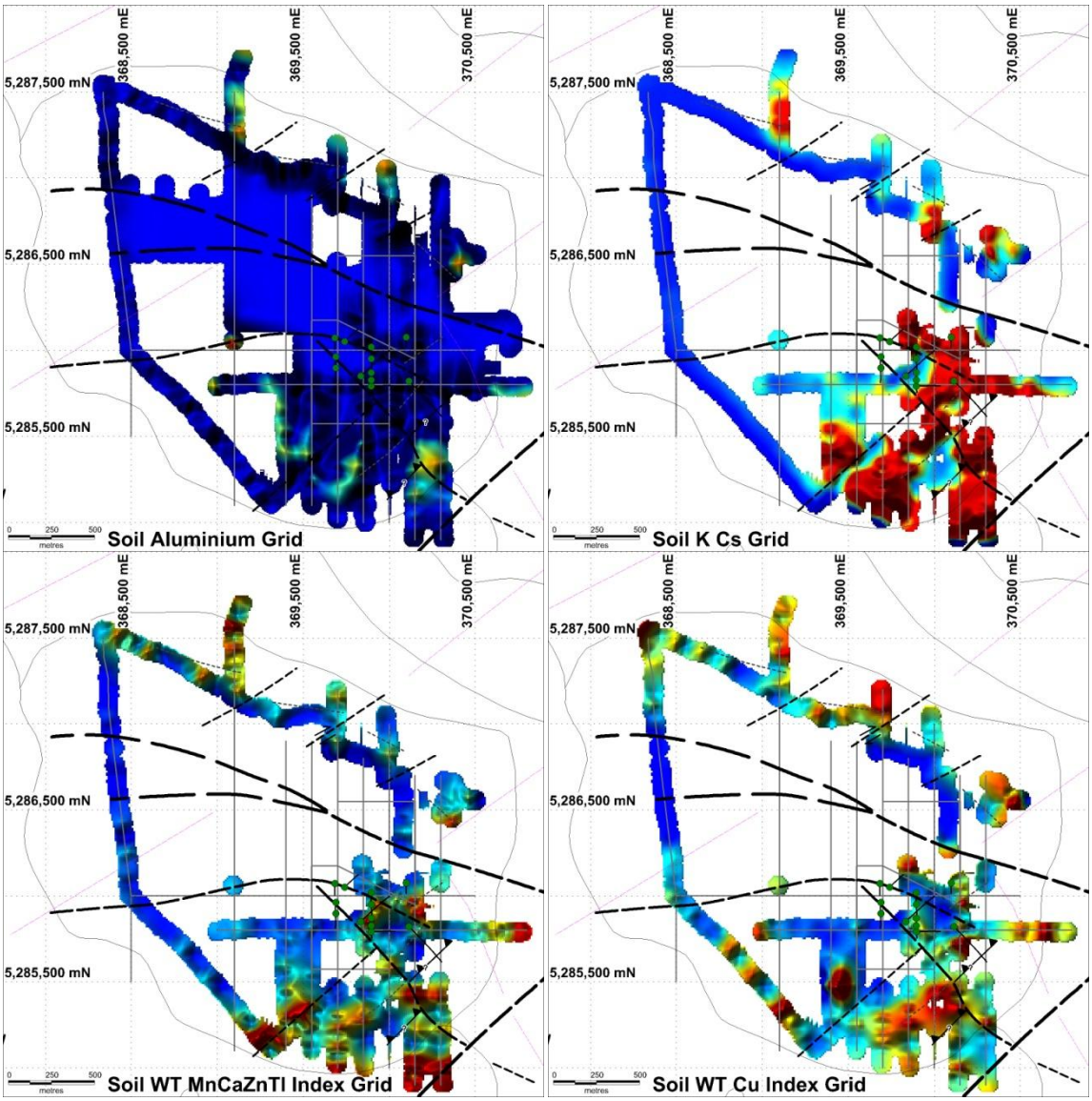

Figure 28: Indices applicable to exploration for Western Tharsis style mineralisation.

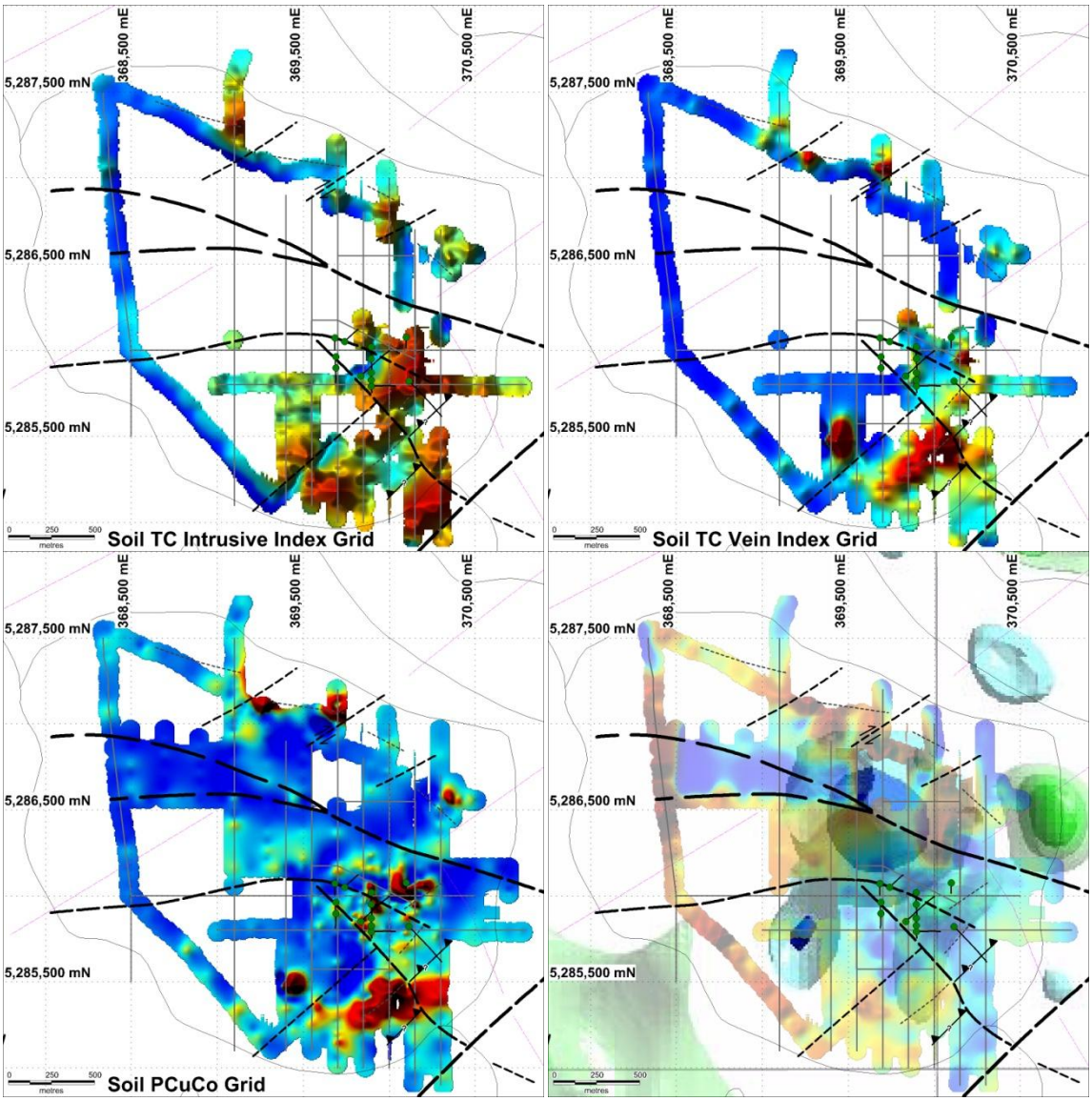

Figure 29: Indices applicable to exploration for Thomas Creek vein and Prince Lyell style mineralisation. Ti/Zr transparency over MobileMT anomalies (bottom right; blue = resistivity & green = conductivity) shows a potential high temperature alteration halo related to early pervasive K Feldspar alteration.

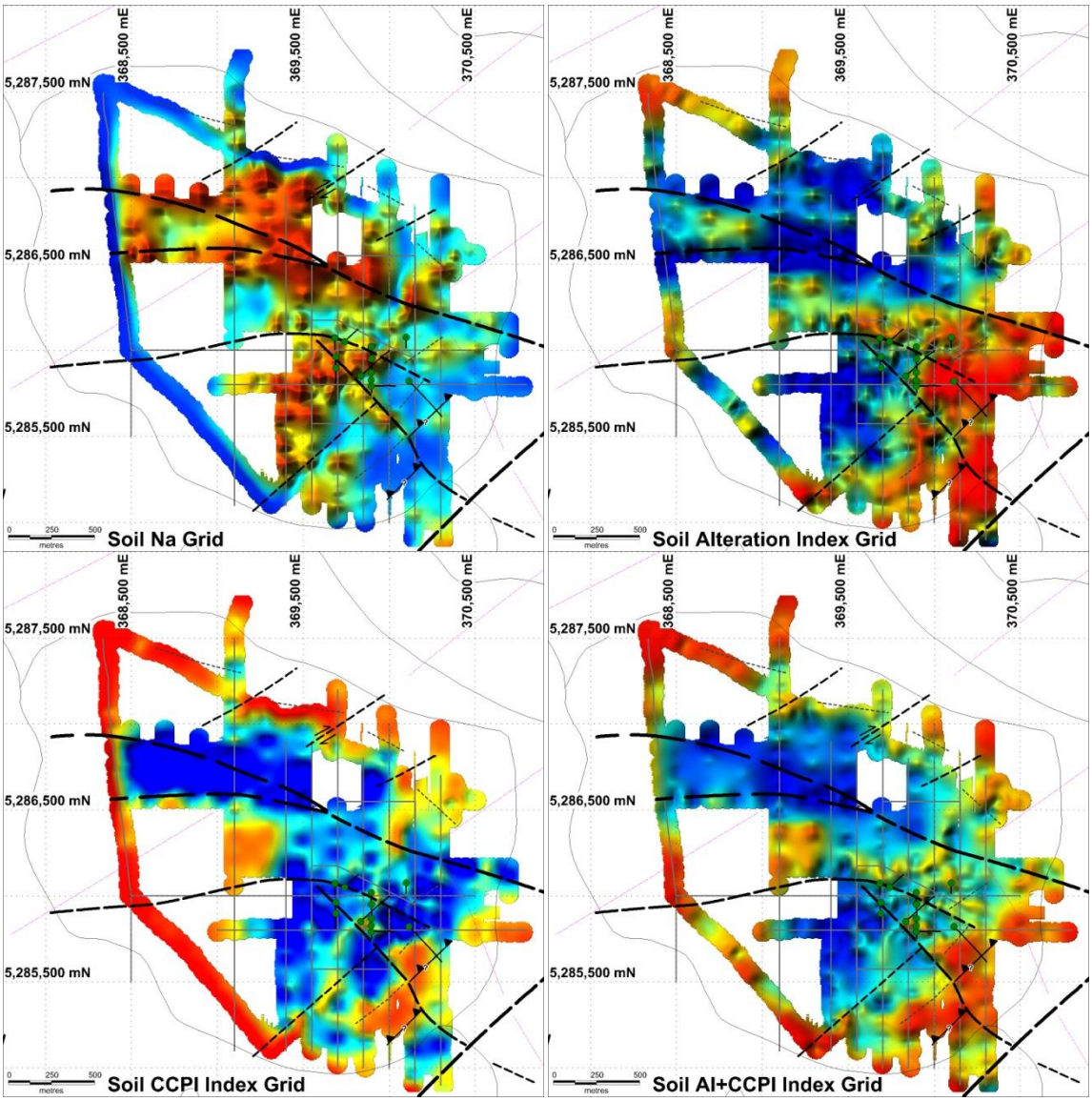

Figure 30: Indices applicable to exploration for Western Tharsis and VHMS style mineralisation.

Soils Discussion and Interpretation

Various elements and indices, as per above, were gridded to aid interpretation of likely mineralisation vectors. Key targets being intrusion related and VHMS related mineralisation styles were assessed via key indicative elements and indices. The SE of the Thomas Creek grid returns many positive vectors with Mt Lyell like and VHMS potential. The NE is less defined with open anomalies and could result in further zones being discovered with extended surveys. Observations follow:-

- Co distribution is similar to previously defined. A new point high is located in the SW of the grid, likely corresponds with veining. Central to the Thomas Creek Prospect is a halo and spot high Co core, suggestive of caldera rim fracture fill or structural intersection.
- Cu has similar distribution to Co in the core of Thomas Creek, whilst forming broad low level anomalies in the grid south.

- Ca defines a NW feature, elongate sub parallel to identified structure trends. For Ca the most intense alteration is concentrated laterally adjacent to inferred fluid focus (Large, 2001). At Thomas Creek Ca mostly covers and extends west.
- Al returns an interesting grid, reflective of lithology distribution and faults. Mn, Nb, Rb, Ga and Li reflect a very similar distribution.
- K reflects pervasive alteration and semi-pervasive veins as well as K-rich micromonzodiorite intrusions. K / Na potentially highlights strongest potassic alteration relative to Na depletion; a strong zone runs NE through the SW of the grid.
- Mg is aligned to structure, in part reflective of Chlorite(?), and the significant intrusive margin in the NW.
- Mo reflects a strong magmatic input. It's very high in the NE near the interpreted structural intersection.
- Na lows indicative of potential VHMS are concentrated in a NE aligned zone through the SE of the Thomas Creek Prospect.
- P defines structure from highly anomalous zones, with a lower tenor broad zone coincident with a MobileMT 224Hz high in the south of Thomas Creek. VHMS potential?
- Pb whilst very low clearly defines highs related to WNW structure.

Key Prospective Zones

Much of the area surrounding the Thomas Creek Prospect remains highly prospective, in part due to the pedigree of alteration and mineralisation noted at Thomas Creek and through a lack of exploration. Significant is the discovery of Cu and Au anomalous rock chips and soils on the Thomas Creek aeromagnetic high northern periphery as well as a soil anomalous zone located on new southern grid extensions. Notes relating to recent field and drilling activities shedding new light on the Thomas Creek prospect and region are outlined below.

Mineralisation potential surrounding Thomas Creek and regional targets were identified utilising a variety of GIS driven data sets with particular regard to new insights including MobileMT modelling. A number of dot points regarding more significant regional targets are made in the following with a summary provided in Table 11.

Thomas Creek Prospect

In the following figures, drill core analyses and various prospectivity indices identified for Thomas Creek were composited to 10m down hole intervals for interpretation purposes. The various indices displayed on drill hole traces were coloured to highlight relative (low to high) anomalous populations within the known distributions; legends are not created as yet. Comparison to soil grids is relative only.

Hole TCDD002 is a clear stand out when comparing intensity and extent of significant Cu intervals, returning 56m @0.1ppm Cu and 219ppm Co at 500ppm Cu cut off (Table 9 & Figure 31). Nearby TCD2 returned 48m of ~0.09% Cu. The most significant Co intervals at 500ppm cut off are 8m @ 0.1% Co in TCDD001 and 3m @ 0.23% Co in TCDD003 (Table 10). Gold alone returns sparse >0.1ppm intervals, with an exception being the sampling high of 2m @ 1.65ppm Au from 424m in TCDD004; where accompanying base metals were low. Notably a low level Co zone towards the base of

TCDD003 is not accompanied by Cu (Figure 31), which are commonly coincident elsewhere; this possibly reflects a late more Co rich vein phase.

The PCuCo additive index returns spot highs down hole, in particular highlighting several zones in TCDD004 (incl. SMS) and 2 zones in TCDD002 (Figure 32). The very similar Thomas Creek vein association (Cu, Co, P, W, Ni & Re) highlights strongest Cu mineralisation in TCDD002. The Western Tharsis Cu index mostly returned values in a low range <100, with elevated potential indicated in the lower sections of TCDD002 and 3. These anomalies project to surface marginal to the Intrusive Index (Figure 33). Correspondingly, the Western Tharsis MnCaTlSb index indicative of proximity to ore, zones away from this area. Further K and Cs depletion is noted as Western Tharsis ore proximal to semi coincident with K multiplied by Cs at Thomas Creek showing similar zonation to the MnCaTlSb index. A low zone exists at the base of TCDD003.

Table 9: Thomas Creek significant intervals; 500ppm Cu cut off, allowing 4m @ 250ppm internal dilution.

Hole_ID	From_m	To_m	Interval	Co_ppm	Cu_ppm
TCDD001	6	12	6	38	569
TCDD001	109	110	1	205	1760
TCDD001	150	171	21	493	943
TCDD001	178	179	1	50	1000
TCDD002	27	31	4	136	1005
TCDD002	78	84	6	115	589
TCDD002	97	104	7	231	974
TCDD002	118	174	56	219	1055
TCDD003	84	96	12	67	744
TCDD003	102	106	4	35	866
TCDD004	199	200	1	837	1590
TCDD004	210	217	7	116	884
TCDD004	292	300	8	153	1184
TCDD004	458	464	6	109	1797
TCDD004	510.9	511.3	0.4	17	1490
TCDD004	605.7	610	4.3	30	1087
TCD1	0	4	4	175	736
TCD2	50	86	36	89	935
TCD2	87	98	11	62	957
TCD3	16	20	4	93	915
TCD3	50	57	7	110	678
TCD3	60	65	5	68	649
TCD3	73	79	6	45	894
TCD3	108	117	9	95	901
TCD5	31	39	8	96	1919
TCD5	40.7	46.5	5.8	57	1616
TCD5	72	76.6	4.6	66	760

Table 10: Thomas Creek significant intervals; 500ppm Co cut off.

Hole_ID	From_m	To_m	Interval	Co_ppm	Cu_ppm
TCDD001	150	158	8	1118	1000
TCDD001	165	166	1	658	2610
TCDD002	100	101	1	510	1215
TCDD002	131	132	1	762	2330
TCDD002	136	137	1	1140	3700
TCDD002	153	154	1	792	4410
TCDD002	157	158	1	665	931
TCDD003	300	301	1	651	14
TCDD003	303	306	3	2263	54
TCDD004	199	200	1	837	1590
TCDD004	294	295	1	638	4710

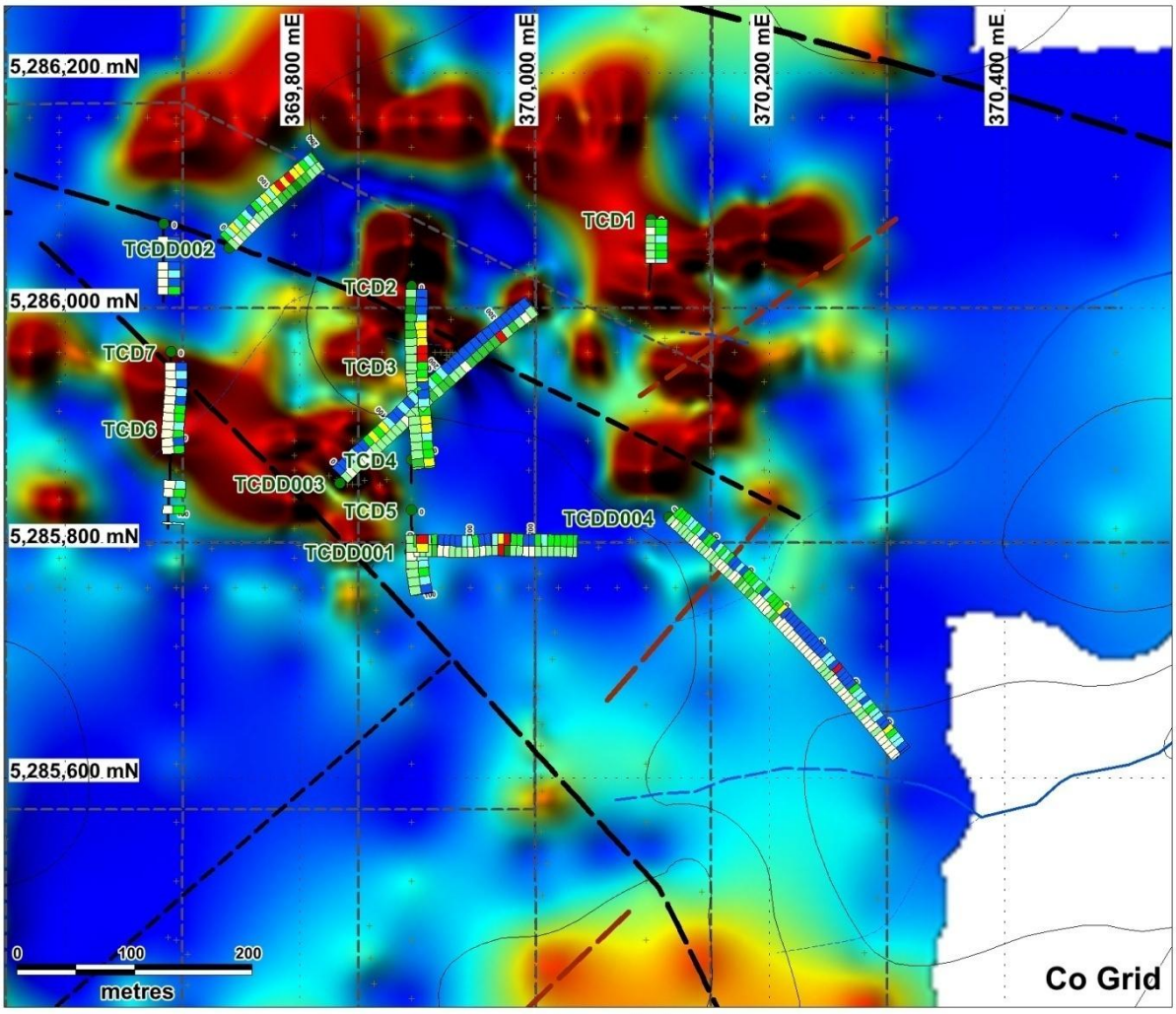

Figure 31: Cu (left of hole trace, low blue to high red) and Co (right of hole trace, low green to high red) surface projected drill hole 10m composite analysis over Co soil grid.

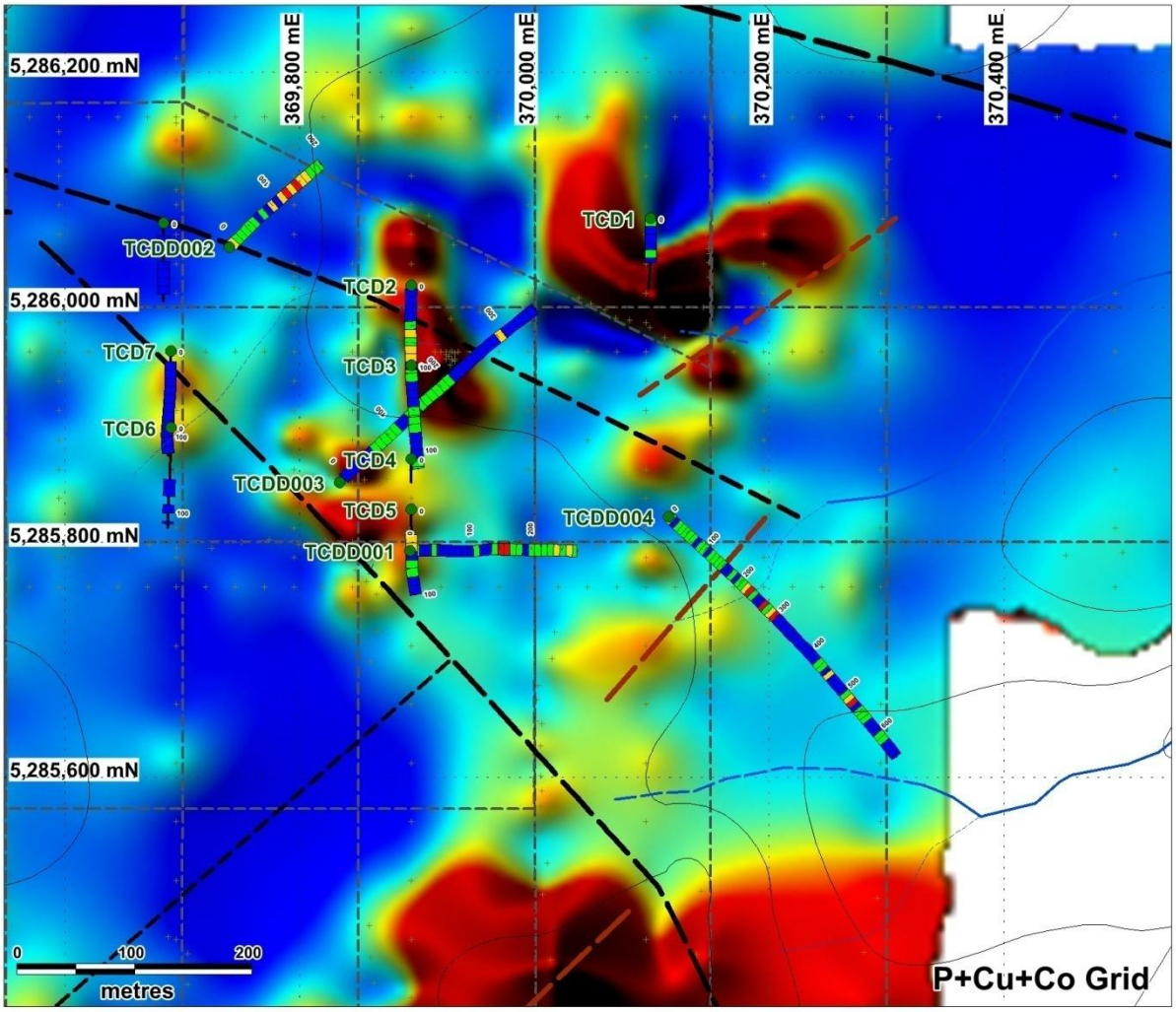

Figure 32: Thomas Creek Prospect down hole relative P+Cu+Co over P+Cu+Co Soil grid.

The distribution of intrusion related elements (K, Ba, Tl & Rb; Figure 33) apparently overlaps with micromonzodiorites and extends as a halo around these. Drill hole intrusive Index distribution mimics soils at surface providing confidence in using this Index as an exploration tool defining areas of potential micromonzodiorite intrusion and associated proximal K-Feldspar-silicate alteration.

Notably the Cu histogram distribution in drill core analysis is weakly bimodal, possibly indicating <200ppm is likely lithogeochemical. Similarly, TCDD004 despite lower sulphide overall, is considerably richer in Fe, likely reflecting significant magnetite in the host andesites (Figure 34).
Overall, geochemical index vectors to exhalative VHMS in the drilled area are east and south, particularly given low Na and high AI and CCPI in soils for this area. Na depletion, a potential VHMS footwall indicator, is evident in the SE of Thomas Creek coincident with elevated Zn VHMS Index in drill holes (Figure 35). Elevated Ba/Sr, a potential VHMS hanging wall indicator, is apparently uniformly low within the drilled area, with some distribution spikes.

Potential VHMS compatible elements in TCDD004 from a volcaniclastic sandstone with hematitic contact and minor chalcopyrite from 510.9 to 511.33m are Ba (2020ppm), Cu (1490ppm), K (6%), Low Na (0.64%) and weak Ag (0.16ppm). High additive Zn VHMS Index totals of 80 to 100 also come

from 402 to 408.65 in TCDD004, corresponding to the margins of an andesite, with pervasive silica and sericite alteration down hole. Further down hole from 516 to 519.45m the range is higher from 110 to 160. This is a positive qualitative indication of potential VHMS presence backing up textural interpretation with the highest Zn VHMS index value corresponding to the suspected VHMS. This interval also favourably bears low Ba/Sr and very low Na @ 0.05%, weakly elevated Cu, Co & Sb (22ppm), Ni, P (4040ppm), Ag (0.26ppm) and very weak Pb. Very high sericite index here suggests amorphous green silica alteration likely includes sericite. A plot (Figure 35) of Zn VHMS index shows elevated values coincident with the 520m potential exhalative VHMS interval, as well as in the top of TCDD001. A DHEM survey of TCDD004 is clearly warranted.

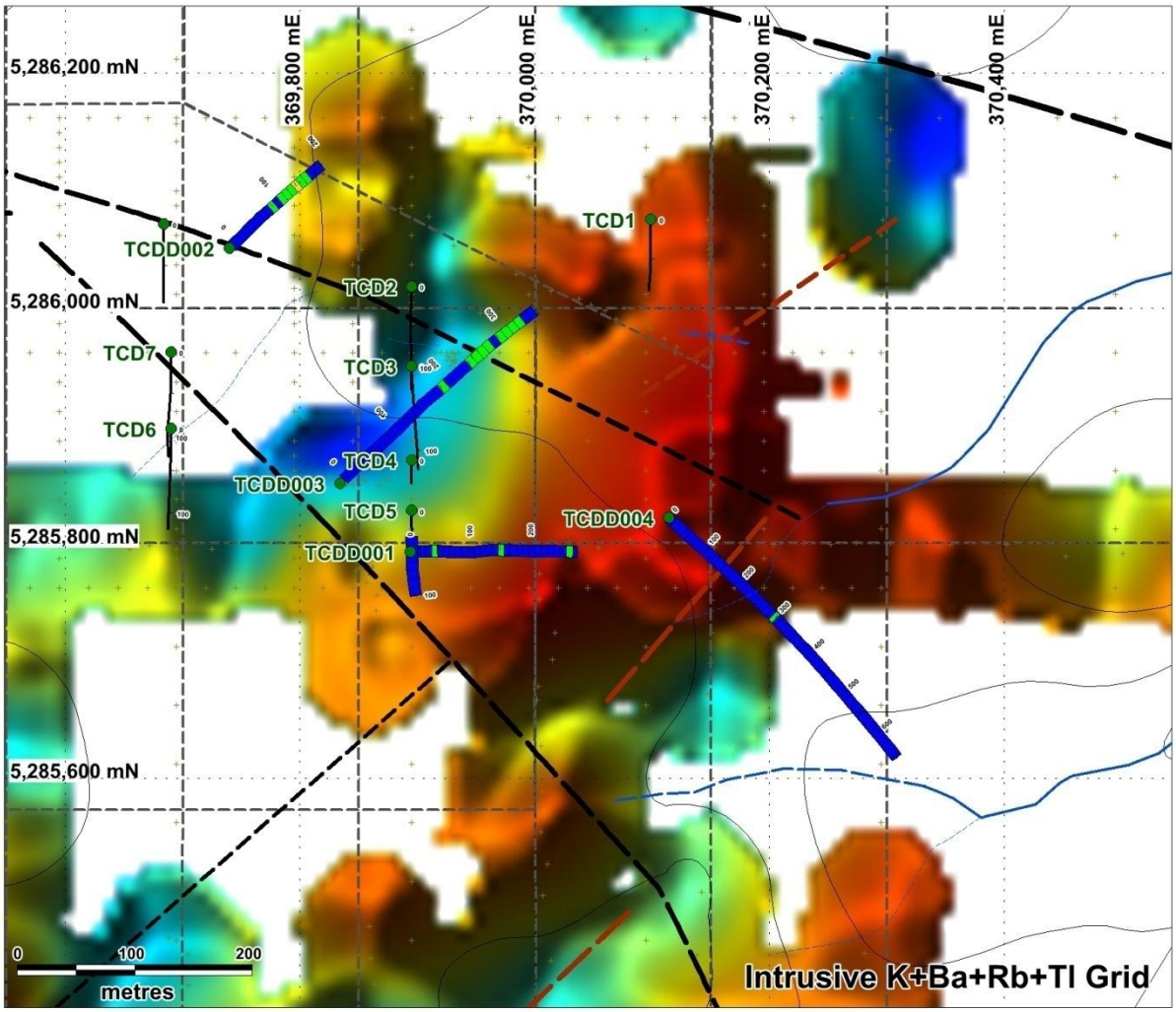

Figure 33: Western Tharsis Cu Index (low blue to high yellow) surface projected drill holes over Intrusive Index soil grid.

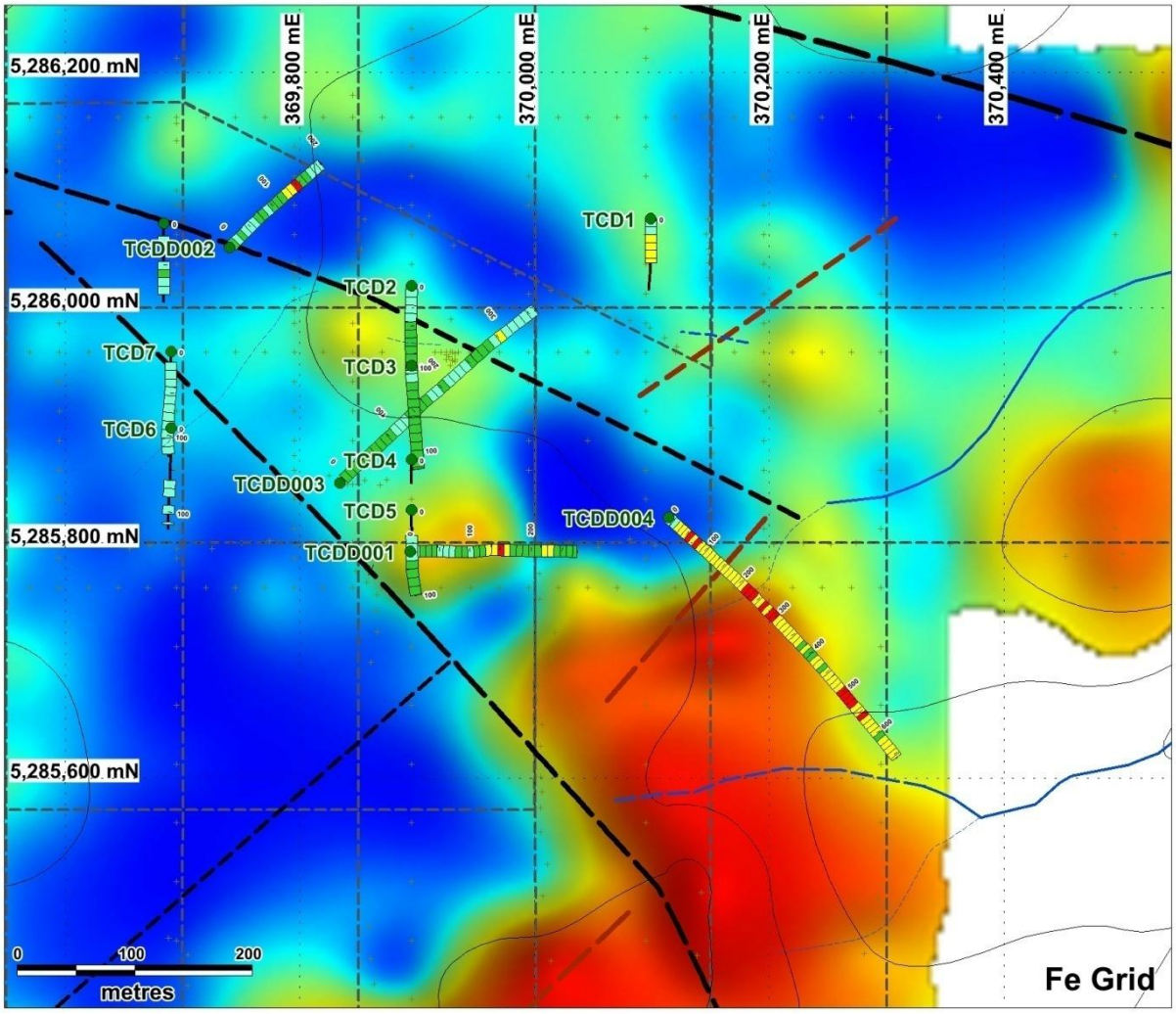

Figure 34: Fe surface projected drill hole 10m composite analysis over Fe soil grid.

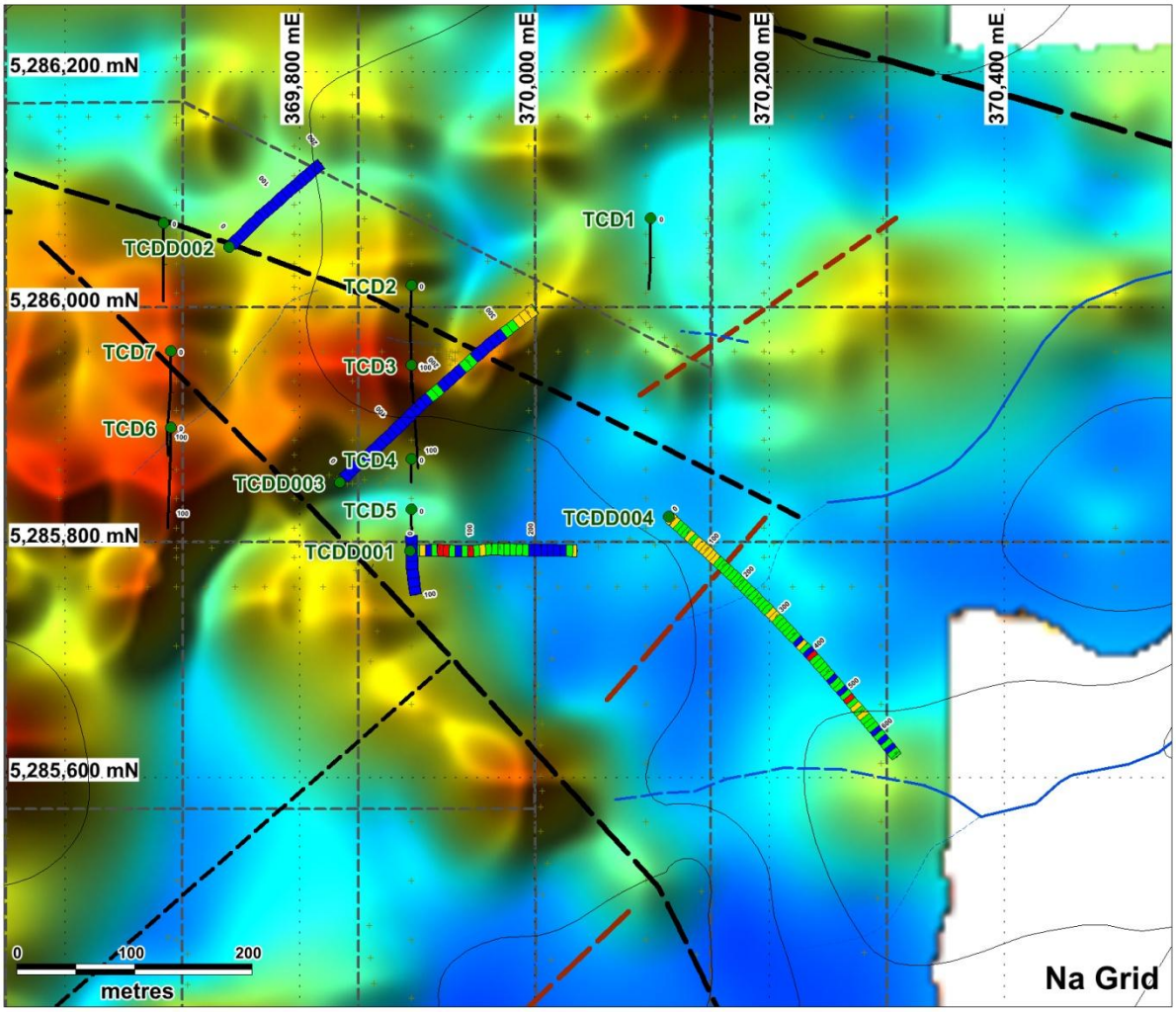

Figure 35: Thomas Creek Prospect surface projected down hole relative Zn VHMS Index over Na Soil grid.

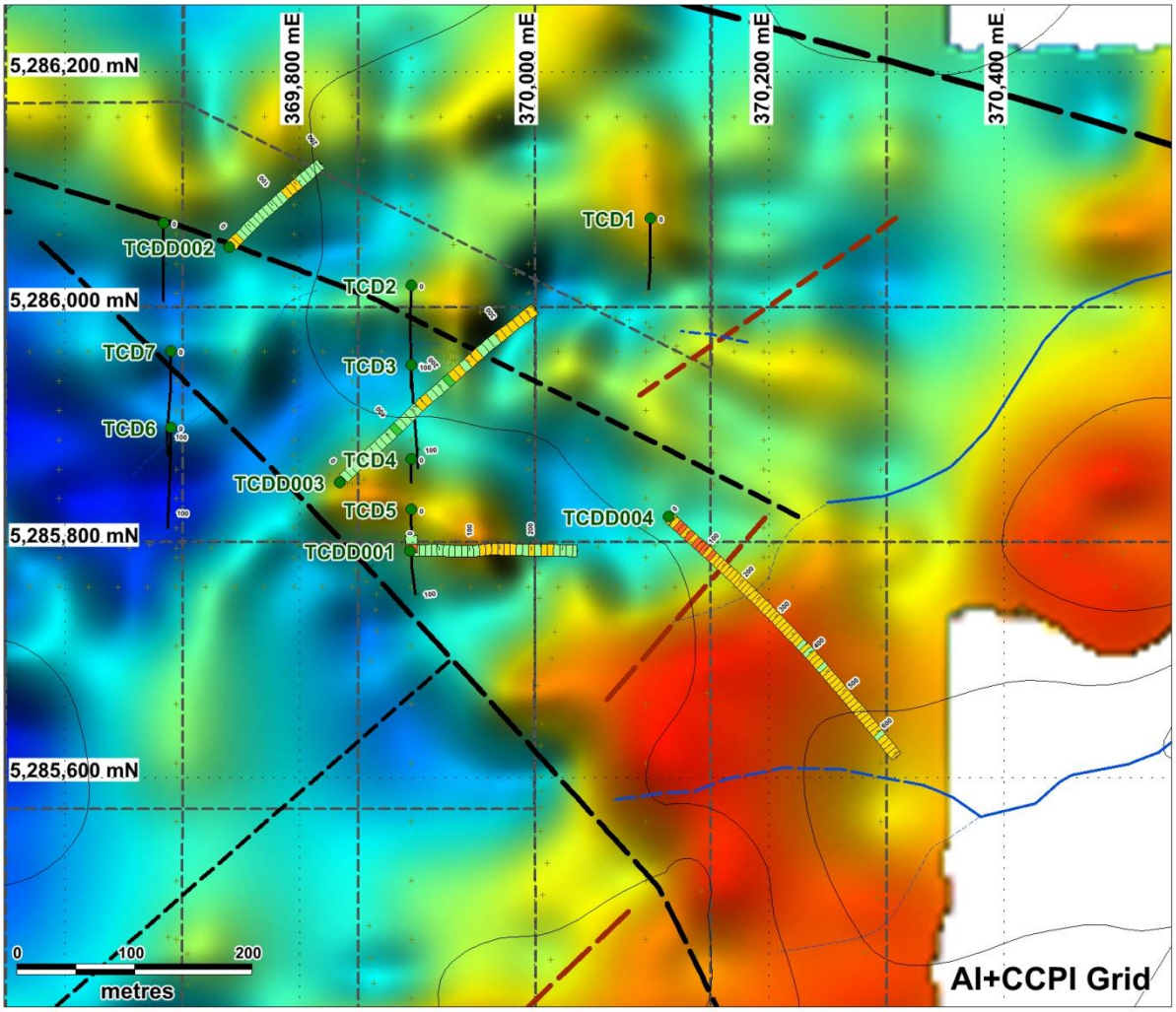

Figure 36: Thomas Creek Prospect surface projected down hole AI + CCPI over AI+CCPI Soil grid.

Sectional Interpretation

Two drill sections were created with 300m envelopes to assess broad geological and geochemical variations (Figure 37, 38 and 39). The NW – SE aligned section through Thomas Creek was created with a wide 100m envelope. Gross patterns observed are a prevalence of silicification to the NW with better Cu grades in TCDD002 and TCD2. This area exhibits a higher Western Tharsis Cu index than elsewhere, zoning to adjacent elevated MnCaZnTl index, consistent with the Western Tharsis model. A possible vector to Western Tharsis style ore is NW along the inferred host structure, and to depth towards the modelled strong core MobileMT resistor.

A number of minor thrust offsets on fractures are identified in drill core. These dip shallowly NW, with steeper similarly dipping faults in the hanging wall. 3D and sectional interpretation (Figure 38) suggests that approximately aligned mill breccia in TCDD001 and 2, with a hydrothermal breccia and faulted zone in TCDD003 (~154 to 160...170m) represents a significant thrust fault surface. This inferred thrust fault in TCDD001 possibly extends from ~150 to 165m, incorporating various hydrothermal breccias and veined zones. Whilst in TCDD002, the thrust is represented by a 10m mill breccia zone with moderate biotite and weak pervasive silica alteration from 180 to 190m. Correspondingly, in TCDD004 is a 8m zone of highly fractured core with local cataclasite, bearing coarse to locally massive (45cm) magnetite-hematite-pyrite veining and fracture fill. These zones

form a relatively flat lying to shallow NW dip possible thrust fault, in concert with the flattest measured striated fractures and faults identified from drilling structural interpretation (Figure 38, 39 & 25). Timing is evidently post mineralised clasts and syn to post micromonzodiorite intrusion, with likely later reactivation.

The inferred thrust clearly coincides with 3D IP modelled chargeability and resistivity features (Figure 39). The thrust model might also help explain the cut off nature of the donut like 10000nT modelled magnetic shell, on the southern rim of the regional scale aeromagnetic high.

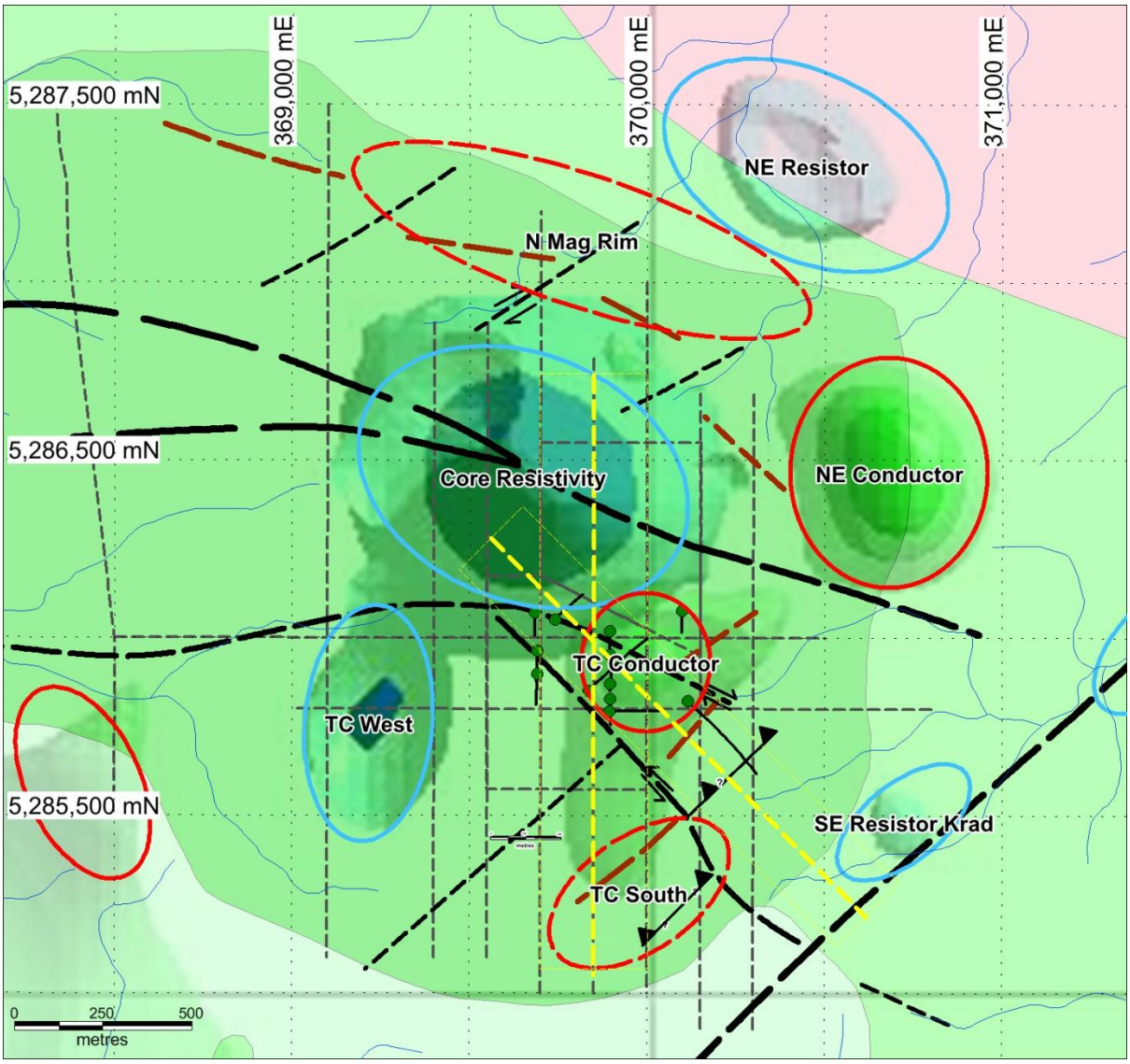

Figure 37: Location of drill sections TEMP and structure interpretation over MobileMT conductors (green) and resistors (blue).

In TCDD004, the lower semi-massive sulphide (/potential VHMS horizon) contact dips 75 to 283TN, roughly projecting up dip towards off section anomalous Cu and Fe in soils (Figure 38). This is in approximate agreement with bedding with a couple of measurements around 500m returning ~30dip to 315TN and 76 to 280TN; local folding variation or facies variation potential noted above.

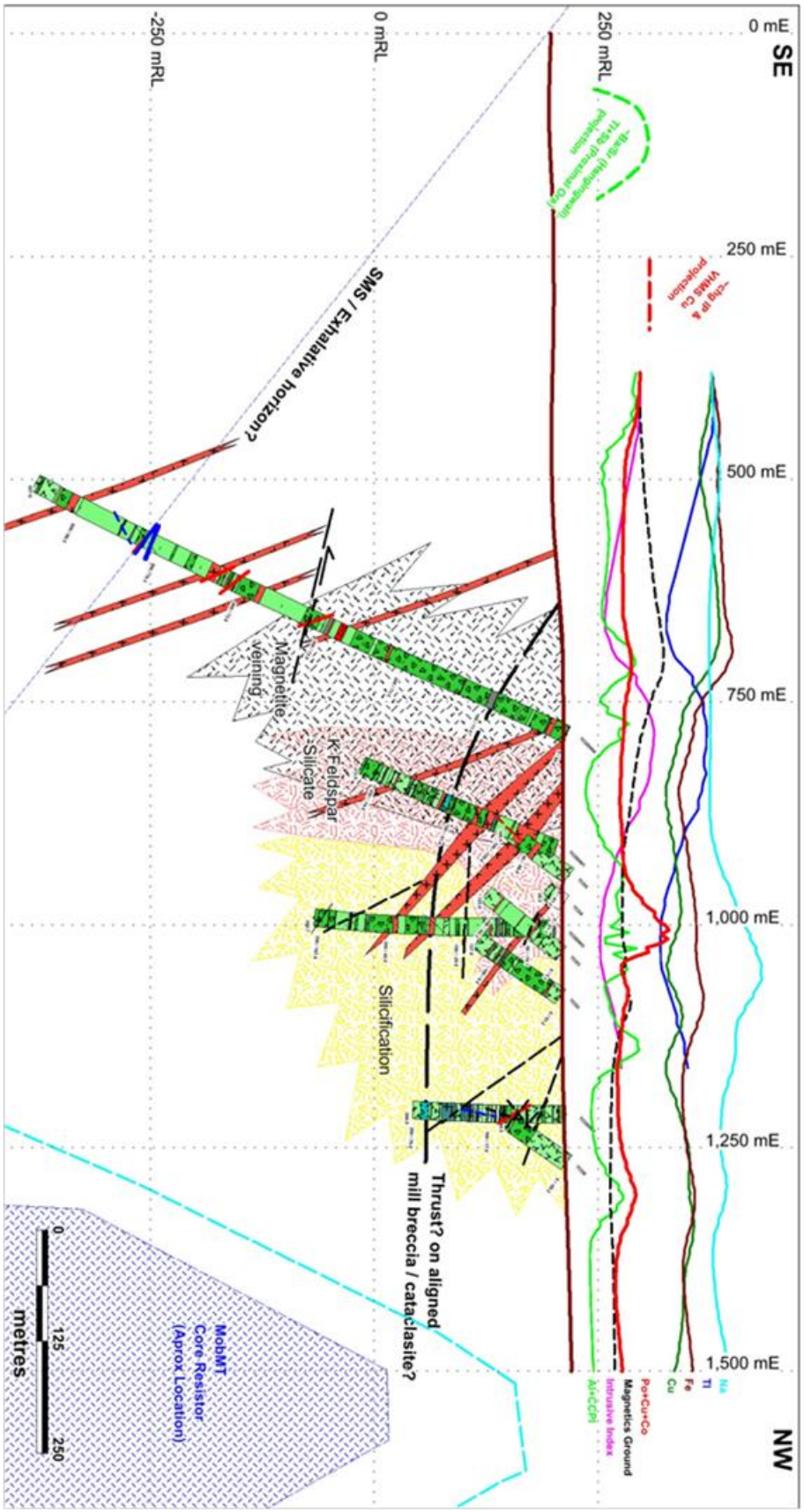

Figure 38: NW aligned section (100m search envelope) showing drill hole geology (micromonzodiorite intrusive highlighted) and broad alteration zonation. Relative soil geochemical trends displayed as surface traces.

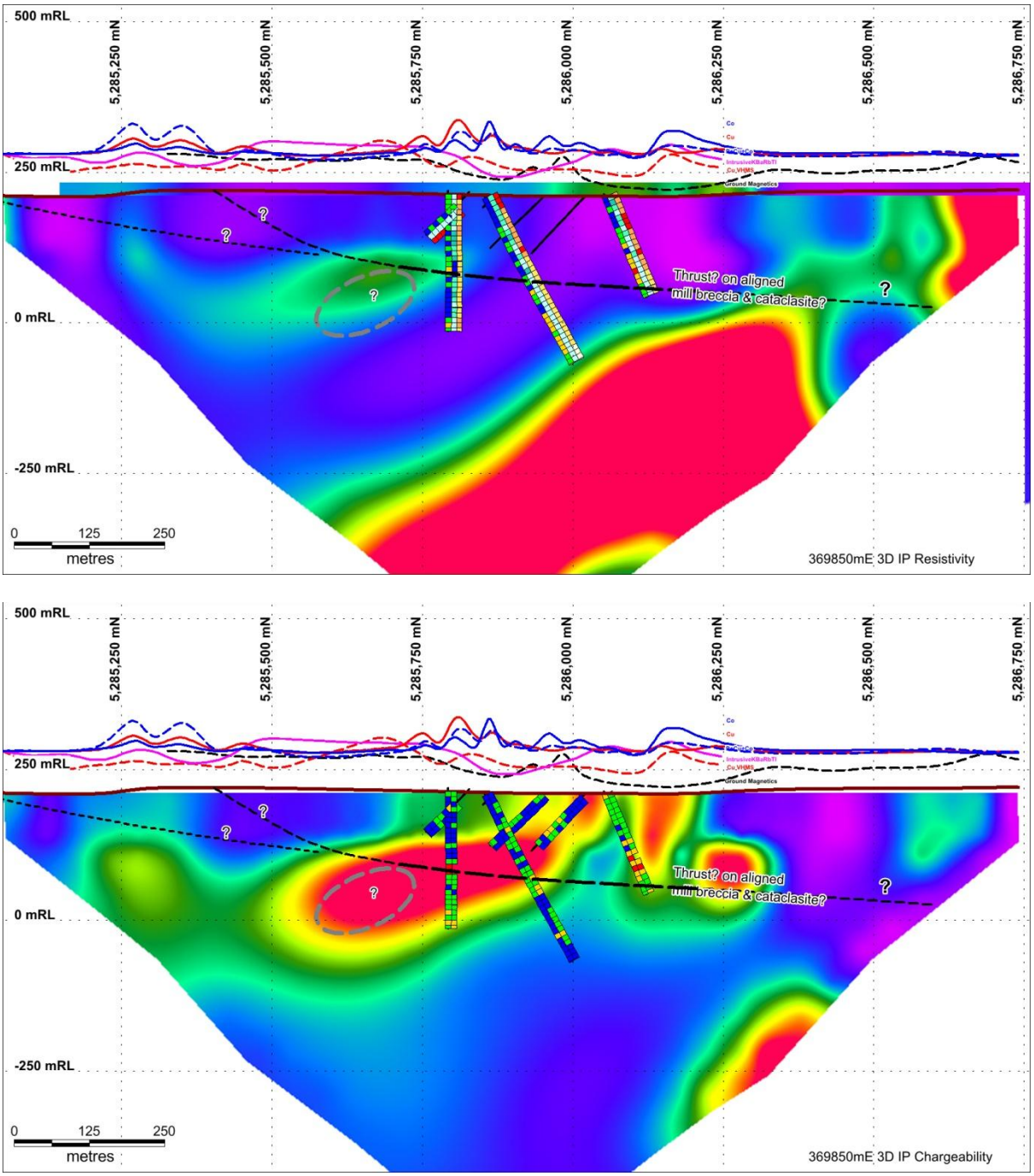

Figure 39: Section 369850mE showing drill hole traces (Left to right; WT, WT distal, KCs Indices), interpretation over 3D IP resistivity psuedosection (Top) and 3D IP chargeability psuedosection (bottom) with PCoCU & Vein indices as drill traces.

Broadly generalised alteration zonation is clearly evident from assessment of spatial distributions in drill holes. Pervasive silica alteration is more common in the NW of the drilled Thomas Creek area, with pervasive K Feldspar silicate dominant in core zone including TCDD001 and 3 (Also TCD3), whilst becoming more diffuse in TCDD002. Magnetite bearing veins are most common in TCDD004 and 1 with minor occurrences elsewhere. Whilst, broad primary(?) disseminated magnetite is prevalent throughout andesites in TCDD004 (Figure 38). Disseminated magnetite is also locally a key

constituent of diorites in the area, as is a local pervasive silica – magnetite alteration association. Biotite is noteworthy in TCDD002, but scarce elsewhere. Biotite associated with pervasive silica is noteworthy in TCDD002 and its coincidence with Thomas Creeks most significant intersection of 56m @ ~0.1% Cu is possibly a proximal indicator to ore, complimented by a high WT index zone/trend. The vector is possibly down plunge north towards the large MobileMT and 3D IP modelled resistor.

NE Conductor

The NE conductor (Figure 37) has high sulphidation Prince Lyell like potential with a likelihood of a late vein overprint. It's a moderate intensity relative MobileMT conductor with no IP or direct field data to compare, but favourable mineralisation and alteration vectors.

The Core resistor within the Thomas Creek Intrusive Complex possibly represents a source intrusion, with broad pervasive alteration hypothetically zoning east through a curious very high Ti/Zr anomaly (Zr / high field strength mobility; Figure 29) coincident with very high K radiometrics, then extending proximaly east to very high magnetics, followed by anomalous Cu in soils to within 100m of the defined NE MobileMT conductor margin (Figure 40). A thin (<50m?) intrusion of silicified diorite, bearing disseminated magnetite and minor pyrite, lies within and immediately south of the gossanous magnetite bearing zone with micromonzodiorite mapped to the north. This hypothetical broad alteration zonation potentially extends west from the fault splay filled large K rich micromonzodiorite; a potential source. i.e. Zonation might extend from devolatilising intrusive source (diorite?), to residual silica-magnetite, generating Ti mobility re-depositing adjacent to outward zoned pervasive K-Feldspar Silicate, driving chlorite-sericite-pyrite-chalcopyrite Prince Lyell like stringer mineralisation to shallower levels.

An approximately E-W 100m wide Cu anomalous soil zone closest to the MobileMT conductor locally bears hematitic (to 10% Fe), chloritic and pyritic (~0.5%) samples returning up to 641ppm Cu and 1130ppm P.

Rock chips from the northeastern area include silicified and magnetite bearing gossanous samples. The gossannous high magnetics coincident subcrop zone has ~20m N-S extent. Extensive cemented iron oxidised creek alluvium from the east flowing creek immediately north, suggests a likely E-W to NW strike. Sparse subhedral quartz crystals to ~2cm with attached dark mineral (tourmaline?) indicated fault hosted veining is nearby. Similarly further west is evidence of faulting along the magnetic rim.

Three rock chip samples (TCR021 to 23) comprised dark brown geothitic hematite and limonite with relict banding and cavities as well as mixed silicified disseminated magnetite bearing diorite. Magnetite – pyrite – silica veining was noted to reach 3% in silicified diorite. Overall, most metals from these highly leached gossanous samples report low. Au weakly detectable to 0.013ppm and Te to 0.13ppm were the only weakly elevated favourable gossanous elements, with Gemmell et al. (1998) noting that Au, Se, Te, As, Sb, Bi, Cd, In, Tl, Hg, Sn and Ba are useful trace elements related to gossanous VHMS. Gossan sample TCR021 returned >50% Fe. KFeldspar - silicate – silica and actinolite altered andesite and relict veined rock chips returned elevated Tl (0.23 & 0.3ppm) and weakly elevated Ba (320 to 1090ppm) from further NE; an intrusive and veined signature.

Core Resistor (MobileMT)

- High resistivity modelled conical plug extending to depth (Figure 37).

- -Ve Na and silica magnetite altered diorite to the immediate south in an area of broad spaced grid.
- High Pb, Zn "Leakage" zones nearby.
- Zoned from Thomas Creek TCDD002?
- Elevated magnetic shoulder to aeromagnetic rim
- Structure intersection coincident
- Large WNW aligned fault bounded high K & Ba anomalies suggesting proximal late volatile source micromonzodiorite (Figure 40)

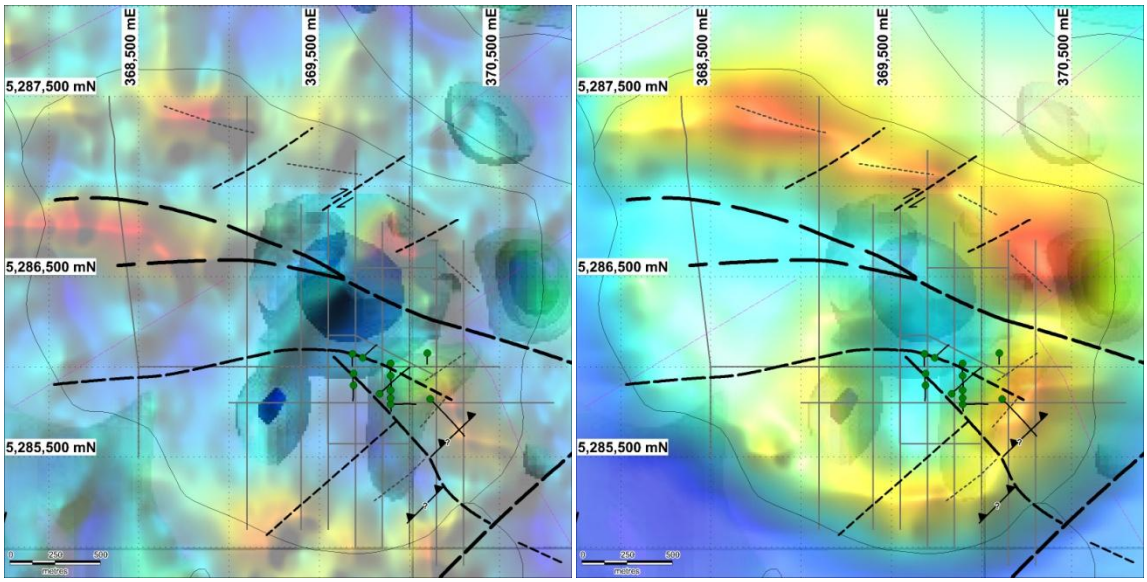

Figure 40: Mobile Magnetotellurics anomalies (green conductors and blue resistors) in the Thomas Creek vicinity displaying K radiometrics (left) and 1996 Geotem aeromagnetics (right) grid transparencies.

Thomas Creek South

The southern to south eastern portion of the Thomas Creek grid (Figure 37) displays a number of mineralisation and alteration features with mostly high sulphidation / Western Tharsis Cu potential, but some VHMS potential. Elevated soil Cu and Au analysis cover a relatively broad SW-NE trending zone.

Features:-

- A strong SW-NE striking soil anomalous zone of coincident high WT, PCuCo and TC vein index's, as well as AI, CCPI, Co, Cu, P , Fe and As.
- Metal and geochemical index anomaly tenor is consistently high w.r.t the core Thomas Creek drilled area.
- Soil Cu is lower tenor but possibly more consistently elevated that the main Thomas Creek Prospect data.
- Na depletion & WT like KCs depleted zone adjacent to south.
- Enveloping Intrusive K Feldspar index highs
- Proximal Aluminium (pyrophyllite?) highs

- High Tl+Sb indicative of Zn VHMS or possibly zoned proximal to Cu VHMS ore is near coincident with surface chargeability highs and rims anomalies
- Very low resistivity on 69850E at <5285210N lies along strike east of strong disseminated pyrite (3 to 8%) and moderate chlorite alteration in soils (high Tl), on the southern margin of a chargeabilty high, open along strike SW.
- At southern end of weak MobileMT conductor extending from the core of hte drilled Thomas Creek Prospect.
- moderately elevated magnetics.
- Strong oxidation in soil locally and micromonzodiorite mapped.
- New strong Cu stream -80# geochem, up-stream from chalcopyrite bearing rock.

Furthest SE possibly has VHMS potential, notably:-

- Coincident are potential VHMS proximity indicators Tl (0.45ppm soil survey high) and Sb in soils.
- At 370300E, 5300N is strong chargeability and low resistivity
- Area potentially projects shallowly to depth towards TCDD004, as a prospective VHMS horizon (Figure 38).
- Coincident K & Tl in the grid SE zone is possibly largely intrusive related? overprinting

Northern Magnetic Rim

- Coincidence of open Au and Cu anomalous rock chips and soils. The 0.1ppm Au & Cu anomaly in the north is possibly early alteration related, since it lacks a Rb, K and Ba intrusive signature.
- A weak restricted MobileMT conductor lies adjacent to the south of the aeromagnetic rim. Further exploration should encompass this feature.
- Pronounced NE (mineralisation) aligned spur extends N / NE to resistive anomaly at the intersection with siliciclastic Owen Group rocks (Potential North Lyell like mineralisation focus). No stream sediment cover.
- An IP chargeability anomaly is coincident with Cu and other indices in soils on 370000E, 5286950N. And at 369100E, 5287200N IP Chargeability lies adjacent to a magnetic high and inferred fault. On 9400E, IP chargeability is lifting at the end of survey.

Regional and MobileMT Interpretation

Clearly, a number of MobileMT anomalies require follow up regionally (Figure 41). Key anomalies are discussed with draft notes on each in Table 11. Some targets are accessible via track extensions from Thomas Creek.

A large resistive cone (2) widens to depth beneath the Thomas Creek NW structural intersection. Silica magnetite altered Diorite is mapped within on the margins of this zone. IP chargeability is notably immediately south east. However, in general IP at surface appears to correlate well with margins to K radiometrics and K in soils.

Notably, 3D modelling & interpretation shows that the peak of the Thomas Creek Prospect core MobileMT conductive body (3) lies between drill holes TCDD002 and 3, beneath TCD2 and is overlain by strong chargeability; a potential VHMS target?. The eastern extension of conductor (3) potentially

fits an interpreted large off hole conductor to the east of TCDD003. The southern end of the conductive blob (4) is coincident with chlorite and significant disseminated sulphides in soils.

Zones of relatively high resistivity extending from depth through WCVS / NCV to the basal Owen Group should be investigated (near surface 6, 9; conceptual deep 11, 18). The limestone of the Timbertops Syncline is notably poorly conductive, with a weakly conductive SW striking linear bisecting, which also hosts a spot high strong conductor (19) in the Upper Owen. 19 has weak potential as a structural target high above Cambrian intrusive, noting that hydrothermal activity at Mt Lyell ceased by around Upper Owen and certainly Gordon Group Limestone time; a Devonian granite – related distal Pb-Zn origin is weakly possible.

The huge resistor to the east (9) lies in a K Radiometric low, adjacent to highs, where aeromagnetics indicates the potential for proximal NCV. This zone lies axial to the Timbertops Syncline, at it's SSE end in an area of dome and basin potential, possibly reflecting a long lived hydrothermal system beneath.

Regionally, a number of conductive MobileMT anomalies to the west of Thomas Creek are evidently 1:250,000 scale mapped fault coincident (eg. 21 to 23). Their nature is as yet unexplained, lying mostly in within the WVS, which has black shale bearing potential. Thus, the series of fault adjacent strong conductors could in part represent fault focusing black shales. Subtle linear trends in 1VD regional aeromagnetics and individual MobileMT frequency grids shows there is potential for further as yet un-mapped andesite units in this area, recognising that VHMS exhalative potential exists regionally near coincident basalt-andesite-black shale horizons. Conductors adjacent to mapped andesite south of Thomas Creek are also of potential interest in this regard.

The NW to WNW fault splay interpreted through Thomas Creek potentially project west towards mapped fault coincident strong MobileMT conductors (21 & 22). Such structural intersections could represent a higher level relative to potentially mineralised intrusion at depth, with the possibility of a high sulphidation epithermal - Prince Lyell like setting requiring investigation. Note also there is some conjecture over where the VHMS prospective Tyndall Group – WCVS boundary sits south of Macquarie Harbour.

Stream coincident conductors beneath Quaternary and Tertiary rock should be interpreted with care. Some strong anomalies are clearly coincident with surficial Quaternary sediments and creek traces; which can also reflect faults. The semi consolidated Tertiary Sediments to the east are particularly conductive, possibly due to clay content and pore waters. Macquarie Harbour graben fill is potentially up to 500 to 750m thick (Forsyth et.al., 2014).

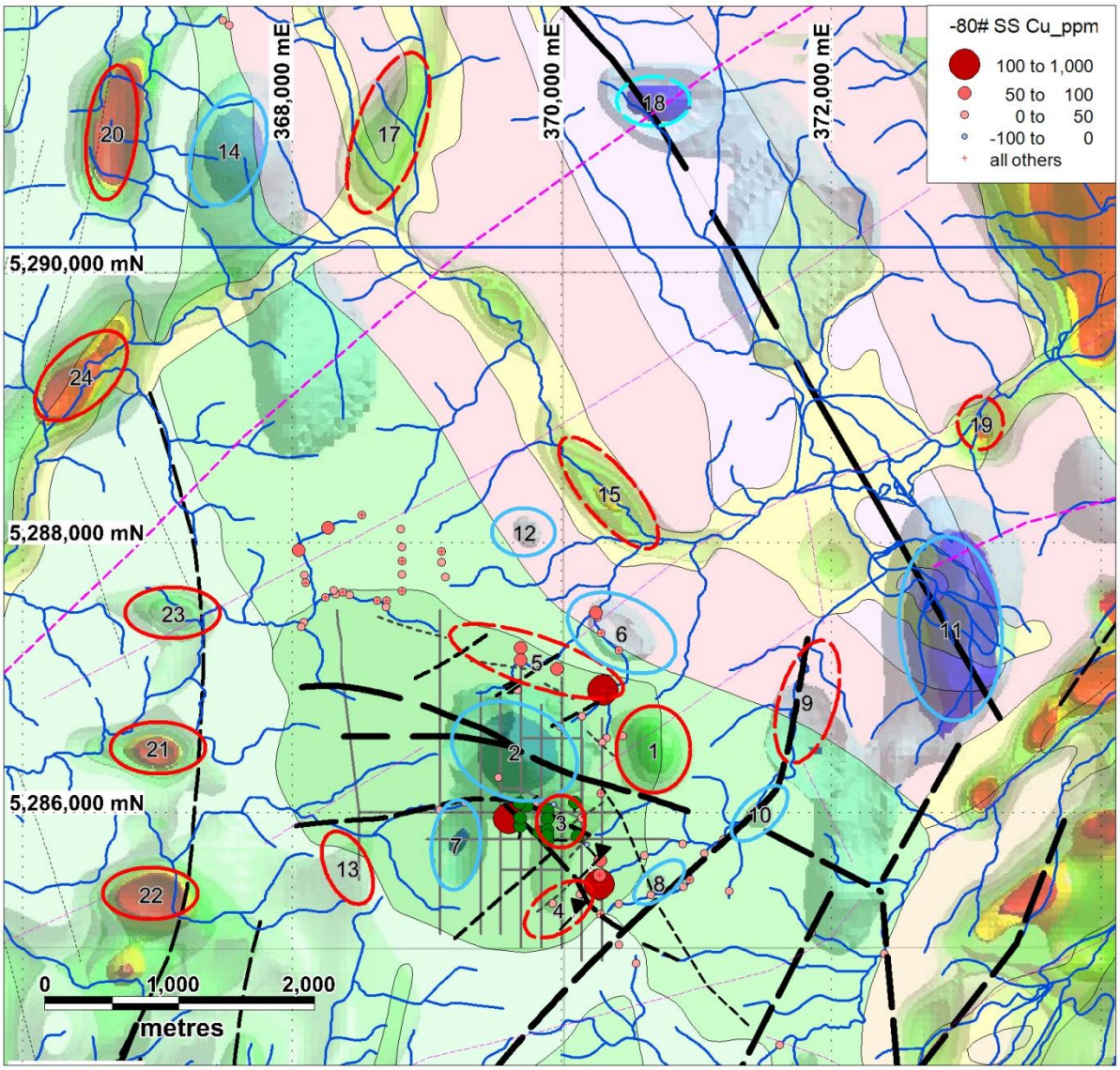

Figure 41: MobileMT anomalies (blue = resistivity & green = conductivity) and prospects in the Thomas Creek Area. DRAFT incomplete assessment focused Thomas Creek proximal.

Table 11: MobileMT anomalies and prospects in the Thomas Creek Area.

ID	MobMtPick	comment	Priority	Target/ Comment	EastGDA	NorthGDA
1	NE Conductor	NE mag / conductor at struc intersection	1	Prince Lyell Cu-Au	370682	5286465
2	Core Resistivity	Core Resitive Anomaly; Silica magnetite altered diorite plug?	3	Metal Source?	369651	5286452
3	TC Conductor	Conductor beneath the central Thomas Creek Prospect	2		369997	5285931
4	TC South	Cond, mag rim, soil anomalous SE TC. mapped / inferred intrusive complex margin	2		369979	5285281
5	N Mag Rim	Mag Rim, K Rad margins, near anomalous Cu soil, rock & drainage	2	Prince Lyell Cu-Au	369815	5287118
6	NE Resistor	Moderate sized Resistor; Silica?; Near Owen Group Contact, N Lyell potential	2	N Lyell, W Tharsis	370446	5287330
7	TC West	Resitive; Silica?; silica magnetite altered Diorite coincident to E	3	Prince Lyell Cu-Au	369216	5285759
8	SE Resistor Krad	Small Reistor; Silica? Resistor at K radiometric trend termination, lineament and rim feature edge.	3	W Tharsis	370723	5285482
9	E Resistor	Broad Resistor plunges SE to depth @ NCV - Owen contact, K Rad anomaly N end = leakage abour a near circular K Rad on fault?	4	N Lyell, W Tharsis	371822	5286821
10		Small Resistor; Silica? Fault intersection	5		371467	5285992
11	Resistivity High1	Strong Resitor; Silica? Fault intersection with Timbertops syncline, above long lived hydrothermal centre?; limestone bearing sequence (Gordon Group). Pb-Zn potential	4	distal N Lyell; broad alluvial cover, braided channels on Google	372884	5287361
12		Small Resistor; Silica?; Near Owen Group Contact, N Lyell potential	4	N Lyell	369719	5288076
13		weak MobMT conductor, mag rim, mapped / inferred intrusive complex margin	6		368412	5285590
14		Extensive Resitive; Silica?; Parallel / Near strong 1VD aeromag on Owen Group Contact, N Lyell potential	3		367529	5290905
15		Conductor parallel drainage; Quarternary fill?	5		370349	5288366
16	TimberTops1	Conductor at structural intersection, Felsic & Andesitic hosts, near Quartz-feldspar porphyry and Aeromag high.	2	VHMS, Porphyry Hydrid / Prince Lyell	367482	5297638
17		Conductor straddles drainage, N Lyell Potential? leakage in Lower Owen	4	N Lyell: Google shows broad flat S end conductor	368717	5291034
18		Radiometrics Lineament intersects Timbertops syncline hinge; limestone bearing sequence (Gordon Group). Pb-Zn potential	5		370681	5291265
19		Point source hgh conductor on weakly conductive K radiometrics lineament. Lower Owen; Late Pb-Zn vein (Devonian)?	3	N Lyell	373107	5288882
20		Strong MobMT conductor coincident with 1VD Aeromag, adjacent to E of sinistral fault and regionally a strong resistive zone extending to depth. = Andesite horizon? W side regional anticline?	3	VHMS?	366665	5291035
21		mod/stong MobMT conductor at Structural intersection of fault extension west of TC? Higher level w.r.t TC intrusives? Prince Lyell potential.	3		367007	5286478
22		Strong conductor at structural intersection of fault extension?? southwest of TC? Higher level w.r.t TC intrusives? Prince Lyell potential.	3		366952	5285398
23		weak MobMT conductor at Structural intersection of fault extension west of TC? Higher level w.r.t TC intrusives? Prince Lyell potential.	4		367118	5287477
24		Strong MobMT conductor at structural intersection? Prince Lyell potential.	4		366438	5289234

Proposed Work

- Further data review, capture, validation and development of GIS for interpretation and targeting.
- Undertake geological mapping, rock chip and stream sediment sampling, as tenement wide target assessment, particularly targeting new MobileMT targets, as well as known airborne magnetics, VTEM and GEOTEM anomalies.
- Gridding, IP, EM and soil sampling NE MobileMT conductive target.
- DHEM test on TCDD004; potential VHMS horizon(s).

Environment

Permission was granted for a work program to undertake up to four diamond drill holes at Thomas Creek within an area defined for gridding to facilitate IP and soil surveys. All works were undertaken within the guidelines of the Exploration Code of Practice.

Disturbance of flora and fauna was minimised during drill pad and grid clearing. Drill sites were cleared of vegetation to provide an approx 15 by 20m area. This allowed drill rig and associated gear to be helicopter sling loaded with enough space to stack loads and still pass freely and safely between. Large timber clearing was minimised where possible. Water required for drilling was sourced from a local creek and pumped >800m to the drill sites using 2 inch poly pipe. At Thomas Creek, a poly pipe T to the camp tank was utilised as required during low rainfall periods. Drilling return waters were bunded to catch drill cuttings before allowing the waters to disperse away from the rig.

Upon hole completion, rods were advanced down the hole with no rotation, enabling 40mm pvc pipe to be extended to the bottom of hole for later down hole EM survey. A reversible sub allowed the drill rod string to then be undone for retrieval leaving the pvc in the hole. All casing was removed. PVC pipe was capped below ground level after DHEM survey completion. A steel can was placed down hole at collar level to allow the covered hole to be relocated by metal detector at a later stage.

All equipment and associated items brought to the drill site were removed on hole completion. This involved “grid" searches for rubbish removal on several later occasions at each site. Rubbish was removed from camp on a regular basis, with portable toilets swapped out as required.

Helicopter flight paths avoided known threatened species locations, principally the Orange Bellied Parrot no fly zone on the Sorell Peninsular from 20th September to 15th November and 15th February to 10th May.

The Thomas Creek camp (Photo 3) comprised a helicopter slung 5.5 by 2.5m hut with generator, portable toilet and shower units provided core services for the Thomas Creek field camp. A 1000l water tank and pressure pump ran the portable shower and plumbed kitchen sink. Gas was utilised for heating and hot water, as well as two fridge freezers. An L shaped tarpaulin covered wooden deck provided shelter around the hut. Personnel were accommodated in Edrill’s 2 helicopter slung pods as well as in tents on removable 2.5m^2 wooden platforms. Wooden walk ways were installed in

camp on high travel routes, elsewhere <15cm branch cording, from site and grid clearing were used where required. Consequently, mud bogs and erosion of the surface around camp was minimised.

A camp at Noddy Creek serviced Young Henry exploration last tenure year and was similarly constructed to the Thomas Creek camp.

Fuels were stored in appropriate containers within designated bund areas at the helipad and in camp. Fuel-spill kits were kept on-site. Firefighting equipment was kept on-site near fuel storage and in camp where mechanical, gas and electrical equipment was used.

Photo 3: Thomas Creek camp and drill pads (TCDD004 on right), view NNW (December 2018, EL06/2013).

References

Berry, R. F., 2014. Middle Cambrian Tectonics – The Tyennan Orogeny Stage 2. In Corbett, K. D, Quilty, P. G., and Calver, C. R., (eds). 2014. Geological Evolution of Tasmania. Geol Soc Aust. Special Publication 24.

Bottrill, R. S. and Unwin, L., 2019. Mineralogical Analyses, Thomas Creek Prospect. Mineralogical / Petrological Report LJN2018-143 by Mineral Resources Tasmania.

Brown, A. V. 1988. Geological Atlas 1:50 000 series. Sheet 78 (7912S). Montgomery. Department of Mines Tasmania.

Brown, A. V.; Findlay, R. H.; McClenaghan, M. P.; Seymour, D. B. 1991. Synopsis of the regional geology of the Macquarie Harbour, Point Hibbs and Montgomery 1:50 000 map sheets. Report Department of Resources and Energy Tasmania 1991/21.

Brown, A. V.; Findlay, R. H.; McClenaghan, M. P. 1993. Summary of the regional geology of the Macquarie Harbour, Point Hibbs and Montgomery 1:50 000 map sheets. Report Department of Resources and Energy Tasmania 1991/02.

Calver, C (etal., 2014). In Corbett, K. D, Quilty, P. G., and Calver, C. R., (eds). 2014. Geological Evolution of Tasmania. Geol Soc Aust. Special Publication 24.

Close, R.J. and Reid, R.O. 1995 Annual Report on Exploration Activity for the 12 months to August 1995. EL's 4/92 and 7/92. Sorell Peninsula. Unpublished Tasmanian Mines Department Report. Plutonic Operations Ltd.

Corbett, K. D, 2014. The Mt Lyell Field. In Corbett, K. D, Quilty, P. G., and Calver, C. R., (eds). 2014. Geological Evolution of Tasmania. Geol Soc Aust. Special Publication 24.

Corbett, K. D, Quilty, P. G., and Calver, C. R., (eds). 2014. Geological Evolution of Tasmania. Geol Soc Aust. Special Publication 24.

Corbett, K.D. and Solomon, M. 1989 Cambrian Mt Read Volcanics and Associated Mineral Deposits. In C.F. Burrett and E.L. Martin (Editors), Geology and Mineral Resources of Tasmania. Geol. Soc. Aust. Spec. Publ. 15: 84-153

Crawford. A. J., Everard. J. L., and Bottrill, R. S. 2014. Mafic-Ultramafic Complexes and Associated Mineral Deposits. in Calver et al., eds 2014).

Forsyth et.al., 2014. Cenozoic Onshore Basins and Landscape Evolution. In Corbett, K. D, Quilty, P. G., and Calver, C. R., (eds). 2014. Geological Evolution of Tasmania. Geol Soc Aust. Special Publication 24.

Gemmell, B. J., Large, R. R., and Zaw, K., 1998 Palaeozoic volcanic-hosted massive sulphide deposits. AGSO Journal of Australian Geology and Geophysics. 17(4). 129-137.

Hall, W. D. M., McIntyre, M. I., Corbett, E. B., McGregor, P. W., Fenton, G. R., Arndt, C. D. And Bumstead, E. D. 1969. Report on Field Work in Exploration Licence 13/65, South-west Tasmania during 1967-68 field season. BHP. Unpublished Company Report for MRT.

Huston and Kamprad (2000), The Western Tharsis deposit, A high sulphidation Cu-Au deposit in the Mt Lyell field, of possible Ordovician age. AGSO Research Newsletter May 2000, no. 32

Kary, G., 1985. Progress Report Twelve Months to September 1985 Sorell Peninsula Exploration Licences 35/83, 36/83 and 37/83 Tasmania. Amoco Minerals Australia Company. Unpublished Company Report for MRT.

Langlands, J. G., 1971. E.L. 13/65 Cape Sorell Peninsula, S. W. Tasmania Exploration for Chrysotile Asbestos in the Hibbs Belt Noddy Creek and Pad 2 to Asbestos Point 1970/71. BHP. Unpublished Company Report for MRT.

McClenaghan and Findlay, 1989 Macquarie Harbour. Geological Atlas 1:50 000 series. Tasmanian Department of Mines.

McClenaghan, M. P.; Findlay, R. H. 1993. Geological Atlas 1:50 000 series. Sheet 64 (7913S). Macquarie Harbour. Explanatory Report Geological Survey Tasmania.

Reid, P.W, van der Stelt, B.J. and Ascough G.L. 2014. Combined Annual Technical Report– Sorell Project EL6/2013 & EL7/2013, Sorell Peninsula, Tasmania, For the period 22nd October 2013 to 21st October 2014. Unpublished Company Report, MRT Tasmania.

Reid, P.W, van der Stelt, B.J. and Ascough G.L. 2015. Combined Annual Technical Report– Sorell Project EL6/2013 & EL7/2013, Sorell Peninsula, Tasmania, For the period 22nd October 2014 to 21st October 2015. Unpublished Company Report, MRT Tasmania

Reid, P.W, Van Der Stelt, B.J. and Ascough G.L. 2016. Combined Annual Technical Report– Sorell Project EL6/2013 & EL7/2013, Sorell Peninsula, Tasmania, For the period 22nd October 2015 to 21st October 2016. Unpublished Company Report, MRT Tasmania

R. Reid, R. O., McClenaghan M. P. and Seymour D. B. 201?. New whole-rock geochemical analyses of the Middle Cambrian Thomas Creek intrusive complex and associated lavas of the Noddy Creek Volcanics, western Tasmania

R. Reid, R. O. 2001. Cambrian Intrusion Related Copper Mineralisation at the Thomas Creek Prospect, Southwestern Tasmania. Masters of Economic Geology Thesis. CODES University of Tasmania.

Raymond, O. L. 1996. Pyrite composition and ore genesis in the Prince Lyell copper deposit, Mt Lyell mineral field, western Tasmania, Australia. Ore Geology Reviews 10(3):231-250.

White, N.C. 1975 Cambrian Volcanism and mineralisation, south-west Tasmania. PhD Thesis (unpublished), University of Tasmania

Appendix

Appendix 1: List of Appended Digital Files

Exploration Work Type	Filename	File format
Report	EL062013_201910_01_Report.pdf	*pdf*
Drilling		
	EL062013_201910_02_SL_1.xls	*xls*
	EL062013_201910_03_DS_1.xls	*xls*
	EL062013_201910_04_DL_1.xls	*xls*
	EL062013_201910_05_Lithologycodes.xls	*xls*
	EL062013_201910_06_DG_1.xls	*xls*
	EL062013_201910_07_DStructure_1.xls	*xls*
	EL062013_201910_08_DGeoTech_1.xls	*xls*
	EL062013_201910_09_DG_PortableXRF.xls	*xls*
	EL062013_201910_10_AnalysisBU18302927	*pdf*
	EL062013_201910_11_AnalysisBU19028743	*pdf*
	EL062013_201910_12_AnalysisBU18302927_QC	*pdf*
	EL062013_201910_13_TCDD004CorePhotos	*zip*
	EL062013_201910_14_TCDD004Hylogger.zip	*zip*
	EL062013_201910_15_LJN2018-130.pdf	*pdf*
	EL062013_201910_16_LJN2018-143.docx	*docx*
Surface sampling		
	EL062013_201910_17_SG_1.xls	*xls*
	EL062013_201910_18_SG_PortableXRF.xls	*xls*
	EL062013_201910_19_AnalysisAD18286728	*pdf*
	EL062013_201910_20_AnalysisAD18286732	*pdf*
	EL062013_201910_21_AnalysisAD18313747	*pdf*
	EL062013_201910_22_AnalysisAD18313753	*pdf*
	EL062013_201910_23_AnalysisAD18313760	*pdf*
	EL062013_201910_24_AnalysisAD19011054	*pdf*
	EL062013_201910_25_AnalysisAD19011059	*pdf*
	EL062013_201910_26_AnalysisAD19011061	*pdf*
	EL062013_201910_27_AnalysisAD18286728_QC	*pdf*
	EL062013_201910_28_AnalysisAD19011054_QC	*pdf*
	EL062013_201910_29_AnalysisAD19011059_QC	*pdf*
	EL062013_201910_30_AnalysisAD19011061_QC	*pdf*
Other (specify)		
	EL062013_201910_31_Expert_MobMtReport.zip	*zip*
	EL062013_201910_32_CG_MobMT_3Dinv.zip	*zip*
	EL062013_201910_33_MobMt_model_final.zip	*zip*
	EL062013_201910_34_SGC_MobMTprelimresults.docx	*docx*
	EL062013_201910_35_SGC_MobMTpreltargets.zip	*zip*
	EL062013_201910_36_SGC_3DINVdxfmodels.zip	*zip*
File Verification Listing *(this file)*	EL062013_201910_37_FileListing.xls	*xls*

Appendix 2: Thomas Creek Soil Geochemistry Correlations

TC Soil Correlations	Au ppm	Ag ppm	Al%	As ppm	Ba ppm	Be ppm	Bi ppm	Ca %	Cd ppm	Ce ppm	Co ppm	Cr ppm	Cs ppm	Cu ppm	Fe %	Ga ppm	Ge ppm	Hf ppm	Hg ppm	In ppm	K %	La ppm	Li ppm
Au ppm	1.00																						
Ag ppm	0.76	1.00																					
Al%	-0.08	0.03	1.00																				
As ppm	0.27	0.30	0.11	1.00																			
Ba ppm	0.06	0.14	0.33	-0.03	1.00																		
Be ppm	-0.01	0.10	0.53	0.23	0.26	1.00																	
Bi ppm	0.21	0.19	0.15	0.47	0.14	0.10	1.00																
Ca %	0.07	0.06	0.10	0.16	-0.01	0.36	-0.02	1.00															
Cd ppm	0.07	0.14	-0.13	0.23	-0.18	0.08	0.01	0.08	1.00														
Ce ppm	0.19	0.32	0.10	0.34	0.39	0.35	0.20	0.16	0.11	1.00													
Co ppm	0.40	0.43	-0.05	0.44	-0.02	0.14	0.22	0.12	0.25	0.27	1.00												
Cr ppm	-0.02	-0.03	0.10	0.08	-0.14	-0.15	0.12	0.04	0.03	-0.11	0.03	1.00											
Cs ppm	-0.05	0.03	0.33	0.09	0.13	0.39	0.09	-0.16	0.07	0.05	0.05	-0.01	1.00										
Cu ppm	0.46	0.44	-0.06	0.42	-0.03	0.09	0.24	0.09	0.16	0.27	0.93	0.02	-0.01	1.00									
Fe %	0.00	-0.07	0.17	0.42	-0.21	0.03	0.19	0.14	-0.05	-0.04	0.08	0.33	-0.03	0.08	1.00								
Ga ppm	-0.02	0.06	0.82	0.25	0.30	0.41	0.24	0.18	-0.10	0.22	0.07	0.16	0.18	0.08	0.36	1.00							
Ge ppm	0.04	0.10	0.27	0.45	0.09	0.25	0.17	0.06	-0.03	0.36	0.13	0.13	0.11	0.14	0.63	0.36	1.00						
Hf ppm	-0.09	-0.01	0.63	0.04	0.48	0.42	0.17	-0.01	-0.09	0.17	-0.07	-0.10	0.21	-0.07	-0.08	0.46	0.08	1.00					
Hg ppm	0.30	0.44	0.08	0.50	-0.13	0.13	0.49	0.11	0.66	0.15	0.51	-0.01	-0.02	0.48	0.17	0.21	0.18	0.27	1.00				
In ppm	0.22	0.24	0.38	0.39	0.08	0.20	0.37	0.21	0.00	0.24	0.28	0.35	0.08	0.36	0.40	0.51	0.37	0.15	0.39	1.00			
K %	0.03	0.17	0.52	0.00	0.78	0.39	0.16	-0.12	-0.05	0.32	0.03	-0.14	0.30	-0.02	-0.19	0.33	0.09	0.52	-0.02	0.07	1.00		
La ppm	0.24	0.36	0.06	0.33	0.36	0.32	0.20	0.12	0.12	0.97	0.27	-0.10	0.03	0.27	-0.06	0.17	0.33	0.15	0.14	0.22	0.29	1.00	
Li ppm	-0.01	-0.01	0.42	0.17	0.12	0.27	0.10	0.06	0.05	0.07	0.04	0.27	0.15	0.01	0.31	0.46	0.24	0.15	0.27	0.40	0.18	0.06	1.00
Mg %	0.04	0.04	0.21	0.12	0.15	0.40	0.05	0.53	0.13	0.20	0.11	0.29	0.04	0.05	0.16	0.25	0.11	0.07	0.28	0.22	0.15	0.17	0.59
Mn ppm	-0.02	0.01	0.22	0.06	0.17	0.39	0.02	0.43	0.04	0.08	0.04	0.18	0.02	0.00	0.17	0.21	0.12	0.08	0.15	0.24	0.12	0.07	0.50
Mo ppm	0.11	0.05	0.03	0.17	-0.02	0.07	0.09	-0.03	-0.02	0.09	0.10	0.03	-0.04	0.13	0.02	0.05	0.03	0.01	0.34	0.05	0.02	0.07	0.04
Na %	-0.04	0.03	0.29	-0.07	0.17	0.43	-0.13	0.49	-0.04	0.03	-0.03	-0.21	0.00	-0.05	-0.12	0.14	-0.08	0.19	-0.02	-0.07	0.09	0.02	-0.02
Nb ppm	-0.12	-0.05	0.63	0.06	0.36	0.35	0.13	0.11	-0.11	0.10	-0.07	-0.08	0.16	-0.07	-0.02	0.52	0.06	0.86	-0.07	0.18	0.39	0.07	0.15
Ni ppm	0.12	0.17	0.13	0.43	-0.03	0.21	0.13	0.31	0.24	0.18	0.50	0.24	0.06	0.30	0.25	0.20	0.20	-0.02	0.62	0.21	0.04	0.14	0.28
P ppm	0.34	0.32	-0.08	0.50	-0.07	0.14	0.18	0.42	0.11	0.42	0.53	0.03	-0.03	0.47	0.23	0.10	0.30	-0.08	0.29	0.33	-0.06	0.37	0.02
Pb ppm	0.00	0.05	0.19	0.20	0.03	0.05	0.16	0.05	0.11	0.08	0.11	0.15	-0.02	0.10	0.25	0.22	0.22	0.18	0.08	0.18	0.06	0.07	0.15
Rb ppm	-0.01	0.15	0.59	0.03	0.66	0.48	0.16	-0.14	-0.03	0.26	0.03	-0.11	0.45	-0.02	-0.19	0.38	0.09	0.56	0.12	0.09	0.90	0.22	0.19
Re ppm	0.29	0.34	-0.07	0.38	-0.04	0.12	0.17	0.13	0.31	0.27	0.80	0.02	0.03	0.63	0.04	-0.01	0.11	-0.09	0.60	0.13	0.06	0.27	-0.01
S %	0.27	0.36	-0.02	0.46	-0.03	0.17	0.17	0.09	0.34	0.26	0.82	0.00	0.13	0.65	0.03	0.02	0.10	-0.04	0.51	0.12	0.08	0.26	-0.02
Sb ppm	0.02	0.10	0.12	0.10	0.01	0.14	0.09	-0.06	0.14	0.05	0.07	-0.01	0.32	0.05	-0.02	0.06	0.06	0.06	0.65	0.04	0.15	0.04	0.01
Sc ppm	0.27	0.36	0.34	0.43	0.18	0.42	0.23	0.27	0.07	0.47	0.59	0.23	0.18	0.64	0.14	0.38	0.29	0.19	0.32	0.53	0.19	0.44	0.26
Se ppm	0.01	-0.02	0.23	0.37	-0.26	-0.11	0.23	0.09	0.04	-0.09	0.06	0.38	-0.04	0.03	0.59	0.39	0.29	0.00	0.07	0.37	-0.19	-0.11	0.28
Sn ppm	0.27	0.27	0.32	0.28	0.18	0.24	0.29	0.20	-0.02	0.33	0.44	0.06	0.00	0.52	0.06	0.42	0.13	0.29	0.40	0.46	0.17	0.32	0.05
Sr ppm	-0.04	0.05	0.37	-0.01	0.37	0.44	-0.02	0.63	0.02	0.17	-0.02	-0.16	-0.02	-0.05	-0.09	0.30	0.00	0.29	0.07	0.08	0.32	0.15	0.09
Ta ppm	-0.11	-0.04	0.61	0.03	0.37	0.39	0.10	0.08	-0.12	0.10	-0.09	-0.16	0.16	-0.08	-0.07	0.47	0.05	0.86	0.21	0.14	0.40	0.07	0.12
Te ppm	0.20	0.18	0.01	0.36	-0.04	0.02	0.64	-0.05	0.01	0.03	0.22	0.13	-0.01	0.20	0.17	0.09	0.07	0.00	0.57	0.15	0.03	0.03	-0.01
Th ppm	0.13	0.17	0.38	0.46	0.10	0.40	0.18	0.24	0.01	0.45	0.15	0.13	0.02	0.20	0.31	0.51	0.47	0.29	0.14	0.44	0.08	0.39	0.21
Ti %	-0.10	0.01	0.72	0.09	0.39	0.41	0.14	0.18	-0.09	0.11	-0.06	-0.07	0.22	-0.06	0.01	0.58	0.12	0.80	-0.08	0.26	0.39	0.07	0.20
Tl ppm	-0.01	0.19	0.63	0.10	0.63	0.52	0.18	-0.11	0.08	0.29	0.10	-0.09	0.49	0.02	-0.16	0.43	0.11	0.55	0.37	0.15	0.85	0.25	0.26
U ppm	0.41	0.41	0.09	0.33	0.10	0.16	0.28	0.07	0.10	0.31	0.89	0.01	0.05	0.93	0.06	0.19	0.16	0.13	0.45	0.35	0.11	0.31	0.02
V ppm	-0.03	0.01	0.36	0.41	-0.04	0.19	0.18	0.30	0.02	0.17	0.09	0.24	0.08	0.09	0.64	0.59	0.42	0.07	0.11	0.41	-0.03	0.08	0.27
W ppm	0.28	0.29	0.26	0.36	0.27	0.21	0.43	-0.07	-0.05	0.25	0.52	-0.06	0.21	0.56	0.07	0.26	0.20	0.30	0.41	0.38	0.38	0.22	0.12
Y ppm	0.23	0.34	0.12	0.45	0.27	0.48	0.20	0.39	0.12	0.82	0.43	-0.05	0.10	0.43	0.07	0.26	0.38	0.15	0.25	0.37	0.23	0.75	0.14
Zn ppm	0.04	0.08	0.17	0.18	0.14	0.28	0.11	0.06	0.39	0.16	0.13	0.19	0.15	0.05	0.14	0.18	0.17	0.03	0.60	0.27	0.16	0.15	0.58
Zr ppm	-0.09	-0.02	0.60	0.03	0.47	0.40	0.16	-0.01	-0.09	0.16	-0.08	-0.12	0.20	-0.07	-0.09	0.43	0.07	0.99	0.25	0.13	0.50	0.15	0.14

TC Soil Correlations	Rb ppm	Re ppm	S %	Sb ppm	Sc ppm	Se ppm	Sn ppm	Sr ppm	Ta ppm	Te ppm	Th ppm	Ti %	Tl ppm	U ppm	V ppm	W ppm	Y ppm	Zn ppm	Zr ppm
Au ppm																			
Ag ppm																			
Al%																			
As ppm																			
Ba ppm																			
Be ppm																			
Bi ppm																			
Ca %																			
Cd ppm																			
Ce ppm																			
Co ppm																			
Cr ppm																			
Cs ppm																			
Cu ppm																			
Fe %																			
Ga ppm																			
Ge ppm																			
Hf ppm																			
Hg ppm																			
In ppm																			
K %																			
La ppm																			
Li ppm																			
Mg %																			
Mn ppm																			
Mo ppm																			
Na %																			
Nb ppm																			
Ni ppm																			
P ppm																			
Pb ppm																			
Rb ppm	1.00																		
Re ppm	0.03	1.00																	
S %	0.10	0.89	1.00																
Sb ppm	0.21	0.09	0.09	1.00															
Sc ppm	0.24	0.42	0.45	0.13	1.00														
Se ppm	-0.18	0.18	0.17	0.03	0.08	1.00													
Sn ppm	0.18	0.25	0.24	0.05	0.59	0.09	1.00												
Sr ppm	0.27	-0.01	-0.02	-0.02	0.14	-0.11	0.18	1.00											
Ta ppm	0.42	-0.09	-0.08	0.04	0.12	0.05	0.33	0.30	1.00										
Te ppm	0.07	0.26	0.26	0.03	0.13	0.23	0.25	-0.10	-0.07	1.00									
Th ppm	0.12	0.06	0.08	0.03	0.42	0.28	0.34	0.11	0.29	0.07	1.00								
Ti %	0.45	-0.08	-0.04	0.10	0.24	0.11	0.36	0.38	0.83	-0.07	0.25	1.00							
Tl ppm	0.91	0.14	0.22	0.19	0.28	-0.11	0.18	0.28	0.44	0.05	0.13	0.48	1.00						
U ppm	0.11	0.58	0.59	0.04	0.60	0.00	0.58	0.03	0.08	0.21	0.25	0.08	0.14	1.00					
V ppm	0.01	0.02	0.05	0.07	0.26	0.47	0.21	0.11	0.10	0.10	0.47	0.30	0.06	0.09	1.00				
W ppm	0.37	0.30	0.31	0.10	0.41	0.06	0.51	0.04	0.27	0.31	0.24	0.29	0.34	0.62	0.16	1.00			
Y ppm	0.22	0.36	0.36	0.05	0.62	-0.03	0.40	0.22	0.12	0.05	0.57	0.15	0.25	0.43	0.31	0.35	1.00		
Zn ppm	0.17	0.12	0.05	0.07	0.25	-0.03	-0.03	0.08	-0.03	-0.02	0.06	0.03	0.24	0.04	0.09	0.03	0.19	1.00	
Zr ppm	0.54	-0.09	-0.05	0.04	0.17	-0.01	0.28	0.29	0.86	0.00	0.27	0.79	0.53	0.13	0.05	0.29	0.14	0.02	1.00

Appendix 3: Thomas Creek Drill Core Geochemistry Correlations

Drill Core Correlation	*Au ppm*	*Ag ppm*	*Al%*	*As ppm*	*Ba ppm*	*Be ppm*	*Bi ppm*	*Ca %*	*Cd ppm*	*Ce ppm*	*Co ppm*	*Cr ppm*	*Cs ppm*	*Cu ppm*	*Fe %*	*Ga ppm*	*Ge ppm*	*Hf ppm*	*In ppm*	*K %*	*La ppm*	*Li ppm*	*Mg %*	*Mn ppm*	*Mo ppm*	*Na %*	*Nb ppm*	*Ni ppm*	*P ppm*
Au ppm	1.00																												
Ag ppm	0.10	1.00																											
Al%	-0.07	-0.26	1.00																										
As ppm	0.11	0.39	-0.28	1.00																									
Ba ppm	0.03	-0.05	0.15	-0.05	1.00																								
Be ppm	0.01	-0.08	0.25	-0.04	0.04	1.00																							
Bi ppm	0.08	0.52	-0.27	0.62	-0.08	-0.01	1.00																						
Ca %	0.03	-0.03	-0.04	0.30	-0.36	-0.02	-0.10	1.00																					
Cd ppm	0.00	0.36	-0.01	0.07	-0.08	-0.09	0.16	0.01	1.00																				
Ce ppm	0.11	0.29	-0.13	0.29	0.09	0.21	0.31	0.05	-0.07	1.00																			
Co ppm	0.04	0.50	-0.17	0.39	-0.16	-0.04	0.40	-0.01	0.11	0.22	1.00																		
Cr ppm	0.03	-0.07	0.06	-0.11	-0.24	-0.29	-0.13	0.25	-0.02	-0.09	-0.04	1.00																	
Cs ppm	-0.01	-0.19	0.20	-0.03	-0.25	-0.01	-0.14	-0.04	-0.05	-0.01	-0.05	0.03	1.00																
Cu ppm	0.15	0.55	-0.29	0.41	-0.11	-0.10	0.36	0.10	0.24	0.25	0.26	-0.03	-0.15	1.00															
Fe %	0.13	0.28	-0.39	0.52	0.01	-0.12	0.33	0.28	0.02	0.27	0.36	-0.04	-0.03	0.39	1.00														
Ga ppm	0.05	-0.12	0.42	-0.05	0.10	0.44	-0.06	0.01	-0.13	0.35	-0.02	-0.22	0.31	-0.15	0.07	1.00													
Ge ppm	0.10	0.28	-0.35	0.38	0.00	0.08	0.43	0.05	-0.07	0.69	0.34	-0.16	-0.02	0.23	0.38	0.27	1.00												
Hf ppm	-0.03	-0.16	0.40	-0.11	0.43	0.31	-0.06	-0.27	-0.13	0.12	-0.17	-0.13	0.04	-0.25	0.02	0.33	-0.11	1.00											
In ppm	0.04	0.19	-0.20	0.25	0.06	0.03	0.23	0.30	0.00	0.27	0.07	0.14	-0.31	0.26	0.34	0.02	0.35	0.00	1.00										
K %	0.04	-0.07	0.28	-0.04	0.85	0.10	-0.03	-0.41	-0.11	0.14	-0.09	-0.30	-0.11	-0.13	-0.04	0.17	0.04	0.49	0.03	1.00									
La ppm	0.10	0.31	-0.10	0.21	0.02	0.22	0.34	0.03	-0.03	0.80	0.44	-0.06	-0.04	0.23	0.23	0.36	0.76	0.05	0.23	0.08	1.00								
Li ppm	0.05	-0.09	0.00	-0.11	0.09	0.14	-0.08	-0.16	-0.15	0.16	-0.16	0.07	0.12	-0.07	0.18	0.35	0.08	0.31	0.13	-0.01	0.09	1.00							
Mg %	0.02	-0.06	-0.01	-0.06	-0.12	-0.16	-0.27	0.55	0.00	-0.01	-0.07	0.52	-0.05	0.06	0.25	0.04	-0.09	-0.20	0.29	-0.28	-0.01	0.28	1.00						
Mn ppm	0.06	0.05	-0.05	0.01	0.32	0.05	0.01	0.02	-0.11	0.16	-0.08	0.09	-0.33	-0.01	0.25	0.11	0.12	0.19	0.44	0.20	0.13	0.44	0.38	1.00					
Mo ppm	0.02	0.40	-0.07	0.26	-0.09	-0.03	0.24	-0.08	0.03	0.18	0.82	-0.03	-0.05	0.07	0.16	-0.01	0.15	-0.09	0.00	-0.04	0.22	-0.12	-0.13	-0.07	1.00				
Na %	-0.09	-0.07	0.50	-0.15	-0.33	0.24	-0.11	0.19	0.12	-0.24	-0.07	0.11	-0.24	-0.06	-0.35	-0.02	-0.38	0.02	-0.08	-0.35	-0.18	-0.21	0.01	-0.10	-0.02	1.00			
Nb ppm	-0.02	-0.06	0.43	-0.09	0.46	0.43	-0.16	-0.01	0.02	0.04	-0.12	-0.16	-0.32	-0.02	-0.09	0.21	-0.21	0.50	0.04	0.48	0.02	-0.06	0.01	0.14	-0.11	0.26	1.00		
Ni ppm	0.03	0.35	-0.22	0.41	-0.24	-0.21	0.31	0.18	0.30	-0.03	0.26	0.07	-0.12	0.68	0.38	-0.32	0.04	-0.36	0.15	-0.28	-0.01	-0.22	0.11	-0.14	0.02	0.11	-0.03	1.00	
P ppm	0.07	0.09	-0.23	0.49	-0.07	-0.01	0.16	0.47	-0.04	0.30	0.02	-0.08	0.02	0.14	0.40	0.10	0.38	-0.16	0.28	-0.09	0.13	-0.08	0.13	0.03	-0.02	-0.12	-0.12	0.14	1.00
Pb ppm	0.04	0.45	-0.07	0.13	-0.07	0.07	0.38	0.02	0.48	0.22	0.46	-0.04	-0.05	0.16	0.18	0.05	0.28	-0.10	0.11	-0.04	0.41	-0.10	0.00	0.01	0.28	-0.03	-0.01	0.15	-0.01
Rb ppm	0.03	-0.13	0.34	-0.08	0.63	0.21	-0.12	-0.16	-0.16	0.17	-0.16	-0.20	-0.03	-0.17	0.13	0.33	-0.01	0.63	0.07	0.78	0.11	0.18	-0.05	0.29	-0.11	-0.21	0.55	-0.33	-0.08
Re ppm	0.04	0.44	-0.09	0.19	-0.19	0.04	0.36	0.04	0.16	0.25	0.42	0.07	-0.14	0.38	0.13	-0.08	0.20	-0.21	0.08	-0.20	0.35	-0.12	-0.03	-0.08	0.43	0.19	-0.03	0.36	-0.01
S %	0.03	0.40	-0.10	0.35	-0.39	-0.21	0.44	-0.05	0.27	0.04	0.55	0.00	0.20	0.49	0.21	-0.22	0.15	-0.35	-0.10	-0.26	0.16	-0.33	-0.18	-0.35	0.31	0.01	-0.28	0.67	0.02
Sb ppm	0.03	0.11	-0.09	0.27	-0.01	0.06	0.11	0.26	-0.03	0.21	0.09	-0.10	0.17	0.06	0.21	0.12	0.13	0.07	0.23	0.02	0.17	0.00	-0.02	0.06	0.05	-0.14	0.01	0.01	0.16
Sc ppm	0.00	0.08	0.17	0.03	-0.17	-0.10	-0.01	0.39	0.09	0.09	0.19	0.45	0.02	0.18	0.22	0.09	0.04	-0.11	0.25	-0.25	0.22	0.13	0.67	0.21	0.02	0.13	0.02	0.24	-0.02
Se ppm	0.00	0.32	-0.18	0.32	-0.31	-0.23	0.27	0.03	0.28	-0.09	0.41	0.05	0.04	0.61	0.27	-0.33	-0.02	-0.35	-0.01	-0.29	-0.03	-0.28	-0.02	-0.25	0.17	0.05	-0.12	0.86	-0.02
Sn ppm	0.07	0.20	-0.04	0.18	0.16	0.13	0.29	-0.08	-0.14	0.36	0.26	-0.15	-0.16	0.01	0.28	0.28	0.41	0.16	0.36	0.25	0.37	0.07	-0.07	0.29	0.28	-0.17	0.09	-0.15	0.13
Sr ppm	0.01	-0.09	0.42	-0.06	-0.06	0.10	-0.19	0.52	0.10	-0.08	0.01	0.11	-0.18	0.00	0.09	0.20	-0.09	0.04	0.03	-0.10	0.07	-0.03	0.37	0.09	-0.08	0.39	0.29	0.03	-0.05
Ta ppm	-0.03	-0.10	0.37	-0.10	0.47	0.56	-0.13	-0.11	-0.06	0.08	-0.10	-0.26	-0.31	-0.12	-0.22	0.21	-0.11	0.44	0.03	0.54	0.09	-0.12	-0.16	0.09	-0.07	0.22	0.89	-0.15	-0.11
Te ppm	0.13	0.44	-0.24	0.72	-0.16	-0.03	0.69	0.13	0.06	0.37	0.35	-0.07	0.07	0.41	0.38	-0.05	0.43	-0.09	0.07	-0.08	0.32	-0.12	-0.17	-0.12	0.21	-0.13	-0.18	0.33	0.30
Th ppm	0.04	0.11	-0.17	0.21	0.01	0.17	0.06	0.19	0.01	0.16	0.13	-0.12	-0.14	0.30	0.29	-0.02	0.19	-0.11	0.24	-0.01	0.14	-0.18	0.09	0.06	-0.04	0.02	0.19	0.35	0.32
Ti %	-0.02	-0.03	0.47	-0.03	0.18	0.02	-0.12	0.31	0.07	-0.07	-0.10	0.21	-0.25	0.06	0.18	0.19	-0.25	0.33	0.15	0.04	-0.06	0.17	0.46	0.29	-0.13	0.39	0.51	0.10	-0.08
Tl ppm	0.00	-0.14	0.38	-0.05	0.65	0.28	-0.07	-0.34	-0.16	0.16	-0.09	-0.29	0.13	-0.17	-0.01	0.34	0.05	0.54	0.05	0.81	0.10	0.08	-0.28	0.14	-0.05	-0.26	0.50	-0.31	-0.08
U ppm	0.03	0.16	0.02	0.08	0.07	0.06	0.28	-0.28	-0.07	0.17	0.26	-0.19	0.04	-0.02	-0.07	0.10	0.16	0.01	-0.03	0.22	0.15	-0.11	-0.35	-0.06	0.36	-0.13	-0.04	-0.10	0.00
V ppm	0.09	0.01	-0.12	0.25	-0.03	-0.03	0.03	0.32	-0.02	0.15	0.01	-0.11	0.20	0.08	0.62	0.39	0.32	0.00	0.28	-0.07	0.06	0.14	0.20	0.08	-0.03	-0.23	-0.14	0.04	0.52
W ppm	0.04	0.17	-0.04	0.32	0.33	-0.01	0.33	-0.13	-0.05	0.25	0.04	-0.22	-0.10	0.12	0.31	0.19	0.32	0.17	0.29	0.31	0.11	0.17	-0.12	0.23	0.01	-0.28	0.03	0.02	0.27
Y ppm	0.11	0.10	-0.21	0.53	0.10	0.15	0.25	0.34	-0.12	0.42	0.04	-0.22	0.00	0.13	0.49	0.24	0.53	0.13	0.43	0.11	0.24	0.04	-0.03	0.10	-0.01	-0.26	0.05	0.01	0.70
Zn ppm	0.06	0.34	-0.11	0.06	0.16	-0.04	0.16	-0.11	0.74	0.09	0.01	-0.05	-0.21	0.21	0.19	-0.01	0.07	0.03	0.20	0.06	0.08	0.20	0.12	0.43	-0.05	-0.04	0.08	0.13	-0.04
Zr ppm	-0.04	-0.14	0.42	-0.13	0.39	0.26	-0.06	-0.28	-0.10	0.12	-0.16	-0.09	0.06	-0.23	-0.01	0.31	-0.13	0.98	-0.03	0.45	0.05	0.30	-0.19	0.16	-0.08	0.04	0.47	-0.33	-0.18

Drill Core Correlation	*Pb ppm*	*Rb ppm*	*Re ppm*	*S %*	*Sb ppm*	*Sc ppm*	*Se ppm*	*Sn ppm*	*Sr ppm*	*Ta ppm*	*Te ppm*	*Th ppm*	*Ti %*	*Tl ppm*	*U ppm*	*V ppm*	*W ppm*	*Y ppm*	*Zn ppm*	*Zr ppm*
Au ppm																				
Ag ppm																				
Al%																				
As ppm																				
Ba ppm																				
Be ppm																				
Bi ppm																				
Ca %																				
Cd ppm																				
Ce ppm																				
Co ppm																				
Cr ppm																				
Cs ppm																				
Cu ppm																				
Fe %																				
Ga ppm																				
Ge ppm																				
Hf ppm																				
In ppm																				
K %																				
La ppm																				
Li ppm																				
Mg %																				
Mn ppm																				
Mo ppm																				
Na %																				
Nb ppm																				
Ni ppm																				
P ppm																				
Pb ppm	1.00																			
Rb ppm	-0.06	1.00																		
Re ppm	0.45	-0.24	1.00																	
S %	0.30	-0.44	0.43	1.00																
Sb ppm	0.04	0.09	0.00	-0.01	1.00															
Sc ppm	0.24	-0.06	0.19	0.15	0.01	1.00														
Se ppm	0.17	-0.40	0.37	0.83	-0.03	0.21	1.00													
Sn ppm	0.23	0.27	0.07	-0.07	0.14	0.03	-0.20	1.00												
Sr ppm	0.09	0.15	0.06	-0.09	-0.10	0.46	-0.04	-0.07	1.00											
Ta ppm	-0.01	0.52	-0.03	-0.33	0.00	-0.18	-0.23	0.13	0.12	1.00										
Te ppm	0.19	-0.14	0.25	0.47	0.12	0.02	0.28	0.20	-0.13	-0.17	1.00									
Th ppm	0.05	-0.03	0.19	0.16	0.08	0.12	0.34	0.04	-0.02	0.21	0.10	1.00								
Ti %	-0.01	0.32	0.04	-0.21	0.02	0.51	-0.04	0.01	0.62	0.22	-0.14	0.01	1.00							
Tl ppm	-0.06	0.78	-0.21	-0.29	0.09	-0.22	-0.30	0.24	-0.09	0.58	-0.10	0.01	0.06	1.00						
U ppm	0.31	0.04	0.26	0.18	0.03	-0.20	-0.02	0.41	-0.30	0.05	0.13	-0.04	-0.29	0.13	1.00					
V ppm	0.00	0.08	-0.10	-0.06	0.20	0.10	-0.09	0.20	0.12	-0.24	0.11	0.17	0.15	0.01	-0.08	1.00				
W ppm	0.02	0.22	-0.05	-0.01	0.17	-0.09	-0.06	0.32	-0.14	-0.01	0.21	0.08	0.04	0.28	0.18	0.32	1.00			
Y ppm	0.01	0.16	-0.09	-0.08	0.23	-0.08	-0.12	0.39	-0.03	0.05	0.41	0.27	-0.04	0.19	0.07	0.55	0.46	1.00		
Zn ppm	0.36	0.08	0.06	0.00	0.05	0.11	0.05	0.07	0.07	-0.02	-0.01	-0.02	0.17	-0.01	-0.09	0.07	0.17	-0.03	1.00	
Zr ppm	-0.09	0.59	-0.20	-0.29	0.06	-0.08	-0.30	0.13	0.05	0.38	-0.08	-0.13	0.34	0.48	0.01	-0.02	0.16	0.10	0.04	1.00